Dissertation

submitted to the
Combined Faculties for the Natural Sciences and for Mathematics
of the Ruperto-Carola University of Heidelberg, Germany
for the degree of
Doctor of Natural Sciences

presented by
Dipl.-Biol. Marta Galach
born in Ostrów, Poland

Oral Examination:
01.12.2014

Molecular mechanisms involved in epithelial differentiation of human induced pluripotent stem cells

Referees: Prof. Dr. Viktor Umansky

Prof. Dr. Jochen Utikal

Summary

The Skin is the largest organ in the mammalian body and serves as a barrier to protect the body from dehydration, mechanical trauma, and microbial invasion. In a healthy organism, the upper skin level - the epidermis regenerates constantly through the duration of life via continual proliferation, migration and differentiation.

To date, skin replacements for patients with large burn injuries are generated with patients own keratinocytes, if possible. But the isolation, expansion in culture, and generation of the skin equivalent are time consuming. Decellularized cadaver skin is used to cover the wounds in the meantime. However, cadaver skin is rare and can cause an immune response.

The application of induced pluripotent stem cells (iPSCs) in regenerative medicine and tissue engineering offers great possibilities. IPSCs display a nearly inexhaustible source of pluripotent cells, which can be differentiated into nearly every cell type of the mammalian organism. This enables to study differentiation processes during embryogenesis, especially in humans, which cannot be addressed *in vivo.*

Furthermore, patient-specific iPSCs can be generated and used to establish patients-specific skin cultures.

The differentiation of iPSCs into keratinocytes is a critical process. In order to use these iPSC-derived keratinocytes for skin replacements a pure cell population is required. Existing protocols for the differentiation of pluripotent stem cells into keratinocytes have been improved during the last years. Nevertheless, these protocols do not lead to a pure population of iPSC-derived keratinocytes.

The aim of this project was to find new regulators, which are involved in the differentiation of pluripotent cells into the epithelial lineage.

Therefore I generated hiPSCs from fibroblasts of healthy donors and validated their pluripotent state by investigating the expression of pluripotency associated markers on RNA and protein level. Furthermore, I performed the termatoma assay, the most stringent test for pluripotency.

The generated iPSCs were differentiated by using a published protocol for 30 day, by culturing them in a defined medium supplemented with BMP4 and retinoic acid. The generated keratinocytes were shown to express basal and suprabasal keratinocyte markers on RNA and protein level.

In order to find new factors which are involved in the development of early epithelial cells, I adapted a high-throughput siRNA screen to the iPSC differentiation. This screen enabled the knock-down of nearly 800 kinases during the differentiation of iPSCs into an epithelial lineage.

HIPK4 was one of the top fifty candidates, which resulted in enhanced expression of the embryonic epidermal marker keratin 18. In further investigations, I could show that HIPK4 resulted not only in enhanced expression levels of keratin 18, but also the expression of other epithelial markers was increased.

I could demonstrate that the knock-down of HIPK4 especially in the first few days has an enhancing effect on the differentiation and that this effect is only present in the presence of retinoic acid in the differentiation medium.

Zusammenfassung

Die Haut ist das größte Organ der Säugetiere und fungiert als schützende Barriere, die den Organismus vor Austrocknung, mechanischen Verletzungen von außen und Infektion schützt. In einem gesunden Organismus regeneriert und erneuert sich die oberste Hautschicht - Epidermis kontinuierlich das ganze Leben lang. Die Erneuerung und Regeneration der Haut wird durch ununterbrochene Zellteilung, Migration und Differenzierung gewährleistet.

Haut-transplantate für Patienten mit großflächigen Verbrennungen werden, wenn möglich, mit Patienten-eigenen Keratinozyten hergestellt. Allerdings ist die Generierung der Haut Äquivalente sehr zeitaufwendig und um die Wunde in der Wartezeit zu bedecken wird dezellularisierte Leichenhaut verwendet. Diese ist aber rar und kann zusätzlich eine Abstoßungsreaktion auslösen.

Der Einsatz von induzierten pluripotenten Stammzellen (iPSCs) in der regenerativen Medizin und dem Tissue Engineering eröffnet viele Möglichkeiten. IPSCs stellen eine nahezu unversiegbare Quelle an pluripotenten Zellen dar, die in fast alle Zelltypen differenziert werden können. Das macht sie zu einem einzigartigen Modelsystem, das die Untersuchung von entwicklungsbiologischen Prozessen des menschlichen Körpers ermöglicht.

Weiterhin können Patienten-spezifische iPSCs generiert werden und somit Patienten-spezifische Hautäquivalente.

Die Differenzierung von iPSCs zu Keratinozyten ist ein kompliziertes Verfahren. Um Keratinozyten für die Generierung von Hautäquivalenten zu verwenden müssen die Differenzierungen eine reine Population ohne andere Zelltypen herstellen. Protokolle wurden immer mehr verbessert, allerdings erzielen sie weiterhin keine reinen Populationen.

Das Ziel dieser Arbeit war es neue Kandidaten zu finden, die eine Rolle während der Differenzierung von pluripotenten Zellen in die epitheliale Richtung spielen, zu finden.

Dafür habe ich Fibroblasten von gesunden Donoren zu humane iPSCs reprogrammiert und ihren pluripotenten Status auf RNA und Proteinebene verifiziert. Außerdem habe ich den Teratom Assay durchgeführt, der kritischste Test um den pluripotenten Status zu verifizieren.

Die reprogrammierten iPSCs wurden dann anhand eines publizierten Protokolls in Keratinozyten differenziert. Das Protokoll basierte auf der Verwendung eines definierten Mediums und der Zugabe von BMP4 und Retinsäure. Es wurde gezeigt, dass die generierten Keratinozyten basale und suprabasale Keratinozytenmarker auf RNA und Proteinebene exprimieren.

Um neue Faktoren zu finden, die einen Einfluss auf die Differenzierung von pluripotenten Zellen zu frühen Epithelzellen haben, habe ich die Differenzierung im Hochdurchsatz siRNA Screening angepasst und etabliert. Dieser Screen ermöglicht durch die Transfektion mit siRNAs den knock-down von nahezu 800 Kinasen während der Differenzierung.

HIKP4 war einer der Kandidaten der top Fünfzig, durch deren knock-down die Expression des embryonalen Epidermis Markers Keratin 18 erhöht wird. Zusätzliche Untersuchungen haben gezeigt, dass nicht nur die Expression von Keratin 18, sondern noch einiger weiterer epithelialer Marker erhöht war, wenn HIPK4 runterreguliert war. Weiterhin konnte ich zeigen, dass dieser Effekt zutrifft, wenn HIPK4 in den ersten 5 Tagen runterreguliert ist und das Medium Retinsäure enthält.

Table of contents

Summary ---- 4
Zusammenfassung ---- 5
Table of contents ---- 6
Abbreviations ---- 9
List of figures ---- 13
1 Introduction ---- 15
1.1 The human skin ---- 16
1.1.1 The skin´s architecture and homeostasis ---- 16
1.1.1.1 Generation and characterization of the different layers ---- 16
1.1.1.2 The basement membrane and the role of laminin and collagen ---- 19
1.1.1.3 Hemidesmosomes and focal adhesions ---- 20
1.1.1.4 Cell-cell adhesion ---- 22
1.1.1.5 Stem cells of the interfollicular epidermis ---- 22
1.1.2 Molecular pathways involved in keratinocyte terminal differentiation ---- 23
1.1.2.1 P63 ---- 23
1.1.2.2 Notch ---- 23
1.1.2.3 NF-κB and IKK ---- 24
1.1.2.4 AP-1 ---- 25
1.1.2.5 AP-2 ---- 25
1.1.2.6 BMPs ---- 25
1.1.2.7 C/EBP ---- 26
1.1.2.8 MAPK/ERK-Pathway ---- 27
1.1.2.9 Hox genes ---- 27
1.1.3 The skin appendages ---- 28
1.1.3.1 The hair follicle ---- 28
1.1.3.2 The sebaceous gland ---- 29
1.1.4 Non-keratinocyte cell types of the epidermis ---- 29
1.1.4.1 Merkel cells ---- 29
1.1.4.2 Melanocytes ---- 30
1.1.4.3 Langerhans cells ---- 30
1.1.5 The embryonic development of the epidermis ---- 30
1.2 Induced pluripotent stem cells ---- 32
1.2.1 History and discovery of induced pluripotency ---- 32
1.2.2 Methods for generating induced pluripotent stem cells ---- 33
1.2.3 Induced pluripotent stem cells for therapeutic purpose ---- 34
1.3 Differentiation of pluripotent cells into keratinocytes *in vitro* ---- 35
1.4 Aim of the project ---- 37
2 Material and Methods ---- 38
2.1 Material ---- 39
2.1.1 Cell culture media and supplements ---- 39
2.1.2 Cell culture media composition ---- 39
2.1.3 Chemicals ---- 40
2.1.4 Kits ---- 41
2.1.5 Buffers and gels ---- 41
2.1.6 Primary antibodies ---- 42
2.1.7 Secondary antibodies ---- 42

2.1.8 siRNA sequences ---- 43
2.1.9 Consumables ---- 43
2.1.10 Machines and devices ---- 44
2.1.11 Material for Microarray ---- 45
2.1.12 Software ---- 45
2.1.13 Plasmids ---- 46
2.1.13.1 TetO human STEMCCA floxed (reprogramming cassette) ---- 46
2.1.13.2 FUdeltaGW-rtTA (transactivator) ---- 47
2.1.13.3 pCMV-dR8.91 (packaging plasmid, Δ8.9) ---- 47
2.1.13.4 pCMV-VSV-G (packaging plasmid, VSV-G) ---- 48
2.1.13.5 pLenti CMV GFP Puro (empty control vector) ---- 48
2.1.13.6 pCW45-HIPK4 (HIPK4 expression vector) ---- 49
2.1.14 QPCR Primer sequences ---- 49
2.2 Methods ---- 50
2.2.1 Plasmid preparation ---- 50
2.2.1.1 Transformation of bacteria ---- 50
2.2.1.2 Preparation of glycerolstocks ---- 50
2.2.1.3 Endo-free plasmid preparation and purification ---- 50
2.2.2 Cell culture methods ---- 50
2.2.2.1 Culture of 293T HEK cells and virus production ---- 50
2.2.2.2 Coating of cell culture plates ---- 51
2.2.2.2.1 Thin Matrigel™ coating ---- 51
2.2.2.2.2 Gelatin coating ---- 52
2.2.2.3 Isolation of primary human fibroblasts and keratinocytes from skin biopsies - 52
2.2.2.4 Isolation of mouse embryonic fibroblasts ---- 52
2.2.2.5 Preparation of feeder cells from mouse embryonic fibroblasts ---- 53
2.2.2.6 Culture and cryopreservation of mouse and human primary fibroblasts ---- 53
2.2.2.7 Culture and cryopreservation of human primary keratinocytes ---- 53
2.2.3 Generation and culture of human induced pluripotent stem cells ---- 54
2.2.3.1 Generation of human induced pluripotent stem cells ---- 54
2.2.3.2 Culture of human induced pluripotent stem cells ---- 54
2.2.3.3 Cryopreservation and thawing of hiPSCs grown on Matrigel™ ---- 55
2.2.4 Epithelial differentiation protocol ---- 55
2.2.5 High-throughput siRNA screen ---- 56
2.2.5.1 Seeding and transfecting cells ---- 56
2.2.5.2 Fixation and immunofluorescence staining ---- 57
2.2.5.3 Automated imaging and data analysis ---- 57
2.2.6 Transfection of hiPSCs with siRNAs ---- 58
2.2.7 Molecular biological methods ---- 58
2.2.7.1 RNA isolation ---- 58
2.2.7.2 Reverse transcriptase-polymerase chain reaction ---- 58
2.2.7.3 Real-time polymerase chain reaction ---- 59
2.2.7.4 Genome wide expression profiling using Illumina BeadChips® ---- 59
2.2.8 Protein biochemistry ---- 60
2.2.8.1 Protein Isolation ---- 60
2.2.8.2 BCA Protein Assay ---- 60
2.2.8.3 SDS page and Western Blot ---- 61
2.2.8.3.1 Preparation of SDS-polyacrylamide gels ---- 61
2.2.8.3.2 Sample preparation ---- 62

2.2.8.3.3 Gel electrophoresis ---- 62
2.2.8.3.4 Blotting ---- 62
2.2.8.3.5 Antibody staining and developing ---- 62
2.2.8.4 Immunofluorescence staining of cells ---- 63
2.2.8.5 Flow cytometry analysis ---- 63
2.2.9 Teratoma assay ---- 64
2.2.9.1 Sample preparation and injection ---- 64
2.2.9.2 Paraffin embedding and hematoxylin and eosin staining of teratomas ---- 64
3 Results ---- 66
3.1 Pluripotency verification of reprogrammed cells ---- 67
3.2 Differentiation of human induced pluripotent stem cells into keratinocytes ---- 70
3.3 High-throughput siRNA screen of differentiating human induced pluripotent stem cells ---- 74
3.4 Investigating the role of HIPK4 during early epithelial differentiation ---- 76
3.4.1 The effect of HIPK4 knock-down on keratin 18 expression during early epithelial differentiation ---- 76
3.4.2 Transfection of hiPSCs with single siRNAs against HIPK4 ---- 80
3.4.3 Serial knock-down of HIPK4 during early epithelial differentiation of hiPSCs ---- 81
3.4.4 The effect of HIPK4 knock-down under different culture conditions ---- 82
3.4.5 Influence of HIPK4 overexpression on differentiating cells ---- 85
4 Discussion ---- 86
4.1 Advantages of using induced pluripotent stem cells ---- 87
4.2 Differentiation of hiPSCs into epithelial cells and the importance of generating efficient protocols ---- 88
4.3 High-throughput screens as the method of choice to find single candidates involved in the development of keratinocyte precursors ---- 89
4.4 The role of HIPK4 during the differentiation of human induced pluripotent stem cells into epithelial precursors ---- 91
References ---- 94
Danksagung ---- 109
Eidesstattliche Erklärung ---- 111

Abbreviations

µg	microgram
µL	microliter
µM	micromolar

A

ADCK2	AarF domain containing kinase 2
ALPL	alkaline phosphatase
AP-1	activator protein 1
AP-2	activator protein 2

B

BCA	bicinchoninic acid
bFGF	basic fibroblast growth factor
BMP	bone morphogenic proteins
BMPR	bone morphogenic protein receptor
BP180	180kDa bullous pemphigoid antigen
BP230	230kDa bullous pemphigoid antigen
BSA	bovine serum albumin
bZIP	basic leucin zipper

C

C/EBP	CCAAT/enhancer binding protein
CBX2	chromobox homolog 2
cm	centimeter
COL7A1	collagen, type VII, alpha 1

D

DAPI	4',6-diamidino-2-phenylindole
DKSFM	defined keratinocyte serum free medium
DMEM	Dulbecco's Modified Eagle's Medium
DMSO	dimethyl sulfoxide
DNMT3B	DNA (cytosine-5-)-methyltransferase 3 beta

E

EB	embryoid body
EBNA1	Epstein-Barr nuclear antigen-1
EGFR	epidermal growth factor receptor
EGFR	epidermal growth factor receptor
EPU	epidermal proliferation unit
Erk	extracellular signal-regulated kinases
ESC	embryonic stem cell

F

FACS	fluorescence activated cell sorting
FAD	F12 and Dublecco´s modified Eagle´s medium
FBS	fetal bovine serum

FGF	fibroblast growth factor
FGFR4	fibroblast growth factor receptor 4
FITC	Fluorescein isothiocyanate

G

g	gram
GEF	guanine nucleotide exchange factors
GM-CSF	granulocyte-macrophage colony stimulating factor
GRB2	growth factor receptor-bound protein 2
GSK3	glycogen synthase kinase 3

H

hESC	human embryonic stem cell
HIPK4	homeodomain interacting protein kinase 4
hiPSC	human induced pluripotent stem cell
HIV	human immunodeficiency virus
HOX	homeobox
HTS	high throughput screen

I

ICM	inner cell mass
IF	immunofluorescence
IKK	inhibitor of kappa B kinase α
IKKα	inhibitor of kappa B kinase α
IL-1α	interleukin-1 α
iPSC	induced pluripotent stem cell
IRS	inner root sheath
ITGA5	integrin-alpha-5
ITGAV	integrin-alpha-V
ITGB1	integrin-beta-1
ITGB1BP1	integrin-beta-1 binding protein
IVL	involucrin
IκBß	NF-κB inhibitor beta
IκBα	NF-κB inhibitor alpha

K

KGF	keratinocyte growth factor
KLF4	krueppel-like factor 4
KRT1/K1	keratin 1
KRT14/K14	keratin 14
KRT16/K16	keratin 16
KRT16P3	keratin 16 pseudogene 3
KRT17/K17	keratin 17
KRT18/K18	keratin 18
KRT5/K5	keratin 5
KRT8/K8	keratin 8

L

L	liter
LAMC2	laminin, gamma 2
LEF1	lymphoid enhancer binding factor 1
LEFTY1	left-right determination factor 1
LEFTY2	left-right determination factor 2
LEP	late envelope protein
LIN28A	lin-28 homolog A (C.elegans)

M

M	molar
MAPK	mitogen-activated protein kinase
MEF	mouse embryonic fibroblasts
mESC	murine embryonic stem cell
mg	milligram
min	minute
mL	milliliter
NF-κB	nuclear factor kappa of activated B-cells

N

NICD	notch intracellular domain
NLK	nemo-like kinase
nm	nanometer

O

OCT4	octamer binding protein 4
ORS	outer root sheath

P

PBS	phosphate buffered saline
PFA	paraformaldehyde
POU5F1	POU class 5 homeobox 1(Oct 3/4)
PPARγ	peroxisome proliferation activated receptor γ
PVDF	polyvinylidene fluoride

R

RA	retinoic acid
RBP-Jκ	recombinant binding protein suppressor of hairless
RT	room temperature

S

SDS	sodium dodecyl sulfate
SG	sebaceous gland
SMA	spinal muscular atrophy
SOS1	son of sevenless
SOX2	SRY (sex determining region Y)-box 2
SPR	small proline-rich protein
ssRNA	single-stranded ribonucleic acid

T

TA	transit amplifying
TAB1	TGF-ß activated kinase 1 binding protein
TAK1	TGF-ß activated kinase 1
Tat	transactivator of transcription
TBS	tris-buffered saline
TCF3	T cell factor 3
TG	transglutaminase
TGF	transforming growth factor
TGM1	transglutaminase 1
TNFR1	tumor necrosis factor receptor 1
TNFα	tumor necrosis factor alpha
TP63	tumor protein p63

Z

ZIC3	ZIC family member 1

List of figures

Figure 1: Schematic illustration of the epidermal architecture ---------- 19
Figure 2: Schematic diagram of focal adhesions and hemidesmosomes ---------- 21
Figure 3: Bright field images of hiPSC line D1 ---------- 67
Figure 4: Alkaline phosphatase staining of hiPSC line D1 ---------- 67
Figure 5: Expression quantities of pluripotency associated markers in hiPSCs compared to NHKs ---------- 68
Figure 6: Immunofluorescence stainings of pluripotency associated markers on human induced pluripotent stem cell colonies ---------- 68
Figure 7: Teratoma assay indicating the pluripotent state of injected human induced pluripotent stem cells (hiPSCs) ---------- 69
Figure 8: Schematic illustration of differentiation experiment ---------- 70
Figure 9: Bright field images of differentiated cells derived from human induced pluripotent stem cells ---------- 70
Figure 10: QPCR analysis of cells at several differentiation steps ---------- 71
Figure 11: Immunofluorescence images of hiPSC-derived keratinocytes at several differentiation steps ---------- 72
Figure 12: Dendrogram based on gene expression array results ---------- 72
Figure 13: Significant fold changes of pluripotency associated genes and keratinocyte markers ---------- 73
Figure 14: Schematic diagram of screen work flow ---------- 74
Figure 15: High-throughput siRNA screen analysis ---------- 74
Figure 16: Distribution of the z-score values of all siRNAs ---------- 75
Figure 17: High-throughput siRNA screen read-out ---------- 75
Figure 18: HIPK4 expression values during in vitro differentiation of hiPSCs into keratinocytes ---------- 76
Figure 19: Illustration of the experimental set-up ---------- 76
Figure 20: Western blot analysis of cells transfected with HIPK4 and non-targeting (control) siRNA ---------- 76
Figure 21: Expression values of keratinocyte markers in differentiated hiPSCs upon HIPK4 knock-down ---------- 77
Figure 22: Flow cytometry analysis of differentiated hiPSCs upon HIPK4 knock-down --- 78
Figure 23: Immunofluorescence staining of Keratin18 (K18) on differentiated hiPSCs upon HIPK4 knock-down ---------- 79
Figure 24: QPCR analysis of differentiated hiPSC line VG2 upon HIPK4 knock-down --- 79
Figure 25: Pool of four single siRNAs against HIPK4 ---------- 80

Figure 26: Expression analysis of differentiated hiPSCs transfection with single siRNAs against HIPK4 ---------- 80
Figure 27: Schematic of serial transfection work flow ---------- 81
Figure 28: QPCR analysis of differentiated cells after serial knock-down ---------- 82
Figure 29: Schematic of varying culture conditions during differentiation ---------- 83
Figure 30: Influence of medium composition on the HIPK4 knock-down effect during differentiation ---------- 84
Figure 31: QPCR analysis of epithelial markers and HIPK4 in HIPK4 overexpressing cells ---------- 85

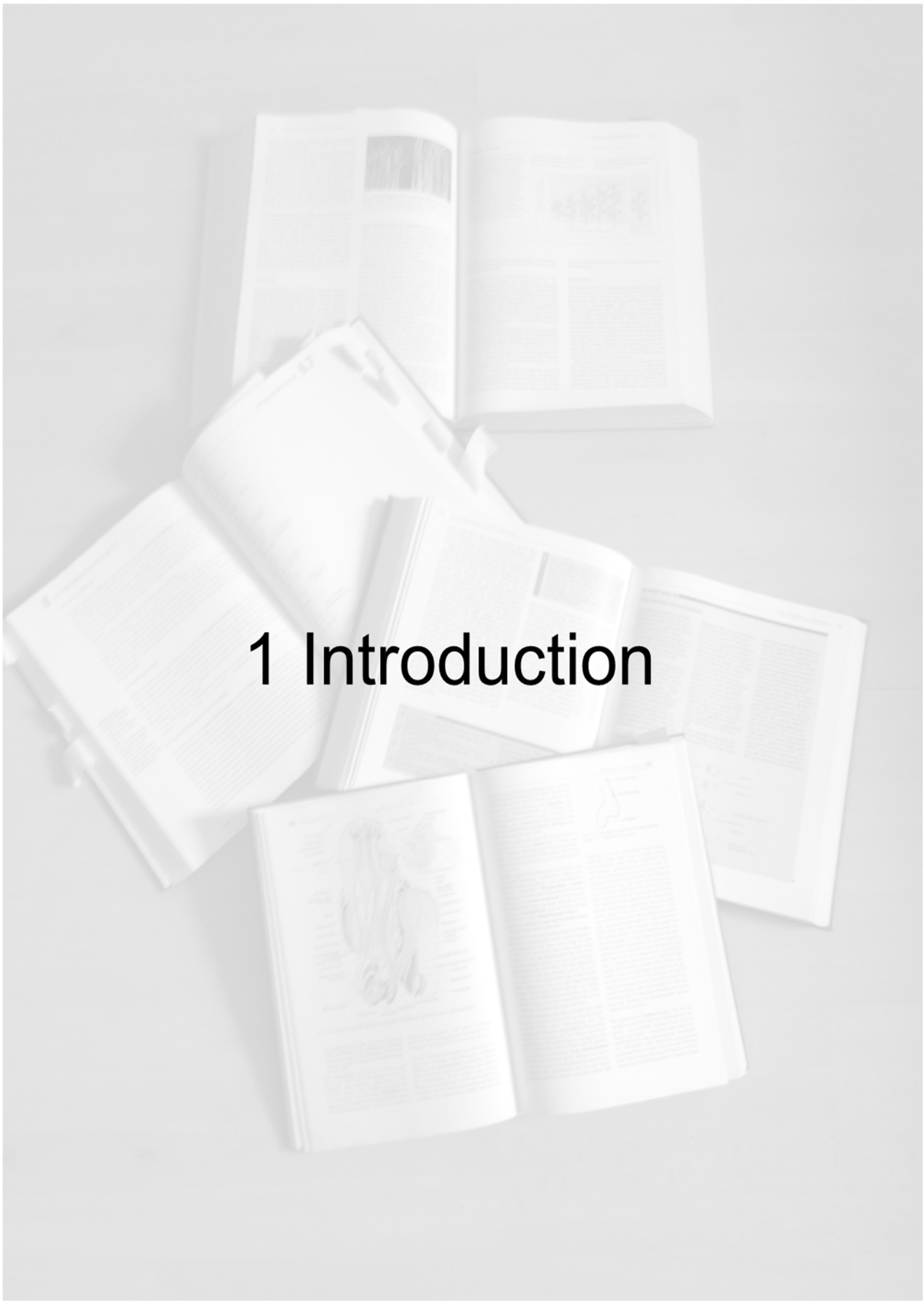

1 Introduction

1 Introduction

1.1 The human skin

The surface of our body, the skin epidermis and its appendages, provides a barrier which protects us against external environmental insults, while keeping essential body fluids inside to prevent us from dehydration. Every day this barrier is exposed to ultraviolet radiation from the sun, mechanical trauma like scratches and wounds, and microbial invasion. The epidermis confronts these traumas through ongoing self-renewal. The process of self-renewal is assured through continuous proliferation, differentiation and migration of the cells and must be carefully balanced to sustain a healthy homeostasis. The human skin epidermis is a tissue with a complex architecture. It is a stratified squamous epithelium consisting of several cell types, including keratinocytes, melanocytes and Langerhans cells. Keratinocytes are the most abundant cell type and appear in different differentiation stages. The epidermis is non-vascularized and receives its nutrients from the blood vessels of the underlying dermis.

1.1.1 The skin´s architecture and homeostasis

1.1.1.1 Generation and characterization of the different layers

The skin epidermis is a self-renewing stratified epithelium maintained by the proliferation, migration and differentiation of keratinocytes. This process starts at the lowermost layer of the epidermis, the basal layer or stratum basale, where keratinocytes proliferate, detach from the underlying basement membrane and migrate upwards. The overlying layer is the stratum spinosum, or spinous layer. This layer is characterized by dense cell-cell connections, named desmosomes, and the expression of the first differentiation markers, including involucrin and transglutaminase 1. The cells of the next layer, the stratum granulosum (or granular layer) cells are rich in granules containing products to assemble various terminal keratinocyte structures. These cells are metabolically active until they reach the next layer, the stratum lucidum, the transition zone between living epidermal cells and dead cells. In this region organelles and nuclei are degraded. The uppermost layer, the stratum corneum, is occupied by dead flattened cells, which consist of a stabilized array of keratin filament covalently crosslinked to a cornified envelope. In the last step, the terminally differentiated corneocytes are shed from the surface, making room for subsequent terminally differentiated cells (Figure 1).

The skin epidermis is a self-renewing tissue with a constant number of cells. This homeostasis is maintained by stem cells in the basal layer. It is still not clear whether all cells in the basal layer have stem cell potential or only a small fraction of cells maintains the stem cell equilibrium. Furthermore it remains unclear if these stem cells divide asymmetrically or symmetrically (the recent findings are further displayed in chapter “1.1.1.5 Stem cells of the interfollicular epidermis”). Basal cells are characterized by their expression of keratin 5 and 14 (K5, K14; also named cytokeratin 5 and cytokeratin 14) (Banks-Schlegel, 1982; Moll et al., 1982). Periodically, basal cells withdraw from the cell cycle, migrate from the basal to the spinous layer and begin to synthesize a new set of structural proteins and enzymes that are characteristic for cornification. These differentiating, migrating cells downregulate the expression of K5 and K14, while keratin 1 and 10 (K1, K10) expression is induced

(Candi et al., 2005). Only suprabasal keratins are able to form heterodimers that assemble into heteropolymers and intermediate filaments (Coulombe and Wong, 2004).

In the upper stratum spinosum and the stratum granulosum, the cells exhibit keratohyalin granules, which contain profilaggrin - the precursor of the interfilament protein filaggrin (Matoltsy, 1975). In addition, a number of other structural proteins are synthesized, including involucrin, loricrin and small proline-rich proteins (SPRs), which are crosslinked by several transglutaminases to reinforce a cornified envelope beneath the plasma membrane. Transglutaminases (TGs) are enzymes that are essential for a correct cornified-envelope assembly, by catalyzing the generation of very stable isopeptide bonds between the structural proteins. In the skin epidermis TG1, TG3 and TG5 are involved in the formation of the cornified envelope (Candi et al., 2005; Simon and Green, 1988).

The structural protein involucrin is highly α-helical and is crosslinked by TG1 to many other structural proteins and thereby contributes to the buildup of a scaffold to which further structural proteins become crosslinked (Rice and Green, 1977). An additional structural protein is loricrin which is the main component of the cornified envelope and constitutes 70-85% of its protein mass. Mainly isopeptide bound loricrin-loricrin crosslinks are found in the cornified envelope, but smaller amounts of loricrin are also crosslinked to SPRs which function as cross-bridging proteins among loricrins (Candi et al., 1995). Even though the amount of loricrin and SRPs is always ~85%, the ratio of SPRs and loricrin varies from 1:100 in thinner epidermal regions to about 1:1000 in thicker epidermal parts, including palm and sole epidermis (Candi et al., 1999). This shows that the flexibility, rigidity or toughness is strongly dependent on the amounts and proportion of crosslinked partners. Furthermore, loricrin crosslinked with SPRs is deposited on a scaffold of involucrin, cystatin A, elafin and desmosomal proteins (Takahashi et al., 1992), and in addition, it is also crosslinked to keratin and filaggrin. This demonstrates that the keratin intermediate filament complex of cornified epidermal cells is covalently bound to the cornified envelope (Steinert and Marekov, 1995). These various crosslinks of loricrin are strengthened by multiple TGs that are required for loricrin crosslinking in the epidermis. Before loricrin is crosslinked to the cornified envelope, it is intermixed with profilaggrin and deposited in the keratohyalin granules in the granular layer of the epidermis (Yoneda and Steinert, 1993).

Profilaggrin is a large complex protein that contains 10 – 12 filaggrin units joined together which accumulates in the keratohyalin granules. Initially, it is highly phosphorylated, but becomes dephosphorylated and proteolytically cleaved during cornification in order to release filaggrin molecules (Gan et al., 1990). Upon release, filaggrin becomes crosslinked to the cornified envelope and thus contributes to the coordination of its structure. Furthermore, it aggregates keratin and other intermediate filament proteins into tight bundles, a hypothetical mechanism named 'ionic zipper' (Mack et al., 1993). This leads to the parallel alignment of keratin and subsequently to a change in cell shape from ellipsoid to flat. Filaggrin becomes degraded into free amino acids after a half live of 6 hours, which results in a high concentration of hydrophilic amino acids in the cornified cell. This is essential for the retention of water and thus for the osmolarity of the cell.

Taken together, in humans the genes encoding involucrin, loricrin, profilaggrin and SPRs are all located in the epidermal-differentiation complex locus on chromosome 1q21 (Mischke et al., 1996). In addition to the aforementioned proteins, genes encoding late envelope proteins (LEPs) are also located in this locus. Late envelope proteins are a new family of proteins that are also substrates for TGs and that are expressed later during keratinocyte differentiation than SPRs.

The assembly of the cornified envelope, which starts in the upper stratum spinosum, is mainly triggered by increasing Ca^{2+}-levels. The increase in the Ca^{2+}-gradient regulates Ca^{2+}-

dependent proteases, which are required for various processes during terminal differentiation (Hennings et al., 1980; Yuspa et al., 1989). They are responsible for the proteolytic processing of the cornified envelope precursor, the degradation of nuclei and mitochondria and the proteolysis of corneodesmosomes during desquamation (Kim et al., 1998). The proteases μ-calpain, cathepsin D and furin are responsible for the proteolytic processing of TGs, which results in their activation. PEP1, capain, furin and matriptase are required for the processing of filaggrin (List et al., 2003; Yamazaki et al., 1997).

Once the cornified envelope is formed, the cell becomes embedded in a lipid envelope, which is essential for the barrier formation of the epidermis and helps to avoid transepidermal water loss. Skin lipids are mainly ceramides, cholesterol, fatty acids and cholesterol esters. Their precursors, glucosylceramides, phospholipids and cholesterols are synthesized intracellularly and stored in lamellar bodies. Beside these lipids, lamellar bodies also contain hydrolytic enzymes, including acid hydrolases (Hamanaka et al., 2005). During cornification the lamellar bodies are extruded into the extracellular space in the upper granular layer, where the activity of the hydrolases leads to complex changes in lipid composition (Freinkel and Traczyk, 1985; Menon et al., 1992). The exocytosis of these lipids is triggered by the increasing Ca^{2+}-level in the differentiating cell at the stratum granulosum/stratum corneum interface. Although it has not been completely determined how the extracellular lipids are connected to the cornified envelope, it is known that long-chain ω-hydroxyceramides located on the extracellular surface are covalently attached through ester linkages to the outer surface of the cornified envelope (Nemes et al., 1999). In addition, other constituents of the lipid envelope have long fatty-acid chains that can cross the plasma membrane and become ester-linked to the cornified envelope.

As one of the last steps of terminal differentiation the cells undergo programmed cell death. The cornified- and the lipid envelope are formed and replace the plasma membrane, the organelles are destroyed and the DNA is degraded (Houben et al., 2007; Lippens et al., 2005). However, the programmed cell death of keratinocytes is distinct from the typical apoptosis. First the terminally differentiated corneocytes are not phagocytosed, and second pathways involved in apoptosis, including the caspase pathway, are not or differently activated. In contrast, the latest member of the caspase family, caspase 14, was found to be exclusively expressed and activated in the epidermis and not during typical apoptosis, suggesting a role for caspase 14 in programmed cell death of keratinocytes (Eckhart et al., 2000; Lippens et al., 2005). Furthermore, the nucleus in cornified cells is completely degraded, whereas it is only partially degraded and nuclear fragments are still detectable during apoptosis (Candi et al., 2005). The DNAse responsible for the nuclear degradation and the pathways that lead to this degradation have not yet been identified. The final step of keratinocyte terminal differentiation and migration is the desquamation, the final shedding of corneocytes from the cell surface. This requires a controlled destruction of cell-cell adhesion structures, especially corneodesmosomes (Chapman and Walsh, 1990). Corneodesmosomes contain the cadherins desmoglein 1 and desmocollin 1, and the glycoprotein corneodesmosin, which is covalently linked to the cornified envelope. For the final shedding, these proteins need to be proteolytically degraded to allow desquamation (Houben et al., 2007). The epidermal homeostasis is a sensitive system that relies on a well-adjusted balance between proliferating cells, which give rise to committed cells and cells that are lost by desquamation.

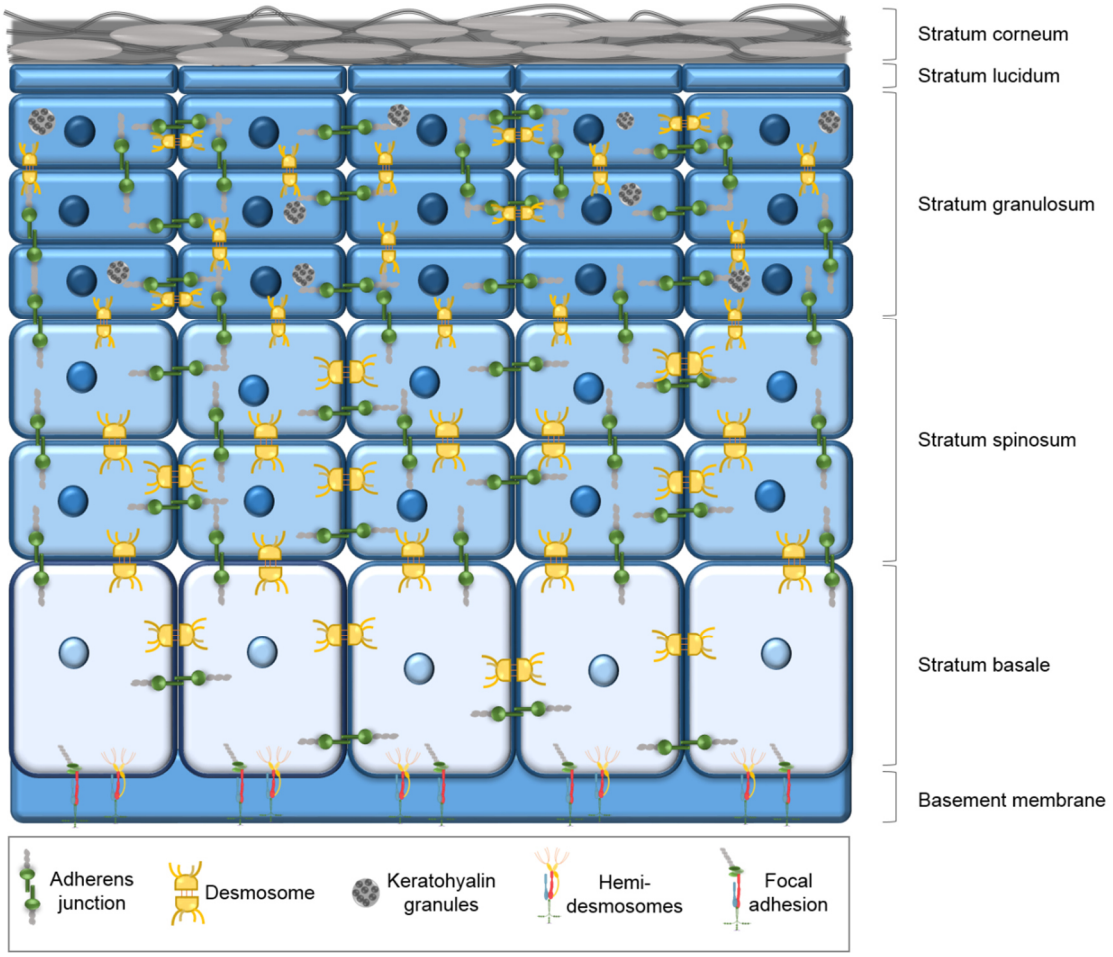

Figure 1: Schematic illustration of the epidermal architecture. The epidermis is a stratified epithelium consisting of stratum basale, stratum spinosum, stratum granulosum, stratum lucidum and stratum corneum. The cells are connected to each other by adherens junctions and desmosomes, and to the basement membrane by hemidesmosomes and focal adhesions. Cells of the stratum granulosum contain keratohyalin granules, which contain profilaggrin.

1.1.1.2 The basement membrane and the role of laminin and collagen

The basement membrane includes a layer of extracellular matrix with a bi-layer structure that is divided into the lamina lucida, the clear layer underneath the basal layer, and the lamina densa, the electron dense layer closer to the dermis (McMillan et al., 2003). The basement membrane acts to determine the polarity of the epidermis. In a healthy skin, homeostasis is ensured by an exchange of signals between the dermis and epidermis. The components of the basement membrane need to selectively facilitate or prevent these signals from crossing. The epidermis and the dermis both contribute to the basement membrane formation (Fuchs and Raghavan, 2002). The basic components of the basement membrane are laminins, collagen IV, nidogens and heparan sulfate proteoglycans, but laminins are the major component, and together with collagen IV, form the basic scaffold of the basement membrane. Laminins are heterotrimeric glycoproteins composed of α, ß and γ chains (Aumailley et al., 2003). There are 5 distinct α, 4 ß and 3 γ chains, which give rise to 15 laminin isoforms. The majority of laminins are able to form networks through self-aggregation by binding their N-terminal short arms that carry binding sides for nidogens or collagen VII. This self-aggregation leads to the incorporation of laminins into the basement membrane. The predominant isoform of laminin in the basement membrane is laminin 5 (also called laminin 3-3-2) (Nishiyama et al., 2000). It consists of three non-identical α3, ß3 and γ2

chains. Due to proteolytic processing laminin 5 has unusually short arms, especially at the α3 and γ2 chains, which prevent the self-aggregation (Aumailley et al., 2003). In contrast to other laminins, laminin 5 does not bind nidogen, a member of the nidogen family of basement membrane glycoproteins that connects the collagen and laminin networks. Laminin 5 incorporates into the basement membrane by forming complexes with laminin 6 and 7 that in turn can self-associate and interact with collagen IV through nidogen (Champliaud et al., 1996). Collagen IV is found primarily in the epidermal-dermal basement membrane. Its C-terminal C_4 domain is not translationally processed, allowing a head-to-head linkage of the collagen fibers. Collagen IV trimers carry a C-terminal NC-1 domain and are able to self-associate to form dimers through the N-terminal domains (Brown and Timpl, 1995). In contrast to other collagen types collagen IV lacks a glycine in every third amino-acid residue, which leads to a flexible sheet formation.

Besides indirect collagen IV binding, laminin 5 can bind directly the NC-1 domain of collagen VII, via the ß3 and γ2 chain short arms (Chen et al., 1999). Collagen VII monomers are composed of 3 α1 chains folded into a triple helix, which then form disulfide-bond stabilized antiparallel-dimers. These dimers then bundle laterally into the so called anchoring fibrils. The anchoring fibrils extend from the lamina densa, where they are bound by laminin 5 at their large NC-1 domain, to the papillary connective tissue (Rousselle et al., 1997). In the connective tissue, these fibrils either loop back to the lamina densa or enter the anchoring plaques (Gipson et al., 1987). Furthermore, other laminin isoforms are present in the basement membrane, but their expression is temporally and spatially restricted during development. For example, during embryogenesis laminin 10 is expressed throughout the entire basement membrane, but becomes restricted to the hair follicles in later stages. In addition, laminin α1 is expressed by the early periderm throughout the basement membrane except for the hair follicles and is then downregulated, whereas the expression of the isoform laminin α2 is restricted to the area surrounding the hair follicles (Aumailley and Rousselle, 1999).

1.1.1.3 Hemidesmosomes and focal adhesions

The cells of the basal layer are strongly connected to the basement membrane by focal adhesions and hemidesmosomes (Figure 2). In both adhesion complexes, integrin receptors play both a structural role, mediating physical attachment of basal cells to the basement membrane, and a signaling role ensuring cellular proliferation and migration.

Focal adhesions contain a transmembrane core of $\alpha_3\beta_1$ integrin, which is intracellularly connected to the actin and microtubule network of the cell. This connection is mediated by numerous actin-binding proteins, including paxillin, vinculin, talin, kindlin, migfilin, and actin isoforms by which the $\alpha_3\beta_1$ integrin is associated with actin (DiPersio et al., 1997). Integrin-$\alpha_3\beta_1$ adheres extracellularly to laminin 5 and this binding is important for assembling and organizing the basement membrane. The β_1 and α_3 integrins are generally involved in the development of hair follicles, but keratinocyte-specific β_1 integrin null mice show extensive epidermal blistering and exhibit a hyperproliferative epidermis (Brakebusch et al., 2000; DiPersio et al., 1997). In contrast, the ablation of α_3 leads to hair loss and basement membrane assembly defects around hair follicles. The fact that no further defects have been described so far suggests that other integrins can compensate for the function of α_3 (DiPersio et al., 1997). Basal keratinocytes also express several other isoforms including $\alpha_2\beta_1$, $\alpha_5\beta_1$, $\alpha_9\beta_1$, and $\alpha_v\beta_5$. These isoforms have various ligands, including fibronectin, collagen and

laminin, suggesting that multiple interactions are involved in anchoring basal keratinocytes according to the physiological or pathological situation (Fuchs and Raghavan, 2002).

Hemidesmosomes ensure a stable and robust adhesion of basal keratinocytes to the basement membrane and the underlying dermis (Borradori and Sonnenberg, 1999). The transmembrane components of hemidesmosomes are $\alpha_6\beta_4$ integrin and the 180kDa bullous pemphigoid antigen (BP180, also known as BPAG2, collagen type XVII α1 or COL17A1) (Hopkinson et al., 1992; McMillan et al., 2003). The cytoplasmic domain of BP180 interacts with the β_4 subunit, while the extracellular domain can bind to both, the α_6 and the β_4 subunit. The β_4 subunit of the $\alpha_6\beta_4$ integrin heterodimer exhibits an unusually long cytoplasmic tail of over 1000 amino acids, which is required for the correct localization within the hemidesmosome and for the interconnection with other hemidesmosomal constituents. The cytoplasmic domains of $\alpha_6\beta_4$ integrin and BP180 are bound to the cytoplasmic plaque constituents bullouse pemphigoid antigen 230 (BP230, also named BPAG1e) and plectin (Hopkinson and Jones, 2000; Simpson et al., 2011). BP230 and plectin belong to the plakin protein family and have the ability to associate with keratin intermediate filaments, providing the bridge between the transmembrane proteins of the hemidesmosomes and the cytoskeleton. Extracellularly the $\alpha_6\beta_4$ integrin heterodimers serve as receptors for laminin 5 (Dowling et al., 1996). This complex consisting of the extracellular portions of the hemidesmosomes and the bound laminin 5 is known as the anchoring filaments, which are attached to the anchoring fibrils (see chapter “1.1.1.2 The basement membrane and the role of laminin and collagen”) to provide a stable adherence of keratinocytes to the underlying basement membrane (Tsuruta et al., 2011).

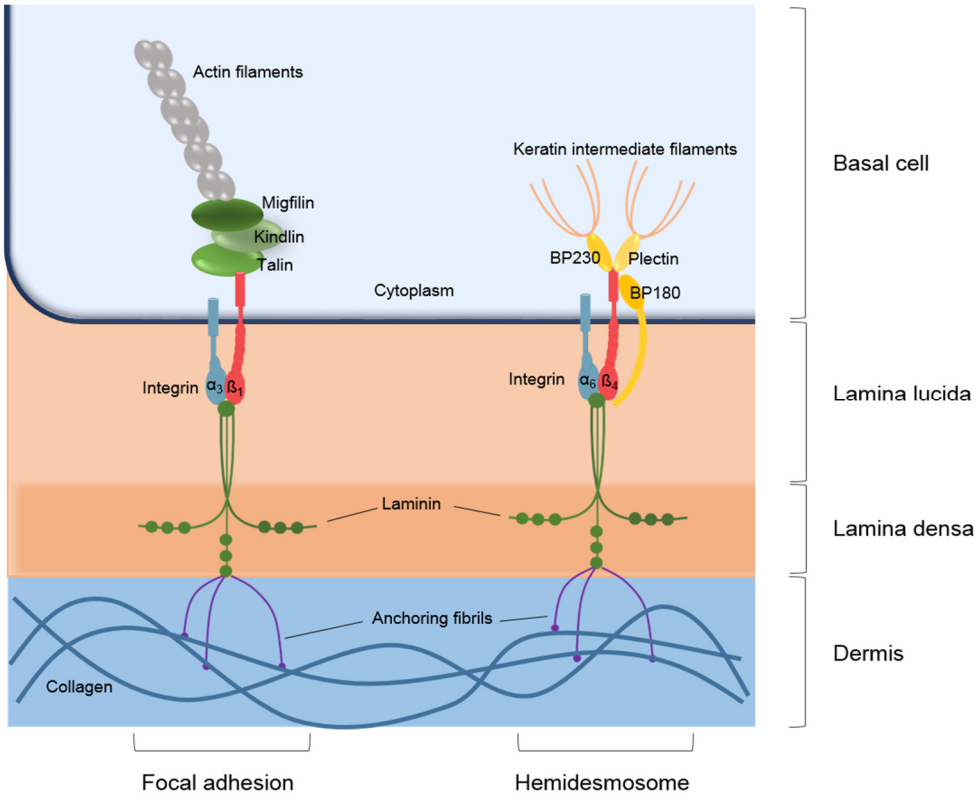

Figure 2: Schematic diagram of focal adhesions and hemidesmosomes. Both are anchored in the basement membrane and the dermis through Laminin and anchoring fibrils. In focal adhesions, $\alpha_3\beta_1$ integrin serves as a laminin receptor, and intracellularly β_1 integrin is connected to the actin filaments through Migfilin, Kindlin and Talin. Hemidesmosomes are connected by $\alpha_6\beta_4$ integrin to BP230 and plectin, which bridge to the kertain filaments, to provide strong adhesion of the cells to the basement membrane and dermis.

1.1.1.4 Cell-cell adhesion

In order for the skin to provide a barrier and protective function, epidermal cells need to be tightly connected to each other through complex junctions (Figure 1). In metabolically active layers, adherens junctions and desmosomes accomplish the formation of an essential sheet.

Adherens junctions consist of the transmembrane protein E-cadherin which is connected to the E-cadherin of the neighboring cells. E-cadherin is connected intracellularly to two proteins, ß-catenin and p120-catenin. ß-catenin recruits α-catenin, which directly binds to the actin filaments of the cell, whereas p120-catenin counteracts cadherin endocytosis and degradation (Perez-Moreno and Fuchs, 2006; Simpson et al., 2011).

Desmosomes are composed of transmembrane desmosomal cadherins, desmocollin and desmoglein, that bridge the gap between neighboring cells. The cytoplasmic tails of these cadherins are bound to plakoglobin, a member of the catenin family that mediates the association between desmosomal cadherins and desmoplakin, the major component of desmosomes. As already mentioned, desmoplakin is N-terminally connected to desmocollin and desmoglein via plakoglobin. The C-terminus of desmoplakin links the transmembrane part of desmosomes and the keratin intermediate filaments, thereby ensuring a strong binding to adjacent cells (Garrod, 1993; Simpson et al., 2011).

1.1.1.5 Stem cells of the interfollicular epidermis

The homeostasis of the epidermis and its appendages is ensured by stem cells, which contribute to the maintenance and repair of the interfollicular epidermis, the hair follicles and the sebaceous glands. These stem cells are characterized by their ability to self-renew and also to give rise to differentiated cells. It is known that stem cells exist in the interfollicular epidermis, and that these epidermal stem cells reside in the basal layer of the epidermis. It was shown that the continuous replacement of terminally differentiated cells is mediated by the presence of so called epidermal proliferation units (EPUs) that are distributed all over the interfollicular epidermis. The EPUs are organized in stacks of cells with a hexagonal surface area on top of 10-11 tightly packed basal cells. It was hypothesized that one EPU harbors one epidermal stem cell and 9-10 transit amplifying (TA) cells, which divide for a few times before differentiating (Potten, 1974, 1981). In contrast, recent studies demonstrated that the basal layer contains only one type of progenitor (named committed progenitors), which choose randomly between self-renewal and differentiation and that these cells have unlimited proliferation capacity (Clayton et al., 2007). Further studies questioned the existence of EPCs and postulated that proliferation of committed progenitors may be achieved simply by contact inhibition, when a nearby postmitotic cell delaminates from the basal layer. This would enable the epidermis to react to the demand for differentiated cells (Doupé et al., 2010).

Furthermore, it was long believed that basal cells divide symmetrically, but recent studies show that basal cells also divide asymmetrically giving rise to one committed cell and one proliferative basal stem cell (Lechler and Fuchs, 2005). Important factors, and possible markers during asymmetrical division are ß1 integrin and α-catenin which both play a role in cell-cell adhesion or cell adhesion to the basement membrane. Loss of function experiments showed that both factors are essential for a proper spindle orientation. Moreover, it was shown that basal cells with the highest ß1 integrin level have the highest proliferative and attachment potential, whereas the cells with lower ß1 level detach and terminally differentiate

(Jones and Watt, 1993). The vast majority of these divisions show a perpendicular mitotic spindle orientation giving rise to two cells persisting in the basal layer. The remaining divisions show a planar spindle orientation with one basal stem cell that resides at the basal layer and one committed suprabasal cell.

1.1.2 Molecular pathways involved in keratinocyte terminal differentiation

1.1.2.1 P63

During the differentiation and migration process of keratinocytes in the epidermis, the first transcription factor specifically expressed in this process is p63. It belongs to the p53 tumor suppressor gene family (Kaghad et al., 1997). The two major p63 isoforms comprise 16 exons and are expressed from two different promoters. The two major isoforms are TAp63 which has an N-terminal transactivator domain, and ΔNp63 which lacks this domain. Alternative splicing of these major isoforms at the C-terminus generates further isoforms named α, ß, γ, and δ. The premature transcriptional termination in exon 10 lead to an additional ε-isoform (Mangiulli et al., 2009). Gain and loss-of function studies revealed that p63 plays an important role in the maintenance of the proliferative potential of basal cells, as well as for the initiation of stratification (Koster et al., 2004b). Furthermore, it is highly expressed in basal cells. The ΔNp63 isoforms are the predominant isoforms in the adult epidermis and have a dominant-negative effect on TAp63 isoforms (Yang et al., 1998). ΔNp63α favors cell proliferation through binding to the promoters of $p21^{WAF/Cip1}$ and 14-3-3σ (member of the 14-3-3 family of intracellular signaling proteins), thus inhibiting their transcription. The important role of p63 becomes apparent in mice lacking p63, which exhibit major defects in all stratified epithelia and die immediately after birth due to a missing protective barrier (Koster and Roop, 2007; Mills et al., 1999; Yang et al., 1999). The detailed role of the different p63 isoforms was unclear for a long time, and it was not known whether the predominant ΔNp63α or the TAp63α isoform regulates the commitment to stratification or the self-renewal potential. The most recent studies showed that $p63^{-/-}$ cells fail to express keratin 5 and keratin 14 as well as differentiation markers keratin 1 and loricrin. In contrast, these cells expressed keratin 18, which is normally expressed in adult single layered epithelia and during embryonic epithelial development prior to stratification. This fact lead to the suggestion, that p63 is essential for the switch from keratin 8 and 18 to keratin 5 and 14. Furthermore, gain-of-function experiments in cells which never express p63 or keratins revealed that only the TAp63α isoform was able to induce keratin 14 expression, whereas ΔNp63α could not. It seems that the switch in expression from TAp63 isoforms to ΔNp63 isoform is required to counterbalance the inhibitory effect of TAp63α on terminal differentiation and to allow keratinocytes to terminally differentiate (Koster and Roop, 2004).

1.1.2.2 Notch

One of the major signaling pathways which is crucial during the early commitment of epidermal differentiation is the canonical Notch pathway. Notch is a cell surface receptor and is activated upon binding to its ligands, which are expressed by neighboring cells. Mice and humans have four Notch homologues and various ligands of the Delta and Jagged family. Notch receptors and ligands are expressed in the basal and suprabasal (spinous and

granular) layers (Watt et al., 2008). The binding of Notch ligands to the receptor results in the cleavage of the intracellular Notch domain (NICD) and its translocation into the nucleus where it forms an active transcriptional complex with the recombinant binding protein suppressor of hairless (RBP-Jκ) to build a bipartite transcription factor (Blanpain and Fuchs, 2006; Rangarajan et al., 2001; Watt et al., 2008). Notch turns this suppressor into an activator of Notch target genes, including HES and HEY family genes. These transcriptional changes are required for the detachment of basal cells from the basement membrane and the commitment to spinous differentiation (Blanpain and Fuchs, 2006; Rangarajan et al., 2001). In vitro studies revealed that the addition of the Notch ligand JAG-1 to keratinocyte cultures resulted in Notch activation and subsequently, during the formation of the cornified envelope, in an induction of loricrin, involucrin, and the peroxisome proliferation activated receptor γ (PPAR γ) expression (Nickoloff et al., 2002). Furthermore, Notch enhances the levels of nuclear factor kappa of activated B-cells (NF-κB) (Guan et al., 1996). These studies indicated that NF-κB works in concert with Notch during epidermal development. Furthermore, RBP-Jκ was shown to bind to the promoter of the cyclin-dependent kinase inhibitor 1 ($p21^{WAF/Cip1}$), a well-known cell cycle regulator. This indicates that $p21^{WAF/Cip1}$ is a direct target of Notch signaling (Rangarajan et al., 2001), which not only influences the commitment of basal cells to differentiation but also the withdrawal from the cell cycle.

1.1.2.3 NF-κB and IKK

The nuclear factor kappa of activated B-cells (NF-κB) transcription factor is a dimer composed of combinations of structurally related proteins, including p50, p52, p65, c-Rel and RelB (Verma et al., 1995). In resting cells NF-κB is inactive and located in the cytoplasm, where it is bound to the NF-κB inhibitory proteins α and ß (IκBα and IκBß). Upon stimulation by tumor necrosis factor α (TNFα), interleukin-1 α (IL-1α), UV irradiation or infection, IκBs are phosphorylated by IκB kinases leading to their degradation and the translocation of NF-κB into the nucleus (Seitz et al., 1998), where the activated form regulates the transcription of target genes. In mammalian skin, NF-κB activity is mediated in part by p50 and p65 subunits (Qin et al., 1999). In the basal layer NF-κB is found to persist in its inactive, bound form in the cytoplasm, whereas suprabasal cells show a nuclear localization of NF-κB. The fact that NF-κB becomes activated in committed cells that withdraw from the cell cycle led to the conclusion, that NF-κB plays a role in the switch from proliferation to growth arrest (Seitz et al., 1998). Similar to p63 and Notch, NF-κB induces $p21^{WAF/Cip1}$ thus inducing growth arrest in cells, rather than inducing the expression of differentiation markers (Seitz et al., 2000). Besides this, it opposes the proliferative activity of TNFR1/JNK during development, demonstrating an orchestrated network of different pathways that are involved in the proliferation/differentiation switch. In contrast to its role as an NF-κB activator, the inhibitor of kappa B kinase α (IKKα) also promotes epidermal differentiation independently of NF-κB function. IKK is an enzyme complex composed of three polypeptides IKKα, ß and γ, where IKKβ represents the catalytic and IKKγ the regulatory subunit. It was shown that the ablation of IKKα results in highly proliferative basal and spinous layers and that granular and cornified layers fail to form (Hu et al., 2001). Furthermore, mutation of the kinase domain of IKKα demonstrated that the kinase activity was not responsible for the induction of differentiation markers like loricrin or filaggrin. It is still not known how IKKα induces the expression of differentiation markers, nor if other proteins are involved in the interaction (Hu et al., 2001).

1.1.2.4 AP-1

The activator protein 1 (AP-1) transcription complex is composed of one protein of the Jun protein family that forms a homodimer with another Jun protein or a heterodimer with a member of the Fos-protein family (Hess et al., 2004). The AP-1 proteins share a conserved DNA-binding domain combined with a basic leucin zipper region (bZIP domain), which is responsible for the dimerization and stability of the dimer. In vitro experiments revealed that the knock-down of c-Jun results in a decreased expression of epidermal growth factor receptor (EGFR) and its ligand HB-EGF and the cells proliferate less and differentiate faster (Zenz et al., 2003). Furthermore, it was shown that AP-1 is involved in a paracrine loop where IL-1 secreted by keratinocytes induces c-Jun in dermal fibroblasts which then produce keratinocyte growth factor (KGF) and granulocyte-macrophage colony stimulating factor (GM-CSF). This process leads to the stimulation of cell growth and proliferation of keratinocytes (Maas-Szabowski et al., 2001; Szabowski et al., 2000). Further studies revealed the involvement of AP-1 in the expression of loricrin (DiSepio et al., 1995), involucrin (Takahashi and Iizuka, 1993) and TG1 (Liew and Yamanishi, 1992), which can be explained by the presence of conserved AP-1 binding sites in the promoters of many differentiation specific genes.

1.1.2.5 AP-2

AP-2 consists of five different isoforms AP-2α-ε; encoded by five different genes (Hilger-Eversheim et al., 2000). AP-2 binding sites are found in the promoter regions of several keratinocyte differentiation markers, including TG1 (Mariniello et al., 1995), involucrin (Kachinskas et al., 1994), $p21^{WAF/Cip1}$ (Zeng et al., 1997), as well as K5 and K14 (Byrne et al., 1994; Leask et al., 1991). Even though *Ap-2α*$^{-/-}$ mice have a normal phenotype, they show increased K1 levels (Maytin et al., 1999). The exact role of AP-2 is still unclear, but the existence of AP-2 binding sites in epidermal genes suggests a necessary, but not sufficient, involvement of AP-2 in epidermal gene regulation (Leask et al., 1991).

1.1.2.6 BMPs

Bone morphogenic proteins (BMPs) are the largest family of secreted molecules of the transforming growth factor (TGF)-ß superfamily. They have versatile functions including the regulation of development, proliferation, differentiation and apoptosis in various organs (Botchkarev, 2013; Li et al., 2003; Mishina, 2003).

BMP signaling is mediated upon BMP binding to its receptors BMPR-I and BMPR-II. While the individual type I and type II receptors display low affinity to BMPs, the heterotetrameric complex of type I and type II receptors shows high-affinity binding to BMPs. Binding of BMP to its receptors leads to the phosphorylation of the intracellular type I receptor domain by type II receptor kinase, resulting in the transmission of an extracellular signal into the interior of the cell. BMP activates two intracellular signaling pathways upon binding to its receptor complex: The “canonical” signaling pathway that includes the Smad family of proteins and the “noncanonical” BMP-mitogen-activated protein kinase (MAPK) pathway.

In the “canonical” pathway, Smad1, Smad5 and Smad8 are activated through receptor type I mediated phosphorylation (now termed receptor-activated Smad, or R-Smad),

assemble with Smad4 (co-Smad) and translocate into the nucleus where they regulate BMP target genes. Other Smads, like Smad6 and Smad7 (inhibitory Smads, I-Smads) antagonize the phosphorylation of Smad1, Smad5 or Smad8, probably through competition with Smad4 for binding to Smad1 (Hata et al., 1998). In the nucleus the Smad complex binds to co-activators or co-repressors and thus activates or inhibits target genes (Kusanagi et al., 2000; Li et al., 2001), including Dlx-3, keratin 1 or involucrin (D'Souza et al., 2001; McDonnell et al., 2001; Park and Morasso, 2002). To date, Smad proteins are the only direct substrates which mediate gene response to the TGF-ß family (Massagué, 2012).

The "noncanonical" pathway is initiated through the activated BMPR complex, interacting intracellularly with the adaptor protein XIAP, which links TGF-ß activated kinase 1 binding protein (TAB1) to the BMPR complex, and TAB1 in turn activates TGF-ß activated kinase 1 (TAK1) (Yamaguchi et al., 1999). TAK1 belongs to the MAPK kinase kinase family and is activated upon TGF-ß1 and BMP4 stimulation (Botchkarev et al., 2002). Once activated TAK1 induces distantly MAPK family member Nemo-like kinase (NLK) which then inhibits the phosphorylation of TCF/Lef1 transcription factors and downregulates Wnt/ß-catenin-dependent transcription (Ishitani et al., 1999). Furthermore, Smad6 was shown to bind and inhibit TAK1, suggesting a link between the canonical and noncanonical pathways (Kimura et al., 2000).

In the embryonic murine epidermis BMP7 is present in the basal layer, whereas BMP6 is located in the suprabasal layer (Lyons et al., 1989; Takahashi and Ikeda, 1996; Wall et al., 1993). The BMP receptor BMPR-IA is largely restricted to proliferating cells in the basal layer. In contrast, BMPR-IB is associated with differentiation and expressed in subrabasal layers (Botchkarev et al., 1999; Panchision and Pickel, 2001). In addition, Smad1, 5 and 6 are also expressed in the developing murine epidermis, suggesting a strong role during development (Dick et al., 1998; Flanders et al., 2001). In the adult human epidermis, BMPR-IA, BMPR-IB and BMPR-II are restricted to suprabasal keratinocytes, whereas no BMP receptors are seen in basal cells (Hwang et al., 2001). Also BMP2 and BMP6 were shown to play a role in the postnatal murine epidermis. BMP6 stimulates K1 and involucrin (D'Souza et al., 2001) expression through the canonical pathway and BMP activates Dlx-3 transcription factor by recruiting Smad1 and Smad4 (McDonnell et al., 2001; Park and Morasso, 2002). Even though not all BMP targets are known yet, it has an important influence on the development, differentiation and proliferation in the epidermis.

1.1.2.7 C/EBP

The CCAAT/enhancer binding protein (C/EBP) family of transcription factors is characterized by a conserved basic-leucine zipper (bZIP) domain at the C-terminus that binds to CCAAT-motifs in the regulatory region of target genes. This domain allows C/EBPs to form homo- and heterodimers with other family members and with other unrelated transcription factors. The family comprises six members (C/EBPα-C/EBPζ) (Ramji and Foka, 2002) and is classified into the class of leucin zipper transcription factors. C/EBPs were suggested to play a role in controlling cell proliferation and differentiation, since levels of C/EBPα and C/EBPß increased significantly in response to calcium-induced differentiation (Maytin and Habener, 1998). The expression patterns of C/EBPs vary within the epidermis; C/EBPα is expressed in the upper suprabasal layers, whereas C/EBPß is already detectable in low amounts in the cytoplasm of basal cells and in the nucleus of suprabasal cells (Maytin and Habener, 1998; Oh and Smart, 1998). Both were shown to be able to bind to the K10 promoter and activate the expression of K10. C/EBPα and C/EBPß are good examples for

the complex network driving keratinocyte differentiation, since their expression is also dependent on AP-2. AP-2 and C/EBPß are both present in the basal layer, where AP-2 represses the expression of C/EBPα. In upper suprabasal layers, the expression of AP-2 is extinguished and C/EBPß is replaced by C/EBPα (Maytin et al., 1999).

1.1.2.8 MAPK/ERK-Pathway

The mitogen-activated protein kinase pathway (MAPK) is a critical regulator for the balance between proliferation and differentiation in keratinocytes (Scholl et al., 2007). During normal homeostasis the pathway is mediated by ligand binding to tyrosin kinase receptors, such as epidermal growth factor receptor (EGFR) or by basal integrins, and is negatively regulated by adhesion molecules. It was shown that reduced EGF signaling resulted in lower proliferation rates, whereas the constitutive EGFR activation increased proliferation (Janes and Watt, 2006). The pathway is initiated upon ligand binding, which activates the tyrosine kinase activity of the cytoplasmic domain of EGFR and tyrosine residues become phosphorylated. This leads to the binding of growth factor receptor-bound protein 2 (Grb2) to the phosphotyrosine residues of EGFR. Grb2 in turn binds SOS1 (son of sevenless; family of guanine nucleotide exchange factors (GEFs)), which once activated, promotes the removal of GDP from Ras. This allows Ras to bind GTP and subsequently activate the kinase activity of Raf. Activated Raf can phosphorylate and thus initiate Mek, which then in a last step phosphorylates and activates extracellular signal-regulated kinases (Erk). Erk regulates the activity of various transcription factors, including c-Myc, c-Fos genes and transcription factors that are important for cell cycle and proliferation.

Many studies which dealt with the role of the MAPK/Erk pathway in keratinocytes investigated the role of Ras during development and differentiation. It was shown that constitutive expression of Ras in the basal layer leads to hyperproliferation and impaired differentiation. The induced expression of Ras in suprabasal layers led to a milder response with focal hyperplasia (Dajee et al., 2002). These data indicate a more influential role of Ras in basal keratinocytes in maintaining cells in a proliferative, undifferentiated state.

Furthermore, Mek1/Mek2 double knock-out mice die 24h after birth due to dehydration and loss of barrier function. The conditional deletion of Mek1 and Mek2 in adulthood resulted in tissue death, indicating that the MAPK/Erk pathway has an additional effect on cell viability (Scholl et al., 2007). Taken together, these data demonstrate, that the MAPK/Erk-pathway plays a central role for the viability and proliferation of keratinocytes.

1.1.2.9 Hox genes

The homeobox (Hox) gene family of transcription factors consists of various crucial regulators of axial patterning and organogenesis. All Hox genes have a conserved binding sequence, named homeodomain or homeobox, and are present in vertebrates and invertebrates. To date, 39 Hox genes were identified in vertebrates and classified in four groups A-D. About 30 Hox genes were found to be expressed in fetal and/or adult human skin (Detmer et al., 1993; Li et al., 2002). In the embryonic epidermis Hox gene expression is limited to the basal layer, whereas in mature epidermis it is significantly down regulated and restricted to the granular layer (Mack et al., 2005). Hox gene function varies depending on the gene, the environment and developmental stage of the organism. They can either

promote proliferation and suppress differentiation or prevent proliferation and allow differentiation. HoxA7, for instance, is activated in proliferating cells and down-regulated in committed cells. It was shown that HoxA7 downregulates TG1, thus lower HoxA7 levels in upper epidermal layers would favor the cross-linking by TG1, which is essential for differentiation (La Celle and Polakowska, 2001). In contrast, HoxB13 is upregulated in committed keratinocytes and seems to have an ant-proliferative function (Economides et al., 2003; Kömüves et al., 2003).

Recent studies revealed that a few genes from the group 13 of Hox proteins interact with Smad proteins (Williams et al., 2005).

Taken together, these data demonstrate that Hox genes are essential regulators of development, proliferation and differentiation in many different tissues.

1.1.3 The skin appendages

1.1.3.1 The hair follicle

The hair follicle morphogenesis begins with an aggregation and invagination of epidermal cells to form the follicular placode. This formation is induced by yet unknown signals from the underlying mesenchyme as well as from neighboring epidermal cells, but ß-catenin is believed to be one of the effectors of this signal (Millar, 2002). The placode signals back to induce condensation in the underlying dermis, and this aggregation of cells will later become the dermal papilla. Initiators of this process are cytokines, receptors and signaling molecules known as placode promoters and placode inhibitors (Millar, 2002). The phase of downward growing through the dermis into the subcutaneous fat is termed elongation phase or anagen phase. The leading front of the elongating hair follicle are the highly proliferative matrix cells, which surround the hair follicle. After elongation is complete, the matrix cells at the bulb region continue to proliferate to give rise to differentiated cells that migrate upwards to build the inner root sheath (IRS) and the hair shaft (Legué and Nicolas, 2005). The IRS cell specification is regulated by BMP and Notch signaling and by the action of transcription factors like CDP and GATA3 (Blanpain and Fuchs, 2006). Furthermore, the IRS acts as a channel to lead the hair shaft to the epidermal surface. The outer root sheath (ORS) surrounds the hair follicle, is continuous with the basal layer of the epidermis and contains the hair bulge below the sebaceous gland, the stem-cell containing niche of the hair follicle. Studies used nucleotide labels in pulse-chase experiments to show that slow-cycling label-retaining cells reside within the bulge (Blanpain and Fuchs, 2006; Cotsarelis et al., 1990; Taylor et al., 2000). Upon activation these stem cells exit the bulge and start to proliferate to give rise to a new hair follicle, populate the epidermis during wound healing and maintain the sebaceous gland (Fuchs and Horsley, 2008). Increased BMP signaling was detected in bulge cells, suggesting a role for BMP in the stem cell control (Blanpain et al., 2004; Morris et al., 2004; Tumbar et al., 2004).

The phase of hair follicle initiation is followed by a degenerative phase or catagen phase. The stop of hair proliferation, involution of the hair and apoptosis of matrix cells accompanied by the loss of two thirds of the hair follicle are characteristics of the catagen phase. The catagen phase ends when an epidermal strand guides the dermal papilla upwards to reach the bulge region. The hair follicle enters now a restoring (telogen) phase during which the bulge anchors the old hair and rests before entering the next hair cycle (anagen phase). The new cycle is initiated by signals between the dermal papilla and the overlying epithelium of

the hair follicle (Davidson and Hardy, 1952; Fuchs et al., 2001). Another important pathway in hair follicle morphogenesis is the Wnt-signaling pathway; especially the nuclear ß-catenin/lymphoid enhancer binding factor 1 (Lef1)/T cell factor 3 (TCF3) complex, as well as BMP and FGF family members are also important regulators (Fuchs et al., 2001).

In postnatal life, the upper portion of the hair follicle and the dermal papilla in the bulb persist, whereas the remaining parts cycle through anagen, catagen and telogen phases (Fuchs et al., 2001).

1.1.3.2 The sebaceous gland

The development of the sebaceous gland (SG) takes place at the same time as the hair follicle morphogenesis. The specialized cells of the SG are lipogenic cells, termed sebocytes, which produce lipids and sebum. Sebum consists of lipids, and through its oily substance it maintains the water resistance of the hair and the skin surface. Terminally differentiated sebocytes release the sebum into a duct and onto the skins surface. Even though the stem cells from the bulge of the hair follicle have the capacity to differentiate into sebocytes, (Blanpain et al., 2004; Morris et al., 2004) pulse-chase experiments identified a pool of slow-cycling progenitor cells in the gland, which maintains the constant turnover of mature sebocytes (Braun et al., 2003; Ghazizadeh and Taichman, 2001). Furthermore, it was shown that these cells are characterized by the expression of the transcription factor Blimp1 (Horsley et al., 2006).

The fate of sebocytes is a result of the inhibition of Wnt signaling. The active ß-catenin/Lef1/Tcf3 complex induces the ectoderm to generate hair follicle, but if this complex is inhibited the cells become sebocytes (Han et al., 2006; Niemann et al., 2003; Takeda et al., 2006). In contrast, hedgehog signaling induces sebocyte development, even ectopically after induction (Allen et al., 2003). Taken together, inhibition of Wnt signaling as well as activation of hedgehog-signaling are both required for SG lineage specification.

1.1.4 Non-keratinocyte cell types of the epidermis

1.1.4.1 Merkel cells

Merkel cells are found in the basal layer of the epidermis, either independently but mostly in clusters (touch domes) (Sidhu et al., 2005). They function as sensory mechanoreceptors and associate with sensory axons to form Merkel cell-neurit complexes.

Merkel cells are the pressure sensors of the skin. Upon deformation by pressure Merkel cells release a neurotransmitter, which activates neurons that are located at the basement membrane. Furthermore, they are considered to be responsible for form and texture perception (Johnson, 2001). The developmental origin of Merkel cells is not completely resolved. Some studies describe a neural crest origin (Le Douarin, 1980; Halata et al., 2003) but there is also good evidence that these cells may have an epidermal origin (Loomis, 2001).

1.1.4.2 Melanocytes

Melanocytes are pigmented, dendritic cells located mostly in the basal layer of the epidermis. During development, melanocyte precursors termed melanoblasts arise from the neural crest and migrate through the dermis and the basement membrane to reach the epidermis. The density of melanocytes varies in different body regions with around one melanocyte per five to ten keratinocytes (Fitzpatrick and Breathnach, 1963).

Melanocytes synthesize melanin in vesicles named melanosomes (Seiji and Fitzpatrick, 1961). These vesicles are delivered to keratinocytes through cytoplasmic processes, to sustain a permanent passage of melanosomes (Ando et al., 2011). The melanosomes are then phagocytosed by the keratinocytes, which results in the aggregation of melanin around the nucleus to protect the nuclear DNA from UV irradiation (Montagna and Carlisle, 1991).

1.1.4.3 Langerhans cells

Langerhans cells originate in the bone marrow and comprise approximately 5% of all epidermal cells. They migrate into the epidermis and reside locally for extended periods with the highest concentration in the spinous layer (Jakob et al., 2001). Their numerous dendrites allow for antigen sampling of nearly the entire surface of the skin. Langerhans cells have an antigen-presenting function and represent a critical immunological barrier to the external environment. Upon inflammation, langerhans cells are mobilized by proinflammatory cytokines like TNF-α and interleucin 1 (IL-1) and migrate rapidly through the lymphatic vessels to the draining lymph nodes (Romani et al., 2001; Stoitzner et al., 2002). These cells are replaced by blood-borne precursors that migrate into the epidermis. Because of their elevated E-cadherin level, langerhans cells are thought to be anchored in the epidermis by the formation of junctions with keratinocytes. Besides E-cadherin, also TGF-ß also might be responsible for the retention of langerhans cells in the epidermis (Geissmann et al., 1999; Riedl et al., 2000).

1.1.5 The embryonic development of the epidermis

The embryonic development of a mammalian organism begins with the fertilization of the oocyte in the ampulla of the oviduct. Once fertilized, the zygote is guided by the cilia in the oviduct towards the uterus. During this migration the zygote begins to cleave. At the 8-cell stage, the zygote is now called blastomere, cell adhesion proteins, like E-cadherin, are expressed and the blastomere becomes a compact ball of cells. After additional cleavages, the 8-cell blastomere becomes a 16-cell morula, which consists of internal cells that are encased by external cells (Barlow et al., 1972). The surrounding external cells give rise to the trophoblast, whereas the inner portion of cells will become the inner cell mass (ICM). The trophoblast cells will form the tissue of the chorion, the extraembryonic membranes and parts of the placenta, whereas the ICM will give rise to the embryo. The segregation into ICM and trophoblast is the first differentiation event that takes place. Upon ongoing cleavages the trophoblast cells secrete fluids into the morula that generate a cavity, the blastocoel. The two cell types become more and more separated as the blastocoel expands, and the morula is now called the blastocyst. During migration the embryo is surrounded by a glycoprotein membrane, the zona pellucida, which prevents the implantation in the oviduct and a tubal

pregnancy. Once the blastocyst has reached the uterus it escapes from the zona pellucida and implants in the uterine wall (O'Sullivan et al., 2001; Perona and Wassarman, 1986). After that, the blastocyst adheres to the endometrium, the epithelial surface of the uterus that has been prepared for implantation by hormonal stimulation and implanting takes place (Ramathal et al., 2011; Wang and Dey, 2006).

The ICM now forms two cell layers, the lower primitive endoderm and the upper epiblast. The primitive endoderm gives rise to extraembryonal structures, such as the yolk sac and is responsible for determining the side of the gastrulation, regulating cell movements in the epiblast and promotion of the maturation of blood cells (Stern and Downs, 2012). The epiblast gives rise to the embryo. Fibroblast growth factor (FGF) signaling within the ICM defines the final fate of either epiblast or primitive endoderm (Yamanaka et al., 2010).

Epiblast and the primitive endoderm now form a structure that is named the bilaminar germ disc.

The next step in development is the gastrulation, a process which proceeds similarly in birds, reptiles and mammals and which is initiated by the formation of a characteristic structure called primitive streak. The primitive streak extends through the midline of the bilaminar germ disc and creates the left-right and anterior-posterior body axes. It is formed by epiblast cells moving towards the midline of the embryo. Subsequently, these cells invaginate and migrate between the epiblast and the primitive endoderm which results in the formation of the primitive groove. The cells that invaginate form the endoderm and mesoderm. During this process the cells undergo epithelial-mesenchymal transition and decrease E-cadherin expression to loosen the cell-cell contacts (Burdsal et al., 1993). Cells of the primitive streak are capable of synthesizing FGF and responding to FGF signals, and these signals seem to be responsible for cell migration and specification (Ciruna and Rossant, 2001; Sun et al., 1999).

The presumptive ectoderm is located anterior and lateral to the fully extended primitive streak. At the end of the primitive streak the neural plate is formed by the thickening of the ectodermal tissue. The neural plate invaginates to form the neural tube, which will later become the central nervous system. The margins of the neural plate break away from the neural plate and give rise to the neural crest which is the origin of the peripheral nervous system and of pigmented cells (melanocytes).

The process that forms the three ectodermal compartments is called neurulation and relies on differential BMP expression. Whereas the specification into the epidermis requires high levels of BMP, cells with a very low level become neural plate and intermediate BMP expression favors the formation of neural crest (Archer et al., 2011).

The epidermis of the embryo starts as a single layer but soon becomes a two-layered structure. The upper layer is termed periderm and represents a temporary cover to protect the embryo from dehydration. The inner layer is the basal layer and contains epidermal stem cells that divide asymmetrically to give rise to one stem cell and one differentiating daughter cell. The cells of the embryonic basal layer differ from the cells of the adult basal layer in that they express of keratin 8 and keratin 18, which are only expressed in adult single layered epithelia and in embryonic epidermis. The daughter cells leave the basal layer, migrate upwards and differentiate. These younger cells push older cells to the border of the skin thus generating a stratified epithelium consisting of four major layers (see paragraph "1.1.1 The skins architecture and homeostasis"). Important factors stimulating the development of the epidermis are BMPs. BMP signaling specifies the epidermis lineage by blocking neural fate and initiates epidermal production by inducing the expression of p63 transcription factor in the basal layer (see paragraph "1.1.2 Molecular pathways involved in keratinocyte terminal differentiation")(Truong and Khavari, 2007).

1.2 Induced pluripotent stem cells

1.2.1 History and discovery of induced pluripotency

In 1981 Martin John Evans and Matthew Kaufman isolated embryonic stem cells (ESCs) from a mouse blastocyst, which was a major breakthrough in the field of biology (Evans and Kaufman, 1981). In the same year, Martin was able to establish a pluripotent stem cell line and culture these cells in a teratocarcinoma conditioned medium (Martin, 1981).

Pluripotent cells have the ability to differentiate into any cell type of the mammalian body including the germ line and they can undergo symmetrical self-renewal to give rise to identical daughter cells. These capacities make them a powerful tool for studying developmental processes in healthy organisms. Furthermore, disease specific mutations carried by the stem cells allow the investigation into the development of diseases.

Thirty years after the first isolation of mouse embryonic stem cells, Thomson and colleagues succeeded in isolating and culturing primate ESCs from Rhesus monkey (Thomson et al., 1995) and only three years later they isolated the first human ESCs (Thomson, 1998). The establishment of human ESCs (hESCs) not only stirred up hopes for various therapeutic applications but also raised ethical concerns. The opinions are divided as to when the embryo has a full moral status and from what point of time on it can be defined as a human being. For example, is there a so called cut-off point at 14 days after fertilization when the nervous system begins to develop? The regulations for using hESCs differ from country to country and make it difficult to use these cells. Therefore, alternative sources of pluripotent cells were examined and the question whether adult somatic cells are restricted to their fate was raised.

Briggs and King could show by transferring nuclei from blastocyst into enucleated frog oocytes, which gave rise to swimming tadpoles that genes are not lost, or permanently silenced, after the cell fate was determined (Briggs and King, 1952). Furthermore, Gurdon transplanted a nucleus from a fully differentiated somatic frog cell into an enucleated egg that then gave rise to a living organism. He demonstrated that somatic cloning derived ECSs provide a new source of pluripotent cells, which are genetically identical to the host (Gurdon, 1962).

In 2006 Kazutoshi Takahashi and Shinya Yamanaka found out that the ectopic overexpression of defined factors reprogrammed mouse adult somatic cells into pluripotent stem cell like cells (Takahashi and Yamanaka, 2006) that show the same characteristics like embryonic stem cells. With this finding these authors created a great deal of enthusiasm in the scientific community and Yamanaka as well as Gurdon were honored with “The Nobel Prize in Physiology or Medicine in 2012 for the discovery that mature cells can be reprogrammed to become pluripotent” (http://www.nobelprize.org/nobel_prizes/medicine/laureates/2012/press.html).

Takahashi and Yamanaka tested a panel of transcription factors and ectopically overexpressed them in mouse somatic cells. They demonstrated that the overexpression of four factors, octamer binding protein 4 (Oct4 or POU5F1), krueppel-like factor 4 (Klf4), sex determining region Y (SRY) box 2 (Sox2) and c-Myc resulted in the reprogramming into a pluripotent state and termed these cells induced pluripotent stem cells (iPSCs) (Takahashi and Yamanaka, 2006). IPS cells show comparable properties to embryonic stem cells, including self-renewal and the potential to differentiate into any cell type of the body. Since the first reprogramming experiment, many other adult cell types of different organisms have been reprogrammed (Galach and Utikal, 2011).

IPSCs offer the remarkable potential to study and manipulate the development of not only a cell type but also whole organs and open new possibilities for studying diseases and their treatment.

1.2.2 Methods for generating induced pluripotent stem cells

To date, many different methods for the reprogramming of adult cells into a pluripotent state have been established. The first approaches used retroviral transduction (Okita et al., 2007; Takahashi and Yamanaka, 2006; Wernig et al., 2007). Retroviral vectors integrate stably into the genome and are usually silenced gradually during reprogramming. The silencing of the transgenes is very important for the generation of stable iPSCs. An iPSC line will only be considered as stably reprogrammed, when the endogenous pluripotency network is upregulated and the transgene has been silenced (Stadtfeld et al., 2008a). Regarding the fact that silenced genes can be reactivated and that each of the reprogramming factors is a potential oncogene makes stable silencing even more important (Friedmann-Morvinski and Verma, 2014).

Even though the transduction efficiency of retroviruses is about 90%, the reprogramming efficiency remains rather low, about 0.01% to 0.1% in human fibroblasts (Stadtfeld and Hochedlinger, 2010).

A slightly higher transduction efficiency is achieved by using lentiviral vectors (Blelloch et al., 2007; Yu et al., 2007), since it allows the transduction of dividing and non-dividing cells. The availability of inducible lentiviral vectors (Tet-ON system) offered the possibility of controlling the transgene expression (Stadtfeld et al., 2008a; Wernig et al., 2008). The use of recombinase-excisable systems enables even the removal of the transgene, but after excision short vector sequences (loxP sites) remain in the host genome. The efficiency of viral vectors can be accelerated when using one single vector carrying all four reprogramming factors in a polycistronic cassette, instead of transducing the cells with four single factor expressing vectors (Somers et al., 2010).

One drawback of lenti- or retroviral transduction is the random distribution of transgenes in the host genome, which could lead to alterations of other genes, for example, tumor suppressor genes. Even though excisable or inducible vectors have solved many safety issues, iPSCs generated by using integrating viral vectors are still potentially harmful especially when they are used for therapeutic application.

Considering that retro- or lentiviral vectors are potentially harmful many researchers engage in finding safer methods for the generation of induced pluripotent stem cells.

Adenoviral vectors offer another possibility for the delivery of the reprogramming factors into the cell, without the risk of genomic integration, by transient expression (Okita et al., 2008; Stadtfeld et al., 2008b; Zhou and Freed, 2009). Even though adenoviral vectors display a safer method, the efficiency of generating iPSCs ranges between 0.0001% and 0.0018%. In contrast, Fusaki and colleagues recently reprogrammed human fibroblasts using F-protein deficient Sendai viral vectors, which transfer the reprogramming genes into the host cell and replicate in the form of negative-sense ssRNA in the cytoplasm (Fusaki et al., 2009). They could show that the efficiency of iPSC induction surpassed even that of retroviral transduction. A major drawback of utilizing Sendai virus for reprogramming is the constitutive replication of the viral vector, representing a challenge to isolate transgene free clones.

Since the first iPSCs were generated, many methods of reprogramming were developed. Besides the already mentioned viral-integrative and viral non-integrative methods, many non-viral delivery methods are also now available.

PiggyBac transposition, for instance, requires only the piggyBac transposons which carry the reprogramming factors (Woltjen et al., 2009). The transposons integrate into already existing sites in the genome and are flanked by inverted terminal repeats required for transposition. The open-reading frame of piggyBac transposons encodes a transposase, which is required to catalyze the insertion. After reprogramming the transgene can be removed by a transposase without leaving any residues in the host genome.

Further reprogramming methods are based on replicating or non-replicating episomal vectors. The oriP/Epstein-Barr nuclear antigen-1-based episomal vectors (oriP/EBNA1), which were derived from the Epstein-Barr virus, stably replicate extrachromosomally and can be subsequently removed from cells in the absence of drug selection (Yu et al., 2009). The replication of the oriP/EBNA1 vector is warranted through the cis-acting oriP element and the trans-acting EBNA1 gene. On the other hand, these vectors are very large (~12kb) and their size results in a very low efficiency of three to six colonies per million cells. In contrast to the very large oriP/EBNA1 vectors, minicircle vectors are much smaller (~3kb), non-integrating, non-replicating episomes (Jia et al., 2010). Minicircle vectors are supercoiled DNA molecules, which lack the origin of replication and the antibiotic resistance gene, that display a longer ectopic expression due to lower activation of exogenous DNA-silencing mechanisms.

Additionally, in order to completely avoid plasmids or viral vectors, synthetic mRNAs can be directly delivered into the host cells through serial transfection (Warren et al., 2010). Even though the mRNA delivery is simple and efficient, its introduction into the host cell results in a relatively high gene dosage of reprogramming factors and this entails an oncogenic risk due to genomic instability caused by high c-Myc levels.

Another way to avoid the introduction of exogenous genetic material is the direct delivery of proteins. To ensure the transduction into the host cell, proteins were fused with peptides, including HIV transactivator of transcription (Tat) or polyarginine (Zhou et al., 2009). A major drawback of this reprogramming method is its slow kinetics and the poor efficiency (0.001%). Furthermore, due to the extensive purification, it is technically challenging to produce the required amounts of protein and therefore difficult to reproduce this experiment.

Recently Anokye-Danso and colleagues have successfully reprogrammed mouse and human somatic cells using lentivirally delivered microRNAs (miRNA-302 cluster) (Anokye-Danso et al., 2011). In contrast Miyoshi and his group repeatedly transfected cells with a cocktail of seven miRNAs (Miyoshi et al., 2011).

In further reprogramming experiments, small molecules were used to replace one or more reprogramming factors or to facilitate the process of dedifferentiation. For example, somatic cells could either be reprogrammed with Sox2 and Oct4 when valproic acid was added to the reprogramming cocktail (Huangfu et al., 2008), or by adding the inhibitor of Mek/Erk pathway together with a glycogen synthase kinase 3 (GSK3) inhibitor, which accelerate the reprogramming of mouse cells (Silva and Smith, 2008).

1.2.3 Induced pluripotent stem cells for therapeutic purpose

Since the first reprogramming experiments many scientist have become interested in using these cells for therapeutic purpose. The iPSC technology offers the possibility of generating genetically matched pluripotent cell lines from patients with known, or suspected, diseases and to obtain an unlimited numbers of differentiated cell types from all major organs of interest. Previously, iPSCs were generated from patients with various diseases, some, but not all, exhibit certain disease properties. IPSCs were generated from patients with spinal

muscular atrophy (SMA) and during the *in vitro* differentiation, a loss of motor neurons was detected (Ebert et al., 2009). In another study, iPSCs derived from LEOPARD syndrome patients were differentiated *in vitro* into cardiomyocytes that had an enlarged cell body, possibly demonstrating the hypertrophic cardiomyopathy involved in this disease (Carvajal-Vergara et al., 2010). Most of these studies were performed with single patients or used hESC lines as controls, and it remains to be determined if these phenotypes are reproducible. Furthermore, these studies need to be repeated with large sets of genetically matched patients. Nevertheless, these first studies exemplify a proof of principle that disease modeling by using iPSC technology is feasible.

The major goal of using iPSCs for therapeutic purposes is not only to investigate the development of a disease but also to find new pathways or drugs that could affect the process of the disease. Thus, disease-specific iPSCs in a disease model *in vitro* would help to replace mouse models, which are not always comparable to the human disease phenotype. Furthermore, disease-specific iPSCs and differentiated iPSCs that display the disease phenotype could be used for high-throughput drug screens in order to find small chemicals that either induce the disease phenotype or prevent it. It is of great interest, if a disease phenotype can also be achieved from iPSCs for diseases that manifest later in life or are caused strongly by environmental factors.

Another milestone of iPSC technology in regenerative medicine would be the use of differentiated iPSCs for cell replacement therapy. To date, cell transplantation for tissue repair has just been realized in the haematopoietic system and the skin. Nevertheless, in many clinical trials, adult stem cells or even differentiated hESCs are used for transplantation therapy. For example, human neural stem cells are transplanted in patients with traumatic spinal cord injury, or human embryonic stem cell derived CD15+ Isl-1+ progenitors are transplanted in patients with severe heart failure.

Before the use of iPSC derived lineage-specific cells for cell-based therapies can be taken into consideration, some obstacles need to be overcome. Protocols need to be established that allow simple and effective differentiation and that yield high amounts of pure differentiated cells of a desired lineage. Indeed, fluorescent activated cell sorting, drug selection or marker isolation are first steps to overcome this problem. Not only the heterogeneity of the differentiated population remains a problem, also the maturation stages of generated cells, even in a homogenous population, can vary. Another problem remains the introduction of generated cells into the organism. Even though cell-based therapies are successful in the haematopoietic system, this may not apply to solid organs. Most solid organs display a complex architecture and are well balanced concerning their number of cells and the arrangement of cell types. It is unclear if the grafted cells can function in concert with the already existing cells. Many studies are still needed to understand the processes that determine a cell fate, the developmental processes in a specific cell type and the role of a cell within a tissue.

1.3 Differentiation of pluripotent cells into keratinocytes *in vitro*

The current treatment for patients with large burn injuries comprises the in vitro expansion of a patient's own keratinocytes to generate skin replacements. The drawback of this therapy is the 3-week delay that is needed to generate an adequate skin replacement. To overcome this time period and to minimize the potential risk of infection or dehydration, decellularised cadaver skin has been used to cover injured skin temporarily, but access to cadaver skin is

limited and there is the risk of immune rejection (Gallico et al., 1984; Guenou et al., 2009). To solve the problem of accessibility, new synthetic biomaterials have been developed but up to now they cannot replace cadaver skin.

One major area in the field of regenerative medicine in dermatology is the application of stem cells in skin grafts. Stem cells offer the remarkable potential of self-renewal through unlimited proliferation and can be differentiated into any cell type of the mammalian body. However, the use of pluripotent cells in cell replacement therapies also entails some problems that have yet to be resolved. First, cells that can differentiate into any cell type can also generate teratomas when injected into an organism. The solution would be to generate a 100% homogeneous population of differentiated cells by clonal isolation and expansion in culture. Furthermore, it is not clear if the differentiation *in vitro* would lead to a cell type that is identical to the corresponding cell type in the organism (Iuchi et al., 2006).

Many studies deal with these problems and many efforts have been made to establish protocols for the generation of keratinocytes from pluripotent cells. The first studies used murine embryonic stem cells (mESCs) (Aberdam, 2004; Coraux et al., 2003; Haase et al., 2007), later on also human embryonic stem cells (hESCs) (Green et al., 2003; Guenou et al., 2009; Ji et al., 2006; Metallo et al., 2008) and human induced pluripotent stem cells (hiPSCs) (Itoh et al., 2011; Tolar et al., 2011) were used for differentiation into the keratinocyte lineage. The differentiation protocols differ from each another based on the culture conditions, medium and supplementation as well as coating or supportive feeder layers. While some studies used cells grown in monolayers others generated embryoid bodies. Embryoid bodies (EBs) are known to recapitulate early embryogenesis and are a favored tool for studying mutations that usually induce early death in embryos (Desbaillets et al., 2000; Rungarunlert et al., 2009). The drawback of EB formation is that after they have been plated to attach, cells grow out and the leading front does not have the same differentiation stage as do the cells near the EB. Therefore many differentiation protocols favor 2D culture of the cells (Coraux et al., 2003; Guenou et al., 2009; Itoh et al., 2011).

Another aspect that differs in various protocols is the medium that is used to convert pluripotent cells into keratinocytes. Some studies used F12 and Dublecco´s modified Eagle´s medium (FAD medium), a commonly used medium for the culture of primary keratinocytes. FAD medium contains hydrocortisone to stimulate keratinocyte growth while inhibiting fibroblast proliferation but also contains fetal calf serum (FCS) (Green et al., 2003; Guenou et al., 2009; Haase et al., 2007). Other protocols prefer ready-to-use media, which are fully supplemented with growth promoting agents like the defined keratinocyte serum free medium (DKSFM) but without the addition of serum (Itoh et al., 2011; Ji et al., 2006; Metallo et al., 2008). The addition of supplements for a defined time frame, such as retinoid acid, ascorbic acid or BMP4, promotes keratinocyte differentiation. BMP4, for example, was shown to permit epithelial differentiation through the inhibition of neural fate, and retinoic acid or ascorbic acid which promote the differentiation into keratinocytes (Coraux et al., 2003).

The most stringent experiment to investigate the functional properties of generated keratinocytes is to test their ability to build whole stratified epithelia by grafting them on organotypic skin cultures (Aberdam, 2004; Coraux et al., 2003; Guenou et al., 2009; Itoh et al., 2011).

Taken together, many protocols for the differentiation of pluripotent cells into the keratinocyte lineage exist, but still no protocol allows for the generation of a 100% pure keratinocyte population.

1.4 Aim of the project

Patients with large burn injuries are treated with skin replacements, which are generated with their own keratinocytes, if possible. However, this method is time consuming, and the wounds need to be covered to avoid dehydration and infection. Decellularized cadaver skin is used to cover the wounds temporarily, and bridge the time until the skin replacement is generated. Nevertheless, the accessibility of cadaver skin is limited and it can provoke an immune response in the patient.

Since the discovery of induced pluripotent stem cells, it was of great interest to use these cells for therapeutic purpose. IPSCs display an unlimited source of pluripotent stem cells, and if differentiated, an unlimited source of nearly every needed cell type.

However, in order to use differentiated iPSCs for tissue engineering, the existing *in vitro* protocols need to be optimized.

In the field of dermatology it is of great interest to establish keratinocyte differentiation protocols and use these iPSC-derived keratinocytes for skin replacements. To date, none differentiation protocol leads to a 100% pure population of keratinocytes. To optimize the protocols, the pathways and mechanisms involved in skin development need to be investigated.

The aim of this project is to find candidates, which are involved in the differentiation of pluripotent cells into epithelial cells.

In detail, hiPSCs will be used as a developmental model and will be differentiated *in vitro* into keratinocytes. It will be investigated, if there are factors, which have an influence on the expression of early keratinocyte markers. Further it will be determined if the overexpression or the knock-down of these factors, can alter the expression of epithelial markers or the number of keratinocyte precursors.

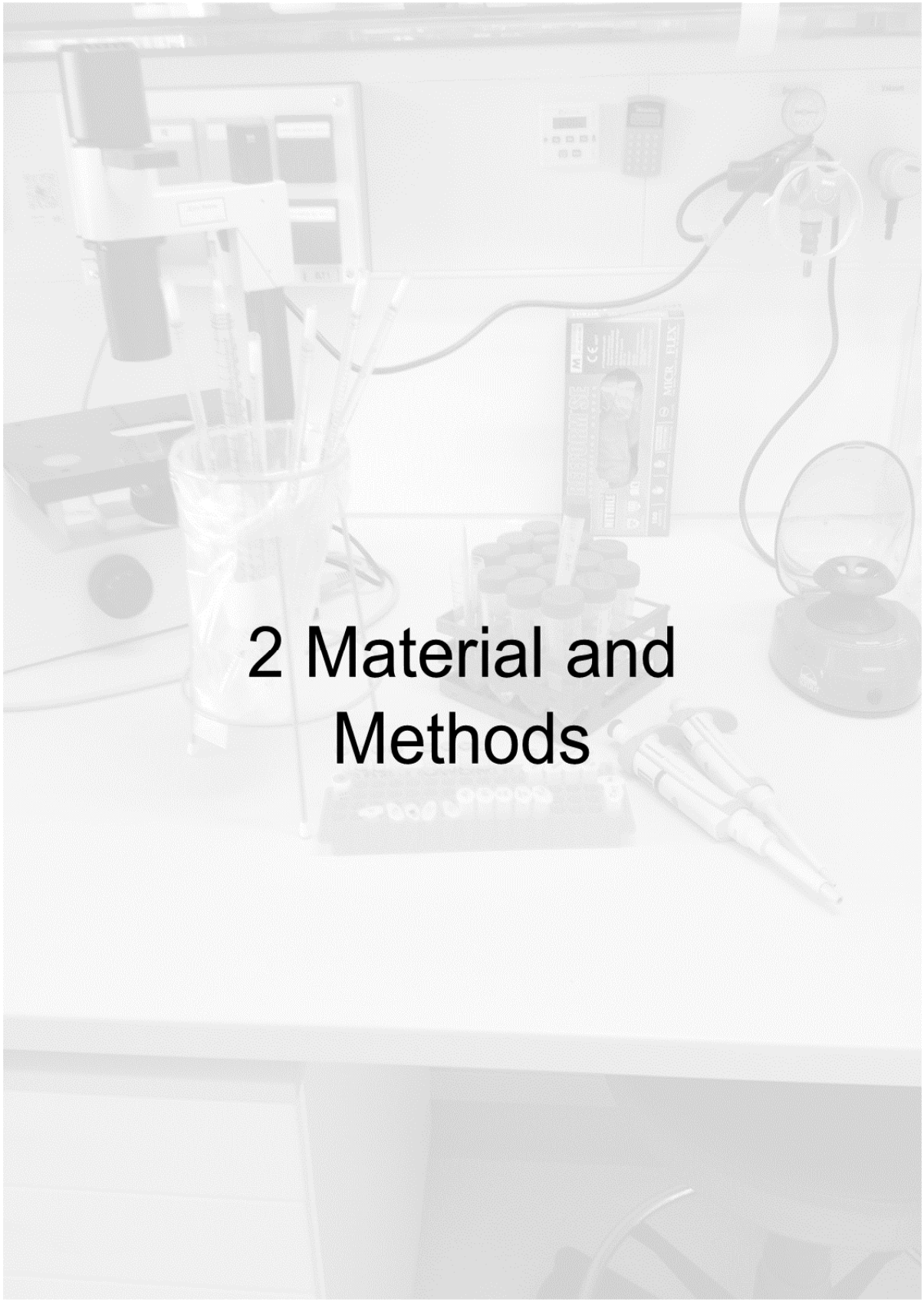

2 Material and Methods

2 Material and Methods

2.1 Material

2.1.1 Cell culture media and supplements

Cell culture media and supplements	Company
all-trans Retinoic Acid	Sigma Aldrich
bFGF	PromoKine
BMP4	PromoKine
Collagen IV	Gibco, Life Technologies
Defined Keratiocyte-serum free Medium (DKSFM)	Gibco, Life Technologies
Dimethyl Sulfoxide (DMSO)	Carl Roth
DMEM GlutaMAX	Gibco, Life Technologies
DMEM/F-12	Gibco, Life Technologies
Doxycyclin	Sigma Aldrich
Fetal Bovine Serum (FBS)	Biochrome AG
Gelatine from porcine skin, Type A	Sigma Aldrich
Glutamine	Sigma Aldrich
Keratinocyte Growth Medium2	Promocell
KnockOut DMEM/F12	Gibco, Life Technologies
KnockOut serum replacement	Gibco, Life Technologies
Matrigel, hES qualified Matrix	BD Biosciences
mFreSR	Stemcell Technologies
mTeSR1 Basal Medium	Stemcell Technologies
Non-essential amino acids	Sigma Aldrich
Normocin	InvivoGen
PBS	Gibco, Life Technologies
Penicillin/Streptomycin	Sigma Aldrich
ROCK-Inhibitor (Y27632)	Stemgent, Miltenyi Biotec
ß-Mercaptoethanol	Gibco, Life Technologies
Trypsin	Biochrome AG
Trypsin/EDTA	Sigma Aldrich

2.1.2 Cell culture media composition

Medium	Composition
CTK solution	H_2O, 0.1 mg/mL collagen IV, 1 mM $CaCl_2$, 20% KnockOut serum replacement, 0.25% trypsin
Differentiation Medium I	500 µL Defined keratinocyte serum free medium (DKSFM), 1 µM all-trans retinoic acid, 10 ng/mL BMP4, 50 ng/mL Normocin

Medium	Composition
Differentiation Medium II	500 µL Defined keratinocyte serum free medium (DKSFM), 50 ng/mL Normocin
Freezing Medium	FBS, 10% DMSO
Gelatin solution	0.1% gelatin in H_2O
hES Medium	500 mL KnockOut DMEM/F12, 20% KnockOut serum replacement, 1% glutamine, 1% non-essential amino acids, 1% penicillin/streptomycin, 4 ng/mL bFGF, 1 µg/mL doxycyclin, 50 µM ß-mercaptoethanol
Matrigel solution	1 aliquot Matrigel™, adjusted to 25 mL mit DMEM/F12
MEF Medium	500 µL DMEM GlutaMAX, 10% FBS, 1% non-essential amino acids, 1% penicillin/streptomycin, 50 µM ß-mercaptoethanol
Washing Medium	DMEM GlutaMAX, 10% FBS

2.1.3 Chemicals

Chemicals	Company
4',6-diamidino-2-phenylindole (DAPI)	Roche
4x Laemmli Sample Buffer	BioRad
Acetic Acid	Sigma Aldrich
Acrylamide	Carl Roth
Ammonium Persulfate (APS)	Carl Roth
Ampicillin	Carl Roth
Braunol®	Braun
BSA	Carl Roth
$CaCl_2$	Carl Roth
Dako Pen	Dako, Agilent Technologies
Eosin	Sigma Aldrich
Ethanol	Sigma Aldrich
Eukitt	Sigma Aldrich
Fluorescence Mounting Medium	Dako, Agilent Technologies
Formalin	Sigma Aldrich
Glycerin	Carl Roth
Hematoxylin	Sigma Aldrich
Isopropanol	Carl Roth
LB-Agar (Lennox)	Carl Roth
LB-Medium (Lennox)	Carl Roth
Lipofectamine RNAiMAX	Life Technologies
Methanol	Sigma Aldrich
Mitomycin C	Carl Roth
Paraform aldehyde	Carl Roth
Polybrene	Sigma Aldrich
Skim Milk Powder	Fluka Analytical™, Sigma Aldrich

Chemicals	Company
Sodium Dodecyl Sulfate (SDS) 20% Solution	G-Biosciences
TEMED	Carl Roth
TRIS Hydrochloride	Carl Roth
Triton-x-100	Carl Roth
Trizma Base	Sigma Aldrich
Tween 20	Carl Roth
X-treme Gene	Roche
Xylene	Sigma Aldrich

2.1.4 Kits

Kits	Company
Amersham™ ECL™ Prime Western Blotting Detection Reagent	GE Healthcare
BCA Protein Assay Kit	Pierce, Thermo Scientific
DNase-Free Dnase Set	Qiagen
EndoFree Plasmid Maxi Kit	Qiagen
RevertAid First Strand cDNA Synthesis Kit	Fermentas, Thermo Scientific
RNeasy Mini Kit	Qiagen
Subcloning Efficiency™ DH5α™ Competent Cells	Life Technologies
FIX&PERM® Cell Permeabilization Kit	An Der Grub Bio Research GmbH

2.1.5 Buffers and gels

Buffers & gels	Composition
Blocking buffer (HTS)	PBS, 3% BSA, 0.05% Triton-x-100
Blocking buffer (IF)	PBS, 3% BSA, 0.1% Triton-x-100
Blocking buffer (WB)	TBS, 5% skim milk powder, 0.02% tween 20
FACS buffer	PBS, 2% BSA, 0.2% sodium azide
Fixation buffer (HTS)	PBS, 4% PFA, 0.2% Triton-x-100
LB agar plates	35 g LB agar powder in 1 L H_2O, autoklaved, supplemented with 100 µg/µL ampicillin
LB medium	20 g LB powder in 1 L H_2O, autoclaved
Lysis buffer	1 complete Mini tablet, in TBS, 0.1% Triton-x-100
PBST	PBS, 0,1% Triton-x-100
Running buffer (WB)	H_2O, 0.19 M Glycin, 0.1% SDS, 25 mM Trisma Base
Separating gel	2 mL H_2O, 1.65 µL Acrylamide (30%), 1.25 mL Tris (pH 8.8, 1.5 M), 50 µL SDS (10%), 50 µL APS (10%), 2 µL TEMED

Buffers & Gels	Composition
Stacking gel	1.4 mL H_2O, 330 µL Acrylamide (30%), 250 µL Tris (pH 6.8, 0.5 M), 20 µL SDS (10%), 20 µL APS (10%), 2 mL TEMED
TBS	H_2O, 150 mM NaCl, 50 mM Trisma Base, pH adjusted to 7.6
Transfer buffer (WB)	H_2O, 39 M Glycin, 20% Methanol, 0.037% SDS, 48 mM Tris, pH adjusted to 8.3
Washing buffer (WB)	0.02% Tween 20 in TBS

2.1.6 Primary antibodies

Target	Host	Application	Dilution	Order No.	Company
Oct3/4	goat	IF	1:250	sc-8628	Santa Cruz
HIPK4	rabbit	WB	1:500	AP52050PU-N	Acris
Involucrin	mouse	IF	1:500	I9018	Sigma
Keratin1	rabbit	IF	1:500	PRB-149P	covance
Keratin14	rabbit	IF	1:250	PRB-155P	covance
Keratin18	mouse	IF/FACS	1:50	11416	Progen
Nanog	rabbit	IF	1:500	ab-21624	abcam
SSEA4	mouse	IF	1:500	9094S	Cell Signaling
Tra-1-60	mouse	IF	1:500	9094S	Cell Signaling
Tra-1-81	mouse	IF	1:500	9094S	Cell Signaling
ß-actin	rabbit	WB	1:10,000	5125S	Cell signaling

2.1.7 Secondary antibodies

Secondary antibody	Application	Dye	Dilution	Order No.	Company
α-mouse IgG HRP-linked Anitbody	WB	HRP	1:10,000	7076S	Cell Signaling
α-rabbit IgG HRP-linked Antibody	WB	HRP	1:10,000	7074S	Cell Signaling
α-goat Alexa Fluor 488	IF	Alexa Fluor 488	1:500	A11055	Invitrogen
α-rabbit Alexa Fluor 488	IF	Alexa Fluor 488	1:500	A11008	Invitrogen
α-rabbit Alexa Fluor 594	IF	Alexa Fluor 594	1:500	A11012	Life Technologies
α-mouse Atto 488	IF	Atto 488	1:500	62197	Sigma
α-mouse Atto 594	IF	Atto 594	1:500	76085	Sigma
α-rabbit Atto 488	IF	Atto 488	1:500	5125S	Sigma

2.1.8 siRNA sequences

siRNA	Sequence
HIPK4 J-004808-09	AGUAUAUGCUCAAGUCGUU
HIPK4 J-004808-10	AGACGAAGGUGCGCCCAUU
HIPK4 J-004808-11	AGAAGGAGGCUGCGGGUAU
HIPK4 J-004808-12	GCAACAACGAGUACGACCA
Non-targeting Pool #2 (1)	UAAGGCUAUGAAGAGAUAC
Non-targeting Pool #2 (2)	AUGUAUUGGCCUGUAUUAG
Non-targeting Pool #2 (3)	AUGAACGUGAAUUGCUCAA
Non-targeting Pool #2 (4)	UGGUUUACAUGUCGACUAA

2.1.9 Consumables

Consumables	Company
10 µL filter tips	Nerbe Plus
100 µL filter tips	Nerbe Plus
1000 µL filter tips	Nerbe Plus
10 µL pipette tips	Nerbe Plus
100 µL pipette tips	Nerbe Plus
1250 µL pipette tips	Nerbe Plus
10 mL serological pipette	Costar , Corning
5 mL serological pipette	Costar , Corning
25 mL serological pipette	Costar , Corning
6well plate	Cellstar, Greiner Bio-One
12well plate	Cellstar, Greiner Bio-One
96well microplates (for BCA)	Greiner Bio-One
96well microplates (for QPCR)	Nerbe Plus
384well plate	Falcon, Becton Dickinson
10cm cell culture dish	TPP
10cm Petri dish	Falcon, Becton Dickinson
T75 cell culture flask	Cellstar, Greiner Bio-One
1.5 mL reaction tube	Eppendorf
2 mL reaction tube	Eppendorf
15 mL conical tubes	Greiner Bio-One
50 mL conical tubes	Greiner Bio-One
cryogenic vial	Nunc, Thermo Scientific
1 mL Syringe	Henke Sass Wolf
50 mL Syringe	Terumo
Needle	Neoject, Dispomed
0.45 µm PVDF filter	Carl Roth
Disposable Scalpel	Feather

Consumables	Company
Amersham Hyperfilm™ ECL	GE Healthcare
Chromatography Paper 3mm	Whatman
PVDF Transfer Membrane 0.45 µm pore size	Immobilon Millipore
Latex Medical Examination Gloves	Blossom
Optical Adhesive Film	Applied Biosystems, Life Technologies
Sealing Tape	Costar, Corning
20 mm ⌀ Glass Cover Slips	Assistent, Glaswarenfabrik Hecht
Glass Object Slides	Thermo Scientific

2.1.10 Machines and devices

Machines and devices	Product name	Company
Aspiration pump	BVC 21	Vacuubrand
Automated Workstation	Biomek FX	Beckman Coulter
Autoradiography Cassette	24X30cm	Dr. Goos Suprema
Bacterial Shaker	Innova 4230	New Brunswick Scientific
Bioimager	BP Pathway 855	BD Biosciences
Biological Safety Cabinet	Hera safe	Thermo Scientific
Blotting Devices	Mini Trans-Blot Electrophoretic Transfer Cell	Bio Rad
Cell Incubator	Cell Incubator	Binder
Centrifuge	5418R	Eppendorf
Centrifuge	5810R	Eppendorf
Centrifuge	Heraeus Multifuge X3 FR	Thermo Scientific
Computer	Precision T3500	Dell
Digital Camera	ORCA-ER	Hamamatsu
Flourescence Microscope	Eclipse T*i*	Nikon
Flow Cytometer	FACSCanto II	BD Biosciences
Freezer	Premium	Liebherr
Freezing Container	Freezing Container	Qualilab
Fridge	Premium	Liebherr
Hemocytometer	Neubauer 0.1 mm	Assistent, Glaswarenfabrik Hecht
Inverted Microscope	Eclipse TS100	Nikon
Laptop	Latitude E6510	Dell
Liquid Nitrogen Tank	Chronos	Messer Griesheim
Microscope	Leica DMLS	Leica
Microscope Camera	EC3 Leica	Leica
Microscope Camera	DS-Qi1Mc	Nikon
Microtome	RM 2065	Leica
Orbital Shaker	Polymax 2040	Heidolph

Machines and devices	Product name	Company
Power Supply	Power Pac 300	Bio Rad
Reagent Dispenser	Multidrop Combi	Thermo Scientific
Real-time QPCR cycler	7500 Real-Time PCR System	Applied Biosystems
Roller Mixer	RM5-30V	CAT
SDS Gelelektrophoresis Devices	Mini-PROTEAN Tetra Cell	Bio Rad
Spectralphotometer	Spectralfluor Plus	Tecan
Spectrophotometer	Nanodrop ND-100	PeqLab
Thermomixer	Thermomixer compact	Eppendorf
Tissue Processor	TP1020	Leica
Vortex Mixer	Vortex Mixer	Heidolph

2.1.11 Material for Microarray

Chemicals and solutions	Company
Illumina Total-Prep RNA Amplification Kit	Life Technologies
Biotin-16-UTP	Roche Applied Bioscience
GEX-HCB Buffer	Illumina Inc.
High Temp Wash Buffer	Illumina Inc.
E1BC Buffer	Illumina Inc.
Blocking Solution (1% Blocker Casein in PBS Hammarsten Grade)	Pierce Biotechnology
Cy3-Streptavidin	Amersham Bioscience

Machines and devices	Company
2100 Bioanalyzer	Agilent
iScan Array Scanner	Illumina Inc.
Human Sentrix 12 Bead Chip Arrays	Illumina Inc.

2.1.12 Software

Software	Company/developer
7500 Software v2.0.5	Applied Biosystems®, Life Technologies
Bioconductor/R	open development project
cellHTS2	M.Boutros, L.Bras, W.Huber
CellProfiler	Broad Institute
Chipster	CSC - IT Center for Science
GraphPad Prism 6	GraphPad Software
ImageJ	W.Rasband, National Institutes of Health
Megallan™ Data Analysis Software	Tecan

Software	Company/developer
Microsoft Office Excel 2007	Microsoft
Microsoft Office PowerPoint 2007	Microsoft
Microsoft Office Word 2007	Microsoft
NIS Elements	Nikon

2.1.13 Plasmids

Plasmid	Label	Received from
Reprogramming vectors	TetO human STEMCCA floxed	Group of K.Hochedlinger, Ref.: Sommer 2009
Transactivator	FUdeltaGW-rtTA	Group of K.Hochedlinger, Ref.: Sommer 2009
Packaging plasmid	pCMV-dR8.91	Group of K.Hochedlinger, Ref.: Sommer 2009
Envelope plasmid	pCMV-VSV-G	Group of K.Hochedlinger, Ref.: Sommer 2009
Empty vector	pLenti CMV GFP Puro	Addgene, Plasmid 17448, Eric Campeau
HIPK4 expression vector	pCW45-HIPK4	The Dana-Farber/Harvard Cancer Center DNA Resource Core; CloneID: HsCD00299059

2.1.13.1 TetO human STEMCCA floxed (reprogramming cassette)

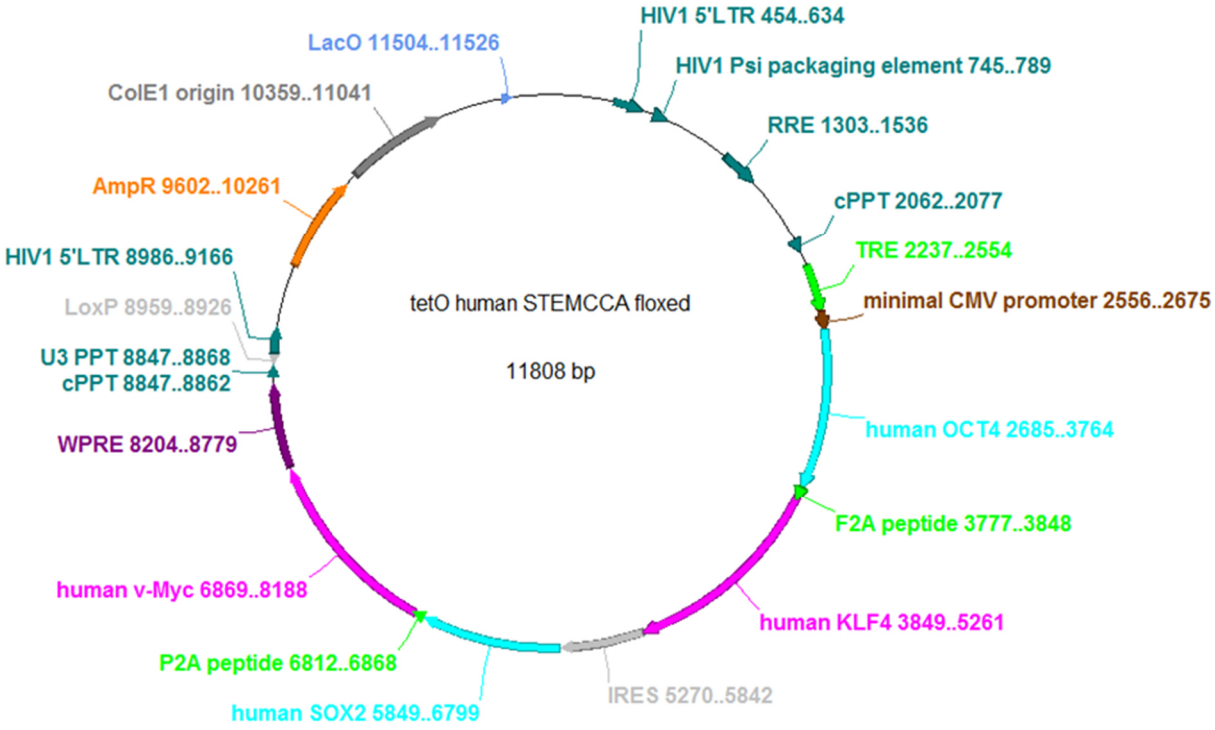

2.1.13.2 FUdeltaGW-rtTA (transactivator)

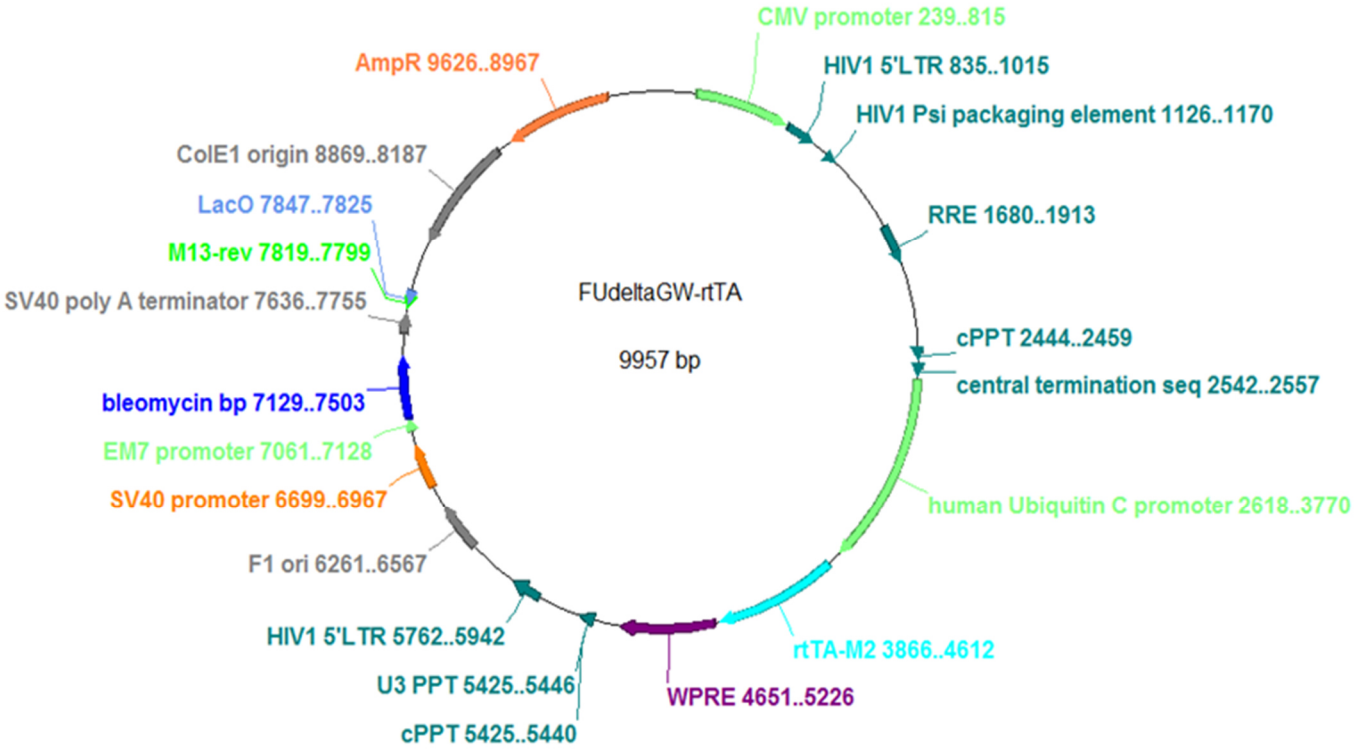

2.1.13.3 pCMV-dR8.91 (packaging plasmid, Δ8.9)

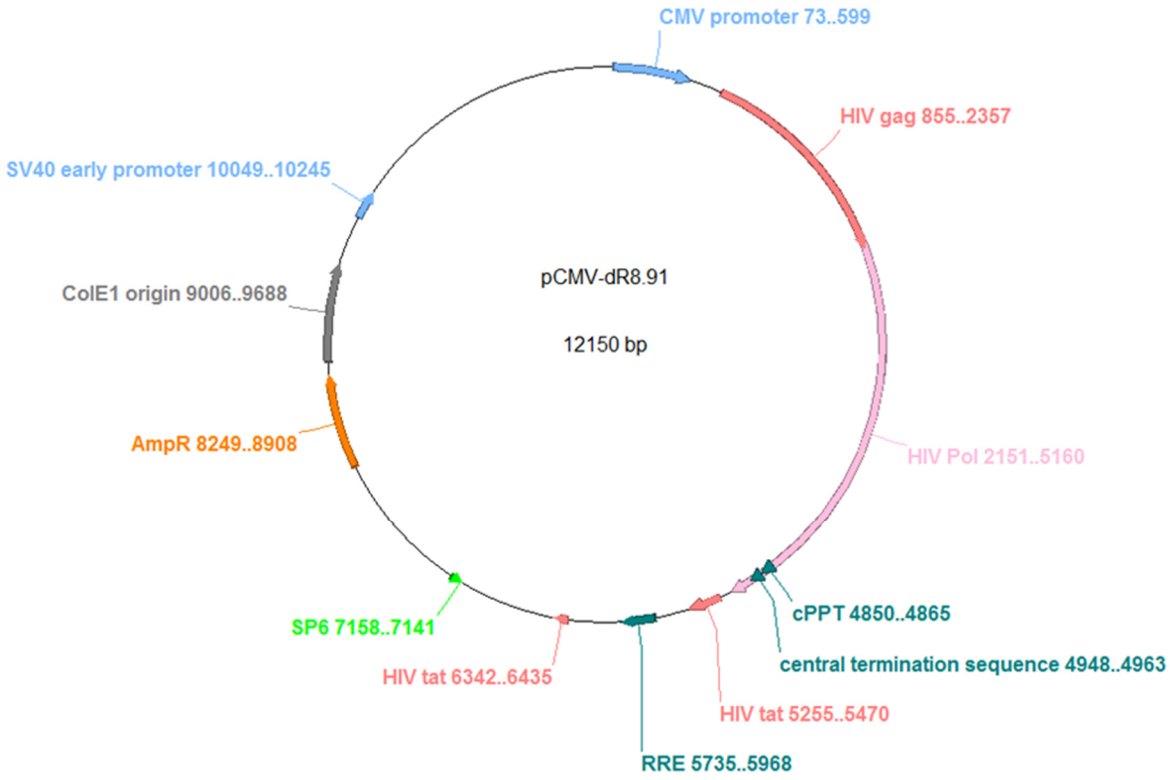

2.1.13.4 pCMV-VSV-G (packaging plasmid, VSV-G)

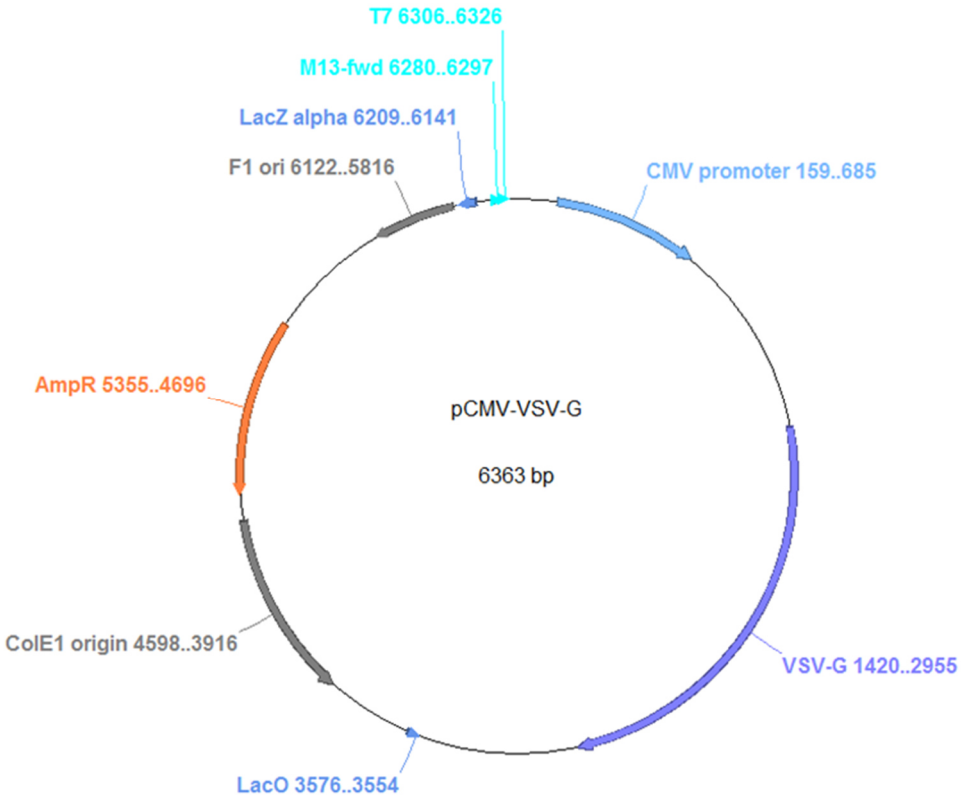

2.1.13.5 pLenti CMV GFP Puro (empty control vector)

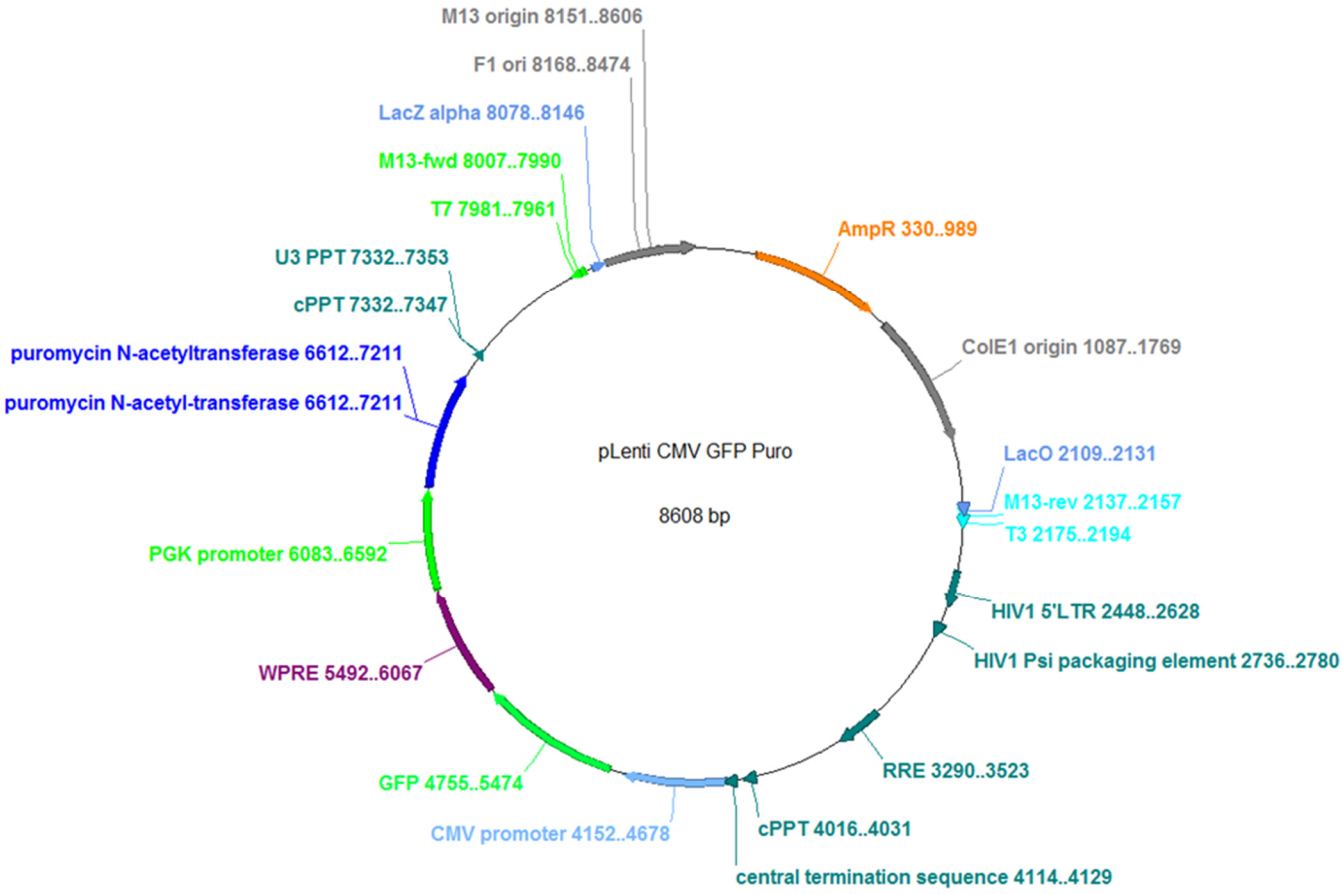

2.1.13.6 pCW45-HIPK4 (HIPK4 expression vector)

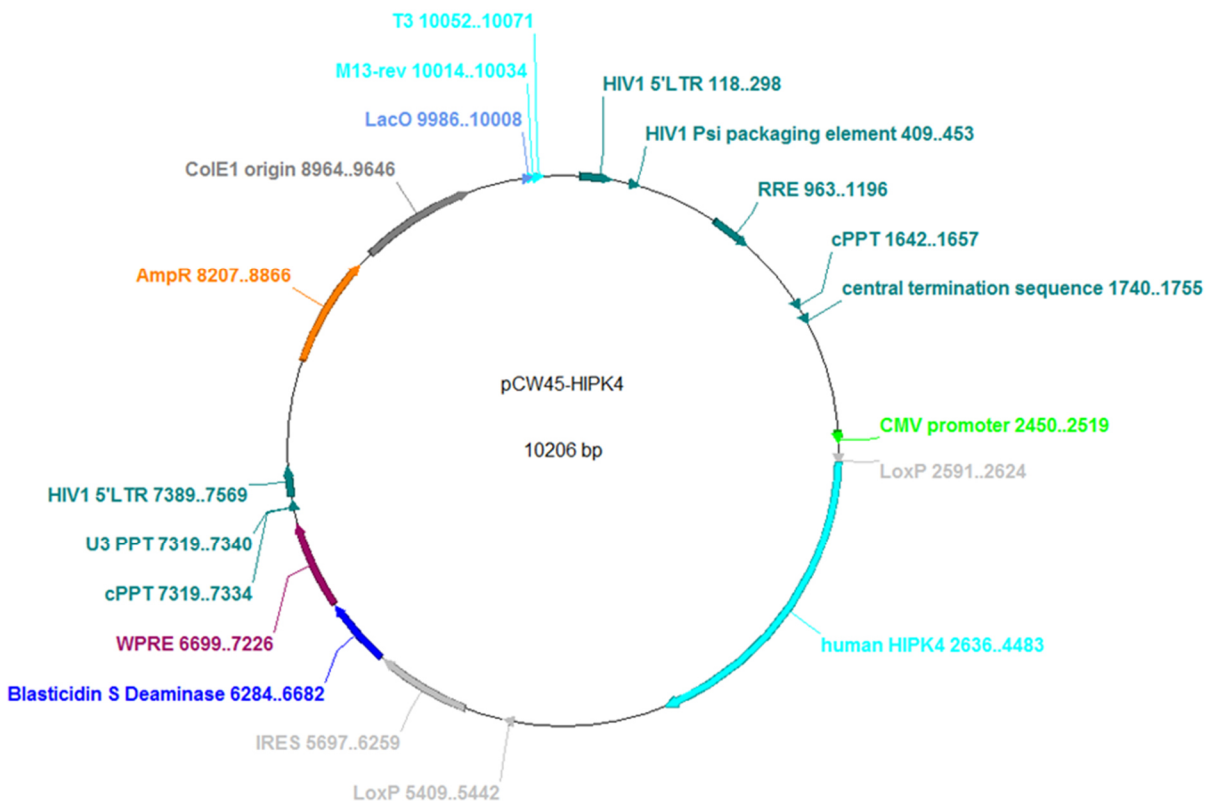

2.1.14 QPCR Primer sequences

Target	Forward Primer 5`-3`	Reverse Primer 3´-5´
18S	GAGGATGAGGTGGAACGTGT	TCTTCAGTCGCTCCAGGTCT
GAPDH	GAAGGTGAAGGTCGGAGTC	GAAGATGGTGATGGGATTTC
HIPK4	GGTCAAGGTGATTGACTTCGG	GGTTGCGCTTGAAGAAGTGG
Involucrin	TGTGAGTCTGGTTGACAGTAGC	ATTCTTGCTCAGGCAGTCCC
Keratin 14	AGGAGATCGCCACCTACCGCC	AGGAGGTCACATCTCTGGATGACTG
Keratin 18	GAGTATGAGGCCCTGCTGAACATCA	GCGGGTGGTGGTCTTTTGGAT
Keratin 5	ATCTCTGAGATGAACCGGATGATC	CAGATTGGCGCACTGTTTCTT
Keratin 8	GATCGCCACCTACAGGAAGCT	ACTCATGTTCTGCATCCCAGACT
Lin28	TGAGGCAGTGGAGTTCACCT	CTTGCATTCCTTGGCATGAT
Nanog	AGGAAGACAAGGTCCCGGTCAAG	TGCTGAGGCCTTCTGCGTCAC
P63	TTCTTAGCGAGGTTGGGCTG	GATCGCATGTCGAAATTGCTC
REX1	TTGGAGTGCAATGGTGTGAT	TCTGTTCACACAGGCTCCAG
Sox2	GTGAGGGCCGGACAGCGAAC	GCGTACCGGGTTTTCTCCATGCT
TERT	GCGTTTGGTGGATGATTTCT	CAGGGCCTCGTCTTCTACAG

2.2 Methods

2.2.1 Plasmid preparation

2.2.1.1 Transformation of bacteria

Competent DH5α bacteria were used as an amplifying system to obtain large quantities of DNA plasmids. Competent bacteria are cells that were treated with $CaCl_2$ in order to increase the permeability of their cell membrane to DNA. For the amplification of naked DNA, DNA plasmids need to be introduced into the bacteria cell, which then makes multiple copies of the DNA.

Frozen stocks of competent *E. coli* DH5α were thawed on ice. 1 µg DNA was added to the thawed bacteria cells and incubated for 15 min. The cells were then heat-shocked for 2-3 min at 42 °C. The bacteria were then placed back on ice. Then 1 mL LB Medium was added to the cells and they were incubated for 30 min at 37 °C while shaking. The transformed bacteria were then plated on agar plates, which contain the appropriate antibiotic and incubated over night at 37 °C.

2.2.1.2 Preparation of glycerolstocks

Transformed bacteria colonies were picked from agar plates with a pipette tip and transferred into 5 mL LB medium containing the appropriate antibiotics. These cultures were inoculated over night at 37 °C vigorously shaking. The next day, 500 µL bacterial culture was mixed with 500 µL glycerol and frozen at -80 °C. Glycerolstocks of every plasmid were prepared for long term storage.

2.2.1.3 Endo-free plasmid preparation and purification

Transformed bacteria grown in colonies on agar plates were picked and transferred into LB medium. Bacteria were incubated over night at 37 °C vigorously shaking. The next day these pre-cultures were used to inoculate large cultures. The plasmids from 200 mL over-night cultures were isolated using the EndoFree Plasmid Maxi Kit from Qiagen, according to the manufacturer's protocol "Plasmid or Cosmid DNA Purification using EndoFree Plasmid Maxi Kit".

At the last step, the plasmid pellet was resuspended in 30 µL endotoxin-free Buffer TE or endotoxin-free water. The concentration of the plasmid was determined using a photometer. The concentration was adjusted to 1 µg/µL for every plasmid.

2.2.2 Cell culture methods

2.2.2.1 Culture of 293T HEK cells and virus production

293T HEK cells were cultured in MEF medium (DMEM GlutaMAX™ containing 10% FBS, 1x non-essential amino acids, 1% penicillin/streptomycin and 50 µM ß-mercaptoethanol) in

T75 cell culture flasks and routinely passaged 2-3 times a week. For passaging the cells, medium was aspirated and cells were washed twice with 10 mL PBS. Trypsin/EDTA was added to the cells just enough to cover the entire surface (~3 mL) and incubated at 37 °C until the cells started to detach. Trypsin/EDTA activity was inhibited by adding 5 mL washing buffer (DMEM GlutaMAX™ supplemented with 10% FBS), cells were rinsed, aspirated and transferred into a 15 mL conical tube. The cell suspension was then centrifuged for 5 min at 1200 rpm. The supernatant was discarded, the cell pellet was resuspended in 5 mL fresh MEF medium and 1/10 of the cell suspension (500 µL) was transferred into a new cell culture flask with 10 mL MEF medium. Cells were cultured at 37 °C and 5% CO_2.

293T HEK cells were used as packaging cells, to produce lentiviral particles. For this purpose, the cells were transfected with an envelope plasmid, a packaging plasmid and a vector that contains the gene of interest. The envelope and packaging vectors provide all required proteins that are needed to produce the viral particles. A list of plasmids used for viral production can be found in the “Material” part (2.1.13 Plasmids).

For the production of lentiviral particles, 293T HEK cells were cultured in MEF medium and grown in T75 cell culture flasks (75 cm^2). On the day of transfection the cells should be 50-70% confluent. Before transfection, the medium was changed to MEF medium without antibiotics, since antibiotics can decrease the transfection efficiency. DMEM GlutaMAX™ and transfection reagent (X-tremeGENE9, Roche) were preheated to room temperature. For one flask 770 µL DMEM GlutaMAX™ was applied to a 1.5 mL reaction tube and 50 µL transfection reagent was added. The solution was mixed by pipetting and incubated for 5 min at room temperature. The DNA was added at following ratios: 1x VSV-G (envelope plasmid), 1.5x Δ8.9 (packaging plasmid) and 2x plasmid of interest. The transfection-mix was then incubated at room temperature for 30 min. After the incubation time the transfection-mix was added to the cells. The medium was discarded after 12-24h and fresh MEF medium was added to the cells. Medium containing the virus particles was harvested after another 12, 24, and 36 hours and stored at 4 °C. After the last harvest the virus-containing medium was filtered, using 0.45 µm PVDF filters. The filtered virus particle-containing supernatant was concentrated by centrifugation using an ultracentrifuge at 40.000 rpm at 4 °C for 2h. The supernatant was discarded, 100 µL PBS was applied directly on the virus pellet and incubated over night at 4 °C. The next day the concentrated virus was aliquoted and stored at -80 °C.

The Virus production was performed in a S2 laboratory, according to the safety instructions.

2.2.2.2 Coating of cell culture plates

2.2.2.2.1 Thin Matrigel™ coating

Human ES-cell qualified Matrigel™ was thawed on ice at 4 °C over night. For aliquot preparation pipette tips and 1.5 mL reaction tubes were kept cool. Thawed Matrigel™ solution was aliquoted in amounts according to manufacturer’s instructions specifically for every lot and stored at -20 °C. For thin Matrigel™ coating aliquots were thawed on ice and pipette tips and cell culture dishes were pre-cooled. One Matrigel™ aliquot was diluted up to 25 mL with ice-cold DMEM/F12. One well of a 6-well plate was rinsed with 1 mL Matrigel™-solution (1 mL per ~10 cm^2). Coated plates were incubated for 1 hour at room temperature. After incubation time plates could be either directly used or were stored up to one week at

4 °C. Prior to use Matrigel™ solution was aspirated and culture plates were rinsed with DMEM/F12 in order to remove surplus Matrigel™.

2.2.2.2.2 Gelatin coating

For coating cell culture plates, 0.1% gelatin solution was added (~1 mL per 10 cm^2) and incubated at room temperature for at least 30 min. After incubation, gelatin solution was aspirated and plates were rinsed with PBS in order to remove surplus gelatin. The plates were then ready-to-use.

2.2.2.3 Isolation of primary human fibroblasts and keratinocytes from skin biopsies

Freshly obtained skin biopsies were transferred into MEF medium and were stored not longer than 24h at 4 °C. The biopsy was transferred into PBS and then on a petri dish without medium. Adipose tissue was removed from the biopsy and cut into small pieces. The pieces were placed in a tissue culture dish containing MEF medium, just enough medium was added that the pieces were completely covered but not floating. The remaining biopsy was cut into small squares, approximately 0.5x0.5 cm in size. These tissue squares were transferred into 35 mm cell culture dishes containing 0.25% trypsin in PBS and incubated overnight at 4 °C. The next day, the epidermis was carefully removed from the dermal part with forceps and transferred into fresh trypsin. The dermal part was transferred into a petri dish. The tissue was then thoroughly chopped with scalpels in order to dissociate it. These tissue fragments were then resuspended in MEF medium, plated in a tissue culture dish and kept at 37 °C and 5% CO_2 until fibroblasts grew out. The epidermal pieces in trypsin were centrifuged at 1200 rpm for 5 min. The supernatant was aspirated and the pellet was resuspended in Keratinocyte Growth Medium (KGM supplemented with 10% FBS and 1% penicillin/streptomycin). The suspension was plated on cell culture dishes and kept at 37 °C and 5% CO_2 until keratinocytes grew out. After 4-5 days medium was added carefully to the cultures and changed for the first time after 10 days. The medium for keratinocytes was replaced by KGM with lower FBS (1%) concentration. Fibroblasts from adipose and dermal tissue were cultured described as below (section “2.2.2.6 Culture and cryopreservation of mouse and human primary fibroblasts”).

2.2.2.4 Isolation of mouse embryonic fibroblasts

14 days after fertilization pregnant mice were sacrificed followed by an abdominal incision. The uterus was excised, the embryos were separated from the amniotic membranes and transferred into a disinfection solution (Braunol®). The embryos were then washed with PBS and the head and the fetal liver were removed using a scalpel. In order to dissociate the tissue, the embryos were placed in a petri dish, bedewed with Trypsin/EDTA and thoroughly chopped with scalpels. The suspension was transferred into a MEF medium containing conical tube. Up and down pipetting led to further dissociation of the tissue. The cells were then seeded on gelatin coated (paragraph “2.2.2.2.2 Gelatin coating”) cell culture plates and kept at 37 °C and 5% CO_2 without moving them for 5 days. Fresh medium was added at day 5 and could be changed when the cells attached to the culture plate. When the cells reached

100% confluency they were either frozen (paragraph “2.2.2.6 Culture and cryopreservation of mouse and human fibroblasts”) or treated with mitomycin c for feeder preparation (see paragraph “Preparation of feeder cells from mouse embryonic fibroblasts”).

2.2.2.5 Preparation of feeder cells from mouse embryonic fibroblasts

Primary MEFs were expanded in a 75 cm^2 cell culture flask in MEF medium until reaching 90% confluency. The MEFs were rinsed twice with PBS and subsequently incubated with DMEM GlutaMAX™ supplemented with 10% FBS and 8 µg/mL mitomycin c for 5 h at 37 °C. After the incubation time the cells were washed two times with PBS with magnesium and calcium and two times with PBS without magnesium and calcium. The mitomycin c treated cells withdraw from the cell cycle and are postmitotic. The feeder cells were then either seeded directly for use with a density of 4000 cells/cm^2 or cryopreserved for later use (see next section).

2.2.2.6 Culture and cryopreservation of mouse and human primary fibroblasts

Mouse and human fibroblasts were routinely cultured in MEF medium. Before reaching 100% confluency cells were passaged. For this purpose, cells were washed twice with PBS and Trypsin/EDTA was added. After 5 min of incubation at 37 °C washing buffer was added and detached cells were rinsed. The cell suspension was transferred into a conical tube and centrifuged for 5 min at 1200 rpm. The supernatant was discarded and the pellet was resuspended in fresh MEF medium. The cells were then seeded on gelatin coated plates in MEF medium. For cryopreservation, 1 mL ($1*10^6$ cells) of cell suspension was transferred into cryogenic vials and 1 mL freezing medium (FBS supplemented with 10% dimethyl sulfoxide (DMSO)). The cryogenic vials were then placed in isopropyl alcohol filled freezing containers and cooled down to -80 °C. The next day the cells were transferred into a liquid nitrogen tank for long term storage.

For thawing mouse and human primary fibroblasts, frozen cryogenic vials were thawed in a water bath at 37 °C. Before the cells were completely thawed, fresh MEF medium was added. The cell suspension was transferred into a conical tube containing 5 mL MEF medium and centrifuged at 1200 rpm for 5 min. The supernatant was aspirated and the pellet was dissociated in MEF medium. The cells were then seeded on gelatin-coated plates in MEF medium and kept in a cell incubator at 37 °C and 5% CO_2.

2.2.2.7 Culture and cryopreservation of human primary keratinocytes

Primary keratinocytes were routinely passaged once after isolation, followed by cryopreservation. In culture, primary keratinocytes differentiate rapidly into terminally differentiated cells, thus isolated cells were cryo-preserved at passage 1.

Isolated and attached primary keratinocytes were grown in Keratinocyte Growth Medium (KGM supplemented with 1% FBS and 1% penicillin/streptomycin. When reaching a confluency of 70-80% primary keratinocytes were passaged. Cells were rinsed with PBS twice and afterwards Trypsin/EDTA was added. After incubation of 5-10 min at 37 °C washing medium was added, the cells were rinsed and transferred into a conical tube. The

cells were then centrifuged for 5 min at 1200 rpm. The cell pellet was resuspended in fresh KGM and plated at a dilution ratio of 1:3 in cell culture dishes. For cryopreservation, $1*10^6$ cells in 1 mL medium were transferred into a cryogenic vial and 1 mL freezing medium was added. The vial was placed in a freezing container and kept at -80 °C overnight. The next day vials were placed in a liquid nitrogen tank for long term storage.

2.2.3 Generation and culture of human induced pluripotent stem cells

2.2.3.1 Generation of human induced pluripotent stem cells

For the generation of human induced pluripotent stem cells (hiPSCs) primary human fibroblasts were co-transduced with the StemCCA plasmid, which contains the four reprogramming transgenes Oct4, Klf4, Sox2 and c-Myc, and the reverse tetracycline dependent transactivator M2.

Fibroblasts isolated from healthy donor biopsies were cultured on gelatin coated plates (see section “2.2.2.2.2 Gelatin coating”) for one passage in MEF medium. The fibroblasts were then seeded on gelatin coated 6well plates with a density of 5000 cells/well. For transduction with lentiviral particles, fibroblasts were rinsed with PBS and 2 mL MEF medium was added followed by 5 µL of M2 and 5 µL of StemCCA concentrated virus. To improve viral transduction 1 mg/mL polybrene was supplemented to the medium. Polybrene (1,5-dimethyl-1,5-diazaundecamethylene polymethobromide) is positively charged and neutralizes the charge repulsion between the viral particle and the cell surface, which facilitates the transduction.

After 24 h, the medium was aspirated and cells were rinsed with PBS, followed by another round of transduction. The next day, cells were washed twice with PBS and a 1:1 mixture of MEF medium with hES medium (KnockOut™ DMEM-F12 supplemented with 20% KnockOut™ serum replacement, 1x non-essential amino acids, 1% glutamine, 1% penicillin/streptomycin, 50 µM ß-mercaptoethanol and 4 ng/mL bFGF) was added to the cells. To induce the transgene expression the medium was supplemented with 1 µg/mL doxycycline. The transduced cells were cultured in the mix-medium for 1 week and afterwards in hES medium supplemented with 1 µg/mL doxycycline for the activation of M2. After four to six weeks appearing hiPSC colonies were picked manually and transferred onto mitomycin c treated feeder cells (see paragraph “2.2.2.5 Preparation of feeder cells from mouse embryonic fibroblasts”). The cells were then cultured for about two weeks until reaching a stable state, thenceforth doxycycline was withdrawn. The hiPSCs where then picked and transferred onto thin Matrigel™ coated cell culture plates and cultured in mTeSR™1 (supplemented with 50 µg/mL Normocin™).

2.2.3.2 Culture of human induced pluripotent stem cells

Stable clones of hiPSCs were cultured in feeder-free conditions in thin Matrigel™ coated cell culture flasks (see section “2.2.2.2.1 Thin Matrigel™ coating”) in mTeSR™1 (supplemented with 50 µg/mL Normocin™). Every second day, medium was changed and colonies were rinsed with DMEM/F12 to remove dead cells. Before changing the medium, cultures were examined under an inverted microscope and differentiating cells or overgrown areas were removed mechanically using a 100 µL pipette tip. Before reaching confluency,

hiPSC colonies were passaged every 5-7 days. Cells were rinsed with DMEM/F12 and incubated for 7 min in CTK solution at 37 °C. Cultures were then washed twice with DMEM/F12 and 1 mL mTeSR™1 was added to the cells. Colonies were disrupted mechanically into smaller clumps by scratching with a pipette tip. Floating small cell clumps were aspirated carefully with a 5 mL pipette to avoid the complete dissociation into single cells. Cell clumps were then transferred into new thin Matrigel™ coated 6well plates and medium was adjusted to a volume of 2 mL/well. The next day, 1 mL mTeSR™1 medium was added per well of a 6well plate. HiPSCs were maintained at 37 °C and 5% CO_2.

2.2.3.3 Cryopreservation and thawing of hiPSCs grown on Matrigel™

Cells were cultured routinely on thin Matrigel™ coated 6well plates in mTeSR™1 medium. For cryopreservation, cells were first rinsed twice with DMEM/F12 and then detached by adding 800 µL CTK solution per well and incubating for 7 min at 37 °C. The CTK solution was aspirated carefully, cells were washed twice with DMEM/F12, and 1 mL of mFreSR™ medium was added to the cells. Cell colonies were then scratched mechanically using a pipette tip, in order to detach whole colonies of hiPSCs. The cell clump suspension was then transferred into cryogenic vials. To achieve a mild cryopreservation, cryogenic vials were placed in freezing containers filled with isopropyl alcohol and stored at -80 °C over night. The next day, vials were transferred into liquid nitrogen containers until further use.

To thaw cryopreserved hiPSCs, cryogenic vials were removed from liquid nitrogen and transferred into a water bath at 37 °C. The cryogenic vials were removed from the water bath, just before the cells were completely thawed. 1 mL of pre-warmed mTeSR™1 medium was added to the cells and the suspension was spun down for 5 min at 900 rpm. After aspiration of the supernatant, 2 mL mTeSR™1 medium was added and the cells were carefully resuspended, without disrupting the clumps. HiPSCs were then plated on freshly Matrigel™ coated 6well plates. The next day 1 mL mTeSR™1 medium was added to the cells. The cells were cultured routinely as described above and kept at 37 °C and *5*% CO_2.

2.2.4 Epithelial differentiation protocol

HiPSCs were cultured on Matrigel™ coated 6well plates, as previously mentioned. 1 h before seeding the cells for differentiation, ROCK-inhibitor (10 µM) was added to the cells to prevent single cell provoked apoptosis. HiPSCs were washed twice with 2 mL DMEM/F12 per well, 800 µL CTK solution was added, followed by 7-9 min incubation at 37 °C. The CTK solution was aspirated when the edges of the colonies started to detach and the cells were then washed twice very carefully with DMEM/F12. Then Trypsin/EDTA was added and incubated for 3 min at 37 °C. Afterwards, mTeSR™1 medium containing ROCK-inhibitor was added, cells were rinsed carefully and transferred into a conical 15 mL tube. The cell solution was centrifuged at 900 rpm for 5 min. The supernatant was aspirated and the cell pellet was resuspended in Differentiation Medium I (Defined Keratinocyte-Serum Free Medium containing 1 µM all-trans retinoic acid, 10 ng/mL BMP4 and 50 µg/mL Normocin). The cell number was determined using a hemocytometer and the cell suspension was adjusted to $1*10^6$ cells per 1 mL. The cells were seeded on Matrigel™ coated plates and dishes at the following density: 150.000 cells per well of a 12well plate (or glass coverslip), 350.000 cells per well of a 6well plate, $2.2*10^6$cells per 10 cm dish. The next day, medium was changed to

fresh differentiation medium and cells were washed carefully with DMEM/F12. On day 4, medium was aspirated, cells were washed twice with DMEM/F12 and fresh Differentiation Medium II (DKSFM supplemented with 50 µg/mL Normocin) was added. Cells were harvested every 5 days for RNA or protein isolation, or were fixed for further stainings. The differentiation was stopped either on day 10 or on day 30.

2.2.5 High-throughput siRNA screen

The knock-down of genes using siRNA is a commonly and frequently used method to determine gene functions. In this experiment a kinome siRNA library (siGenome, Dharmacon) was used to knock down certain kinases during the differentiation of hiPSCs into the epithelial lineage. After 10 days of differentiation, the cells were stained for immunofluorescence against keratin 18 (K18), which is a marker for simple or embryonic epithelia.

2.2.5.1 Seeding and transfecting cells

a384well plates were coated with 10 µL Matrigel™ (see "Thin Matrigel™ coating") per well

384well plates were coated with 10 µL Matrigel™ (see "Thin Matrigel™ coating") per well using a reagent dispenser (Multidrop™ Reagent Dispenser, Thermo Scientific). The plates were sealed with silver foil and stored at 4 °C until use.

SiRNAs (siGenome, Dharmacon) which were used to transfect the cells, were provided in three stock plates in a concentration of 250 nM in a pool of four single siRNAs. After aspirating the Matrigel™ solution, 5 µL of each siRNA was pipetted into the corresponding plate using an automated workstation (Biomek® FX, Beckman Coulter), resulting in three plates per run. Conditions maintaining pluripotency served as negative control (wells D2 to M2) and conditions promoting differentiation served as positive control (wells D3 to M3).

Transfection was performed by mixing 4.95 µL DMEM/F12 with 0.05 µL transfection reagent (Lipofectamine®RNAiMAX Transfection Reagent) (amount for 1 well), incubating for 10 min and adding to the wells using a reagent dispenser. After another 20 min of incubation the plates were ready for seeding the cells.

HiPSCs were dissociated as previously described (see paragraph "2.2.4 Epithelial differentiation protocol"). Two cell suspensions with different media and cell number were prepared:

1) hiPSCs in Differentiation Medium I, 100.000 cells/mL
   a. hiPSCs in mTeSR™1 (supplemented with 50 µg/mL Normocin), 50.000 cells/mL

40 µL of the cell suspensions were added to the plates using a reagent dispenser. The plates were shortly spun down and kept at 37 °C and 5% CO_2. On culture day 5 additional 50 µL medium was added. Instead of Differentiation Medium I, Differentiation Medium II was added to the cells. The cells were cultured until day 10.

2.2.5.2 Fixation and immunofluorescence staining

Fixation, blocking and fluorescence staining were performed using an automated workstation.

After 10 days of differentiation, medium was aspirated and 50 µL of fixation buffer (1xPBS with 4% PFA and 0.2% Triton-x-100) for high-throughput screens (HTS) was pipetted into each well and incubated for 30 min at RT. The fixation buffer (HTS) was aspirated and the cells were washed with 50 µL PBS twice. Then 50 µL blocking buffer (1xPBS with 3%BSA and 0.05% Triton-x-100) (for HTS) was added and incubated for 45 min at RT. The K18 primary antibody dilution was prepared and pipetted into a 384-deepwell plate using a multichannel pipette. This plate was then placed into the automated workstation as a reservoir plate. After aspirating the blocking buffer, the cells were washed with PBS and 10 µL K18 primary antibody diluted in blocking buffer was pipetted from the 384-deepwell plate into the wells. It is to mention that with the automated workstation not the whole liquid in the well can be aspirated, there is a residual amount of about 10 µL remaining. These 10 µL residual amount must be taken into consideration when calculating the dilution of the primary antibody. Thus the concentration must be doubled (1:25 for K18).

The plates were sealed with silver foil and incubated over night at 4 °C. The next day, the antibody solution was aspirated and the cells were washed three times with 50 µL PBS. The secondary antibody (α-mouse Atto 594) was diluted with PBS, just as for the primary antibody the double concentration was used (1:250). In addition, 4´,6-diamidino-2-phenylindole (DAPI, 1 ng/mL) was added to the dilution, for nuclear staining. The dilution was then pipetted into a 384-deepwell plate, which was placed in the automated workstation. There the dilution was added to each well and incubated for 1 h at RT under exclusion of light. After incubation the staining solution was aspirated and the cells were washed four times with PBS. As a last step 20 µL PBS were pipetted into the wells, the plates were sealed with silver foil and stored at 4 °C until imaging.

2.2.5.3 Automated imaging and data analysis

Imaging was performed using an automated BD Pathway 855 Bioimaging System (Becton Dickinson) with a 20x objective (NA: 0.75) and a Hamamatsu digital camera (Orca-ER). Per well 25 fields were imaged for both filters, Hoechst (nuclei staining) and FITC (K18 staining).

Images were analyzed using the Cellprofiler image analysis software Version 2.0. Object selection was based on adaptive intensity and fixed size thresholds for every single object. The segmentation of objects was optimized in order to reach the best resolution even in dense cell clusters. For data analysis, parent objects were segmented in channel 1 (Hoechst), and in channel 2 (FITC) the mean intensity of child objects was measured. Based on the mean intensity of every nucleus, nuclei were categorized into a K18-positive and K18-negative cell, according to the manually set mean intensity threshold. The values of K18-positive cells were used for further analysis. To prevent strong viability effects, wells with less than 1000 cells were excluded from the analysis.

For data analysis, the cellHTS2 software was used. The fraction of K18-positive cells per well were normalized per assay plate and the z-scores were calculated using the R package cellHTS2. The correlation between the data of replicates was estimated using the Spearman rank correlation coefficient.

2.2.6 Transfection of hiPSCs with siRNAs

To examine the role of HIPK4 during the early differentiation of hiPSCs into keratinocyte lineage, HIPK4 was knocked down using a set of four siRNAs. The cells were transfected on day 1 after seeding, and differentiated for 10 days.

The cells were seeded on Matrigel™ coated dishes as described before (see Differentiation of hiPSCs) in Differentiation Medium I. For transfection with siRNAs, transfection reagent was added to DMEM/F12 and incubated for 10 min (for exact amounts, see information below). After incubation time, either the set of four siRNAs against HIPK4 or the non-targeting siControl were added and incubated for 20 min at RT. Then the transfection mix was added to the cells. The final siRNA concentration amounts to 25 nM. After 2 days, medium was aspirated, the cells were washed twice with PBS and fresh Differentiation Medium I was added. At day 4 of differentiation, the medium was aspirated, the cells washed again and cultured in Differentiation Medium II. The medium was changed every 2 days and the cells were harvested either on day 5 and day 10 or only on day 10.

	12well plate (1 well)	6well plate (1 well)	10cm dish
growth area (in cm²)	3.7	9.6	60
cell number	150,000	350,000	$2.2*10^{10}$
transfection mix	108.9 µL DMEM/F12 + 1,1 µL RNAiMAX	217.8 µLDMEM/F12 + 2,2 µL RNAiMAX	1306.8 µL DMEM/F12 + 2.2 µL RNAiMAX
total volume	1.1 mL	2.2 mL	13.2 mL
HIPK4 siRNAs, set of 4 (µL/siRNA)	0.7	1.4	8.3
siControl (in µL)	2.75	5.5	33

2.2.7 Molecular biological methods

2.2.7.1 RNA isolation

For total RNA isolation from cultured cells the RNeasy Mini Kit from Qiagen was used and performed according to manufacturer's protocol. Furthermore, an on-column DNase digestion was carried out using the DNase-Free DNase Set (Qiagen) in order to eliminate contaminating DNA.

In the last step, the RNA was eluted using 30 µL RNAse-free water. The concentration of eluted RNA was measured with a photometer and RNA samples were stored at -80 °C.

2.2.7.2 Reverse transcriptase-polymerase chain reaction

The reverse transcriptase-polymerase chain reaction (RT-PCR) was performed in order to transcribe RNA into cDNA. Therefore, the RevertAid First Strand cDNA Synthesis Kit (Thermo Scientific) was used and performed as directed in the "First Strand cDNA Synthesis" protocol. In every experiment 500 µg RNA were reverse transcribed .The transcribed cDNA was adjusted with nuclease-free water up to 200 µL and used for real-time PCR analysis.

2.2.7.3 Real-time polymerase chain reaction

The real-time polymerase chain reaction (QPCR) method allows quantifying the expression level of genes. For the QPCR 2.5 µL cDNA (preparation described in section "2.2.7.2 The Reverse Transcriptase-Polymerase Chain Reaction") was pipetted in each well of a 96-well plate. Per well following solutions were added 0.15 µL primer-solution (mix of forward and reverse primer, concentration: 10 µM), 5 µL SYBR®Green and 2.35 µL water. The plate was sealed with a foil and spun down.

The experiment was performed using the Applied Biosystems® 75000 Real-Time PCR System. For all experiments the Quantitation – Comparative C_T ($\Delta\Delta C_T$) program type was used with following run methods:

holding stage	50 °C	for 2 min	
	95 °C	for 10 min	
cycling stage	95 °C	for 15 sec	
	60 °C	for 1 min	cycling stage repeated for 40 cycles
melt curve stage	95 °C	for 15 sec	
	60 °C	for 1 min	
	95 °C	for 30 sec	
	60 °C	for 15 sec	

The data were analyzed using the 7500 Software v2.0.5 (Applied Biosystems®).

2.2.7.4 Genome wide expression profiling using Illumina BeadChips®

Genome wide expression profiling using Illumina BeadChip® HumanHT-12 v4 was performed at the Genomics and Proteomics Core Facility at the DKFZ. With this method it is possible to analyze the expression level of 31,000 annotated genes (48,107 genes in total) on one chip in a high-throughput process. For this purpose, RNA was isolated (see paragraph "2.2.7.1 RNA isolation") from normal human keratinocytes (NHK), hiPSCs and cells after 10 days of differentiation. From all samples (respectively three biological replicates per sample) 1 µg RNA was used for the profiling. The following steps were carried out by the members of the Core facility.

In order to determine the quality of the provided RNA, the samples were checked on an Agilent 2100 Bioanalyzer (Agilent Technologies) using the total RNA Nano chip assay. Samples that display a greater RNA index value were used for expression profiling. 500 ng RNA was used for cDNA synthesis. In the next step the Illumina® Total Prep™ RNA Amplification Kit (Life Technologies) was used to amplify/lable the samples in order to synthesize biotin-labeled cRNA, achieved by the addition of biotin-16-UTP (Roche Applied Science). The quality of purified cRNA was determined using the RNA Nano Chip Assay on an Agilent 2100 Bioanalyzer. The first hybridization step was performed at 58 °C with 100 ng cRNA/µL in GEX-HCB Buffer (Illumina) in a wet chamber for 20 h. Spike-in controls for low, medium, and highly abundant RNAs, mismatch control and biotinylation control oligonucleotides were added. The microarray chip was washed with High Temp Wash Buffer (Illumina) at 55 °C followed by two washing steps with E1BC Buffer (Illumina) at RT. In between the washing steps with E1BC Buffer, the microarray chip was washed with ethanol at RT. Next the chip was blocked using 4 mL blocking solution (1% (wt/vol) Blocker Casein in

phosphate buffered saline Hammarsten grade (Pierce Biotechnology) for 5 min, and the signals were developed by a 10 min incubation step in 2 mL Cy3-streptavidin (1 µg/mL; Amersham Bioscience) and 1% blocking solution. Finally the chip was washed with E1BC Buffer, dried and scanned.

The microarray was scanned using the iScan Array Scanner (Illumina). The data were extracted for each bead individually and outliners (>2.5 median absolute deviation) were removed. The remaining values were used to calculate the mean average signal for a give probe, and a standard deviation for each probe was calculated.

For data analysis the received raw data were uploaded to CHIPSTER software. All values (9 in total) were normalized to each other using CHIPSTER. To compare the values of the samples, a three group test (empiricalBayes) was done. Furthermore, the p.value adjustment method BH (Bejamini-Hochberg) was performed and the p.value threshold was set to 0.05. These calculations resulted in a list of 5471 genes. These genes were represented in a heat map, and hierarchically clustered by the added dendrogram (pearson distance method), which was clustered by samples and genes.

The logarithmic fold changes of gene expression of NHK compared to hiPSCs and 10 day differentiated cells compared to hiPSCs were calculated using CHIPSTER.

2.2.8 Protein biochemistry

2.2.8.1 Protein Isolation

To isolate proteins from adherent cells, cells were washed twice with PBS and Trypsin/EDTA was added. After 5 min at 37 °C cells were rinsed with washing medium (DMEM GlutaMAX™ containing 10% FBS) and transferred into a conical 15 mL tube. The cells were centrifuged at 1200 rpm for 5 min and the cell pellet was washed with PBS. After additional centrifugation PBS was aspirated and the cells were lysed with 50 µL lysis buffer (complete Mini tablet in 1xTBS supplemented with 0.1% Triton-x-100) (50 µL for < $5*10^6$cells; 100 µL lysis buffer for > $5*10^6$ cells). The lysate was incubated for 15 min on ice, followed by centrifugation at 13.000 rpm and 4 °C for 15 min. From the protein containing supernatant 10 µL were used to measure the concentration. The remaining protein was frozen at -80 °C.

2.2.8.2 BCA Protein Assay

To measure the concentration of a protein lysate the BCA (bicinchoninic acid) Protein Assay Kit (Thermo Scientific Pierce) was used. A standard curve for bovine serum albumin (BSA) was developed using the purified BSA standard, diluted to obtain following concentrations:

Conc. 1:	2.000 µg/µL	Conc. 6:	250 µg/µL
Conc. 2:	1.500 µg/µL	Conc. 7:	125 µg/µL
Conc. 3:	1.000 µg/µL	Conc. 8:	25 µg/µL
Conc. 4:	750 µg/µL	Conc. 9:	H_2O = Blank
Conc. 5:	500 µg/µL		

Protein samples from the lysed cells were diluted 1:10 and 1:20 with H_2O. 10 µL per sample were added to a well of a 96well plate. Each sample as well as the BSA standard concentrations were measured in duplicates.

To every sample, 196 µL of BCA Reagent A and 4 µL of BCA Reagent B were added (BSA standard and protein samples). The plate was sealed and the solutions were mixed by shaking the plate for 90 sec using an orbital shaker. The plate was then incubated for 30 min at 37 °C. The absorbance was measured using a plate-reader at a wavelength of 560 nm.

The replicated absorbance values of the BCA standard were averaged and the value of the blank was subtracted. Then the mean absorbance values were plotted against the standard protein concentration to generate a standard curve. In parallel the values of the protein samples were averaged, subtracted from the blank and multiplied by the dilution. The slope of the standard curve was used to calculate the concentration of each sample of interest according to its mean absorbance value.

2.2.8.3 SDS page and Western Blot

2.2.8.3.1 Preparation of SDS-polyacrylamide gels

To separate proteins of a sample according to their size, SDS polyacrylamide gel electrophoresis (SDS-page) was performed. For preparing 10% polyacrylamide gels a spacer plate and a short plate were fixed in a casting frame and arranged in a casting stand. First the components of the separating gel were mixed as follows:

H_2O	2 mL
30% Acrylamide	1.65 mL
1.5M Tris, pH 8.8	1.25 mL
10% SDS	50 µL
10% APS	50 µL
TEMED	2 µL

The separating gel solution was applied in between the short glass plate and the spacer plate and rinsed with isopropanol until hardening, then the isopropanol was removed using a piece of filter paper. Then the components of the stacking gel were mixed as follows:

H_2O	1.4 mL
30% Acrylamid	330 µL
0.5M Tris, pH 6.8	250 µL
10% SDS	20 µL
10% APS	20 µL
TEMED	2 µL

The stacking gel solution was carefully pipetted on the separating gel and the combs were immediately inserted into the gel. After hardening the gels were used for electrophoresis.

2.2.8.3.2 Sample preparation

For each sample 25 µg protein were used, 2x Laemmli buffer was added at the appropriate amount and the sample was adjusted to a volume of 20-30 µL with lysis buffer. The probes were spun down and heated at 95 °C for 5 min. The Laemmli buffer contains ß-mercaptoethanol, which reduces the intra and intermolecular disulfide bonds and SDS to denature the proteins. The probes were then loaded on the gel.

2.2.8.3.3 Gel electrophoresis

The polyacrylamide gels were fixed in the electrode assembly module and placed in a tank. Running buffer (25 mM Tris base, 0.19 M glycine, 0.1% SDS in H_2O) was filled into the inner chamber, the space in between the two gels, and in the outside chamber. The combs were carefully removed from the gels. The probes and the protein ladder were then loaded into the wells. The electrophoresis device was plugged on a power supply and electrophoresis was run until the sample dye reaches the bottom of the gel, at 80V.

2.2.8.3.4 Blotting

After electrophoresis, the gel containing glass plates were taken out of the tank. The short glass was carefully lifted and the stacking gel was removed using a spatula. Then the gel holder cassettes were assembled in following order: cathode side, foam pad, 3 pieces of filter paper, gel, PVDF membrane, 3 pieces of filter paper, foam pad, anode side. The PVDF membrane was incubated for 2 min in methanol in order to activate its protein binding capacity, and then washed with water. The gel holder cassette was placed in the electrode. A cooling unit was fixed in the tank, transfer buffer was poured in and the whole tank was placed in a Styrofoam box filled with ice. Blotting was set up for 2h at 60V in order to transfer the proteins from the gel onto the PVDF membrane.

2.2.8.3.5 Antibody staining and developing

After the successful transfer of proteins from the gel onto the PVDF membrane, the membrane was removed from the gel holder cassette. In order to block non-specific antibody binding, the membrane was incubated in blocking buffer (1xTBS with 0.02 Tween 20 and 5% milk powder) (for western blot) for 1h at RT on an orbital shaker. The membrane was then placed into a conical 50 mL tube. Primary antibody was diluted in 10 mL in blocking buffer, and added to the membrane (used antibodies and concentrations are described in section “2.1.6 Primary Antibodies”). The membrane was incubation in antibody solution over night at 4 °C on a roller mixer. The next day the membrane was washed three times for 10 min with washing buffer (1xTBS, 0.02% Tween 20) on an orbital shaker. Then the secondary antibody was diluted in 10 mL blocking buffer and incubated for 1 h at RT while shaking. The membrane was washed three times for 10 min with washing buffer on an orbital mixer.

To detect the antibody binding Amersham™ ECL™ Prime Western Blotting Detection Reagent (GE™ Healthcare) was used. It is a chemiluminescent substrate to detect the horseradish peroxidase activity of the secondary antibody. For this treatment Solution A and

Solution B were mixed at the ration of 1:1, poured on the membrane and incubated for 1 min while shaking. The membrane was then transferred into an autoradiography cassette. The evaluation of the signal intensity was performed by exposing a photographic film (Amersham Hyperfilm™ ECL).

To control if every lane owns the same amount of loaded protein loading controls were set up. Therefore an additional antibody staining was performed on the same membrane by using a primary antibody against the housekeeping gene ß-actin. The staining and development of the film was performed as described above.

2.2.8.4 Immunofluorescence staining of cells

For immunofluorescence stainings, cells grown on coverslips were washed twice with PBS in order to remove dead and floating cells. Cells were fixed with 4% paraformaldehyde in PBS for 30 min. After incubation cells were rinsed three times with PBST (0.1% Triton-x-100 in 1x PBS).

Cells were then treated with blocking buffer (3% BSA, 0.1% Triton-x-100 in 1x PBS) (for immunofluorescence stainings, IF) for 45 min to prevent unspecific antibody binding. Primary antibodies were diluted in blocking buffer (for antibody dilutions see “Material” part). 500 µL antibody-solution was added per coverslip and incubated over night at 4 °C. The primary antibody solution was aspirated and cells were washed three times for 5 min with PBST. The secondary antibody was diluted in blocking buffer 1:1 with PBS, 500 µL per coverslip were added and incubated for 1 h at room temperature, under exclusion of light. After aspirating the secondary antibody solution, cells were rinsed three times with PBS. Stainings of the nuclei were performed with 4´,6-diamidino-2-phenylindole (DAPI) fluorescent stain. In PBS diluted DAPI (1 µg/mL) was added to the cells and incubated for 5 min, followed by three washing steps with PBS. For permanent preservation of stained cells, object slides were labeled and coverslips were fixed with mounting medium on the object slides. Imaging was performed using an inverted microscope (Nikon).

2.2.8.5 Flow cytometry analysis

Flow cytometry is a method used for sorting and counting cells by size, granularity or the expression of certain markers after fluorescence staining. It is a laser-based method, where single cells in suspension are passing the lasers in a fluid stream, allowing them to analyze their characteristics, including size, granularity or fluorescent tag.

To prepare the cells for the staining, the FIX&PERM® cell permeabilization kit (ADG) was used and performed according to manufacturer´s protocol, with minor changes.

Grown cells were washed twice with PBS and Trypsin/EDTA was added to the cells. After 5 min at 37 °C, washing medium (DMEM GlutaMAX™ containing 10% FBS) was added, the cells were rinsed and transferred into a conical tube. After centrifugation for 5 min at 1200 rpm the supernatant was aspirated, the pellet was resuspended in PBS, the cell number was determined using a hemocytometer. The samples were then divided in order to prepare three conditions for each sample: non stained cells, cells stained only with the secondary antibody and cells stained with primary and secondary antibody. After an additional centrifugation step the pellets were resuspended in 100 µL Reagent A

(fixation reagent, provided with the kit) and incubated for 15 min at RT. Then, 5 mL PBS were added to each sample in order to dilute the fixation reagent, and the cells were spun down for 5 min at 1200 rpm. In the meantime the primary antibody K18 was diluted 1:50 in Reagent B (permeabilization reagent, provided in the kit). The supernatant was aspirated, the cells were resuspended in 100 µL Reagent B/primary antibody dilution and incubated for 30 min at RT. After incubation, 5 mL PBS were added and the samples were spun down, washed with PBS and again spun down. The secondary antibody was diluted in Reagent B (1:500), and 100 µL of this dilution was added to the cells, followed by 30 min incubation at RT. The cells were then washed twice with PBS and passed through a 70 µm cell strainer. This step is important in order to avoid cell clumps, which block the cell stream during flow cytometry. The cells were then again centrifuged and resuspended in 500 µL FACS buffer (PBS supplemented with 2% BSA and 0.2% sodium azide) and transferred into a 5 mL FACS tube. The samples were measured with the BD FACSCanto™II cell analyzer using the BD FACSDiva™ Software and analyzed with FlowJo Analytical Software.

2.2.9 Teratoma assay

2.2.9.1 Sample preparation and injection

The teratoma assay is a very stringent test to verify the pluripotency of stem cells and reprogrammed cells.

HiPSCs were cultured on thin Matrigel™ coated (see section “2.2.2.2.1 Thin Matrigel™ coating”) 10 cm cell culture dishes in mTeSR™1 medium (supplemented with 50 µg/mL Normocin™). The cells were rinsed twice with DMEM/F12, CTK solution was added to the cells and incubated for 7 min at 37 °C. The CTK solution was aspirated and the cells were washed twice with PBS. Then 840 µL ice-cold PBS were added to the colonies, which were then scraped in order to detach them from the cell culture plate, while preserving the colony formation. One 50-80% confluent 10 cm cell culture dish yielded six injections of 140 µL. The cell clump suspension was divided into six aliquots of 140 µL, and 60 µL undiluted Matrigel™ (30%) were added to the aliquots. The aliquots were kept on ice until injection to prevent Matrigel solidification.

Two NOD-SCID mice were held and 200 µL were injected subcutaneously into each flank. After 12 weeks the mice developed teratomas. They were sacrificed, dissected and the teratomas were carefully removed. Teratomas were fixed in 4% formaldehyde overnight, and paraffin embedded as described in the following paragraph.

2.2.9.2 Paraffin embedding and hematoxylin and eosin staining of teratomas

The isolated teratomas were fixed in 4% formaldehyde at RT overnight. Embedding in paraffin requires processing of the tissue. Therefore the teratomas were placed in a Tissue Processor (Leica), were the dehydration, clearing, and infiltration with paraffin takes place. Dehydration is ensured by incubating the tissue in baths of progressively increasing alcohol concentrations followed by the paraffin infiltration steps in the following order:

10% formalin	1.5 h
10% formalin	1.5 h
70% ethanol	1.5h
80% ethanol	1.5 h
96% ethanol	1.5 h
99% ethanol	1.5 h
99% ethanol	1.5 h
xylene	1.5 h
xylene	1.5 h
paraffin 55 °-65 °C	1.5 h
paraffin 55 °-65 °C	1.5 h
paraffin 55 °-65 °C	1.5 h

After removing the samples from the Tissue Processor, they were placed in a metal box, which serves as a frame for the embedding. The tissue was then doused with paraffin and left to cool down for 30 min. After paraffin hardening, the metal frame was removed and 1 µm thick sections were prepared using a microtome.

The hematoxylin and eosin (HE) staining is a routinely and most widely used staining in hematology. It serves to distinguish different structures of tissues. The staining based on the addition of hematoxylin, which stains basophilic structures, including the nuclei. After applying hematoxylin the nuclei show a brownish-red color. The addition of water increases the pH and leads to a color change into blue. The second dye is eosin, which stains eosinophilic structures, like the cytoplasm, in various shades of red. The staining steps were performed in following order:

xylene	10 min
99% ethanol	5 min
95% ethanol	5 min
70% ethanol	5 min
hematoxylin	3 min
dH_2O	5 min
4% acetic acid	90 sec
eosin	90 sec
dH_2O	5-10 sec
70% ethanol	5 min
96% ethanol	5 min
99% ethanol	5 min
xylene	5 min

In the last step the sections were mounted with Eukitt® mounting medium.

3 Results

3 Results

3.1 Pluripotency verification of reprogrammed cells

Induced pluripotent stem cells offer a great promise for therapeutic purposes, especially because of their ability to differentiate into all cells of the mammalian body. In order to use reprogrammed cells, they have to be examined for their pluripotency, their ability to differentiate into all cells of the mammalian body and their ability to self-renew indefinitely. Therefore, a number of required tests have to be performed to prove their pluripotent state and to demonstrate their similarity to human embryonic stem cells (hESCs). In a first step the morphology of the generated hiPSC line D1 was examined. HESCs grow in colonies of small cobblestone-like cells and are tightly packed with sharp edges. During the reprogramming process and also after establishing stable hiPSCs lines, the cells were investigated for their morphology. Figure 3 shows the generated hiPSC line D1. The cells had the desired morphology of sharp-edged colonies with small cobblestone like cells.

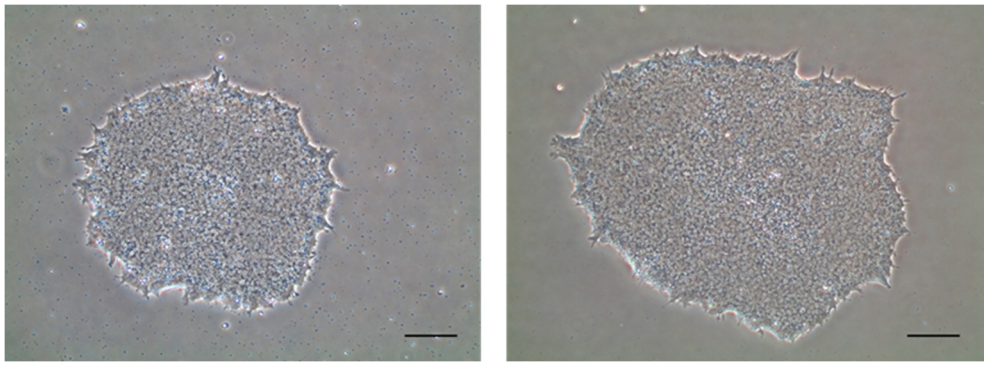

Figure 3: Bright field images of hiPSC line D1. Scale bar: 100 µm

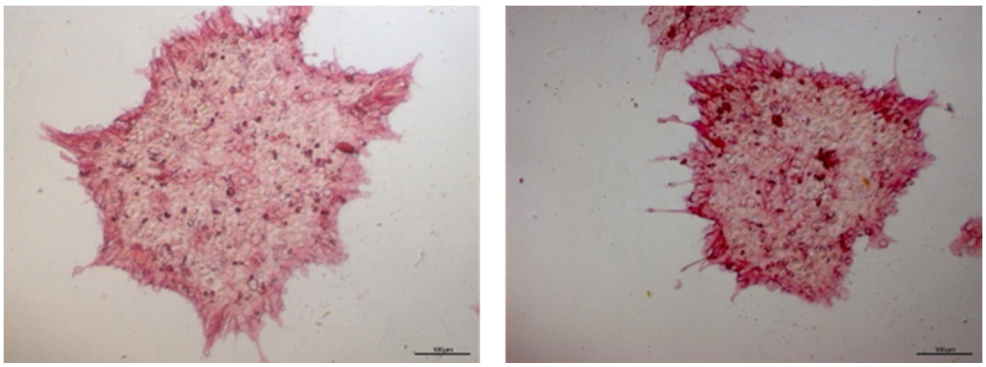

Figure 4: Alkaline phosphatase staining of hiPSC line D1. Scale bar: 100µm

Pluripotent cells also display elevated levels of alkaline phosphatase on their cell membrane (Martí et al., 2013), which serves as a marker for pluripotency. Figure 4 shows the positive alkaline phosphatase staining of the hiPSC line D1.

During the reprogramming process, the RNA expression levels of certain genes alter. Stem cells display the expression of certain pluripotency-associated markers. Figure 5 shows the expression levels of pluripotency-associated markers LIN28, SOX2, REX1, TERT and NANOG of the generated hiPSC line D1 compared to NHKs, analyzed by QPCR. Furthermore, the cells were tested for the expression of pluripotency-associated genes on protein level. Immunofluorescence stainings performed on fixed hiPSC line D1 showed the expression of OCT4, NANOG, SSEA4, TRA-1-60 and TRA-1-81 (Figure 6). OCT4 and NANOG were localized in the nucleus, whereas SSEA4, TRA-1-60 and TRA-1-81 are surface markers. Immunofluorescent stainings of the hiPSC line D1 showed clear expression of all tested markers, as a proof for their pluripotency.

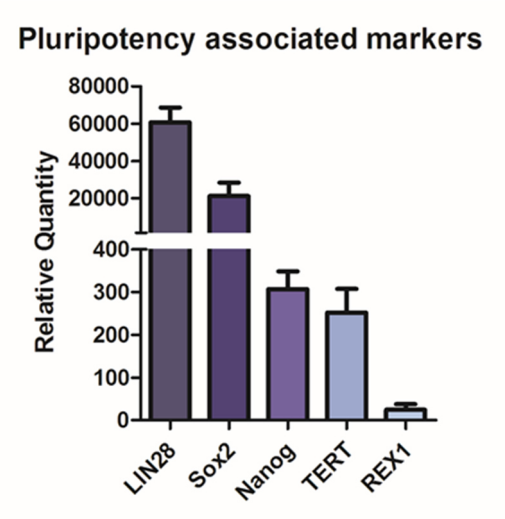

Figure 5: Expression quantities of pluripotency associated markers in hiPSCs compared to NHKs. QPCR expression analysis of SOX2, LIN28, REX1, TERT and NANOG in human induced pluripotent stem cells (hiPSCs). Normalized to GAPDH. Normal human keratinocytes were used as a reference sample.

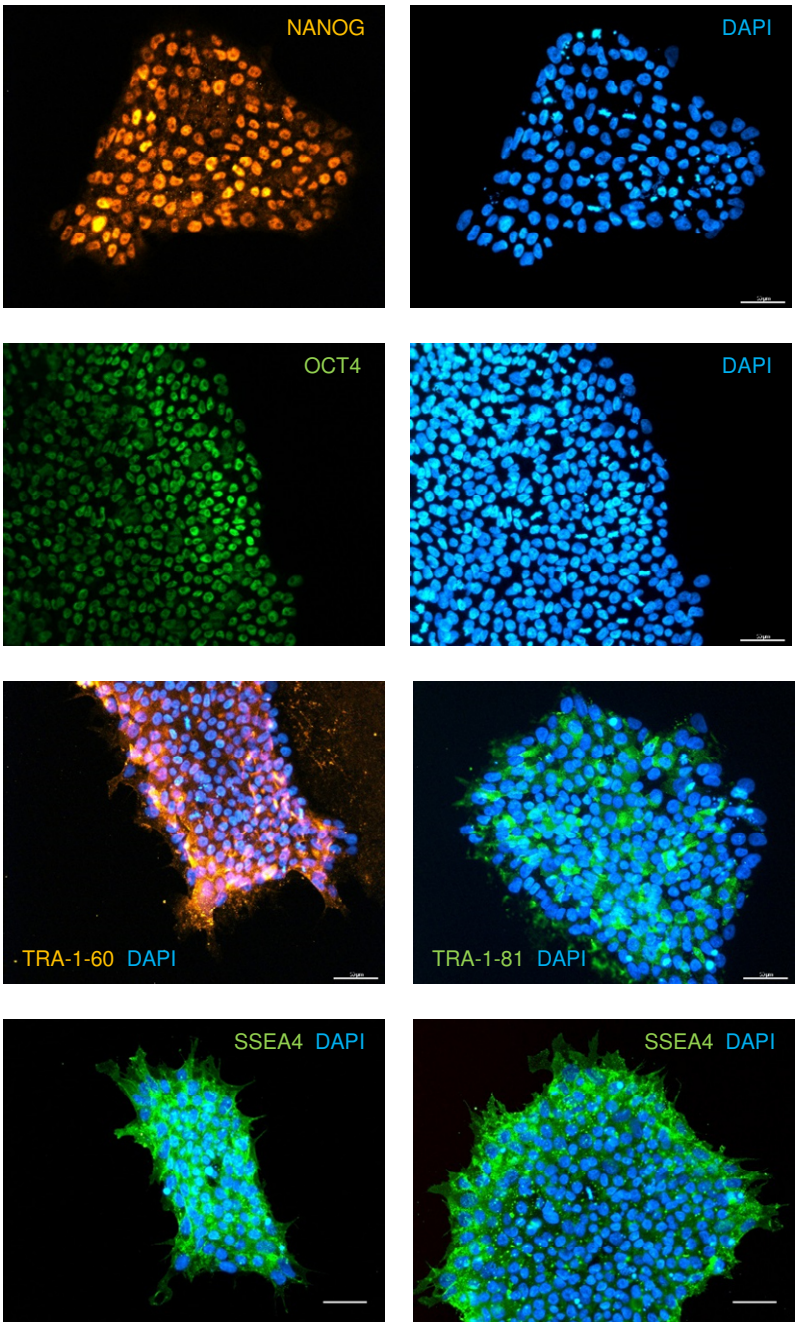

Figure 6: Immunofluorescence stainings of pluripotency associated markers on human induced pluripotent stem cell colonies. The images show nuclear NANOG and OCT4 stainings and the corresponding staining of the nucleus. The staining images for the surface markers TRA-1-60, TRA-1-81 and SSEA4 are merged with the nuclei staining. Nuclei were stained with 4′,6-Diamidin-2-phenylindol (DAPI). Scale bars are 50 µm.

The most stringent of the pluripotent state of a cell is the teratoma assay. HiPSCs D1 were injected, as previously described (“2.2.9 Teratoma assay”), subcutaneously into the flanks of two NOD-SCID mice. Both mice developed teratomas after three months (Figure 7A). The teratomas were fixed, paraffin embedded and the prepared sections were stained for H&E. The teratomas contained pigmented cells and epidermal structures, representing the ectodermal lineage (Figure 7B, first row). Furthermore, muscle fibers and cartilage, originating from the mesoderm and gut-like epithelium with endodermal origin, were detected.

The performed experiments proved the pluripotent state of the generated hiPSCs on RNA and protein level and in an *in vivo* experiment.

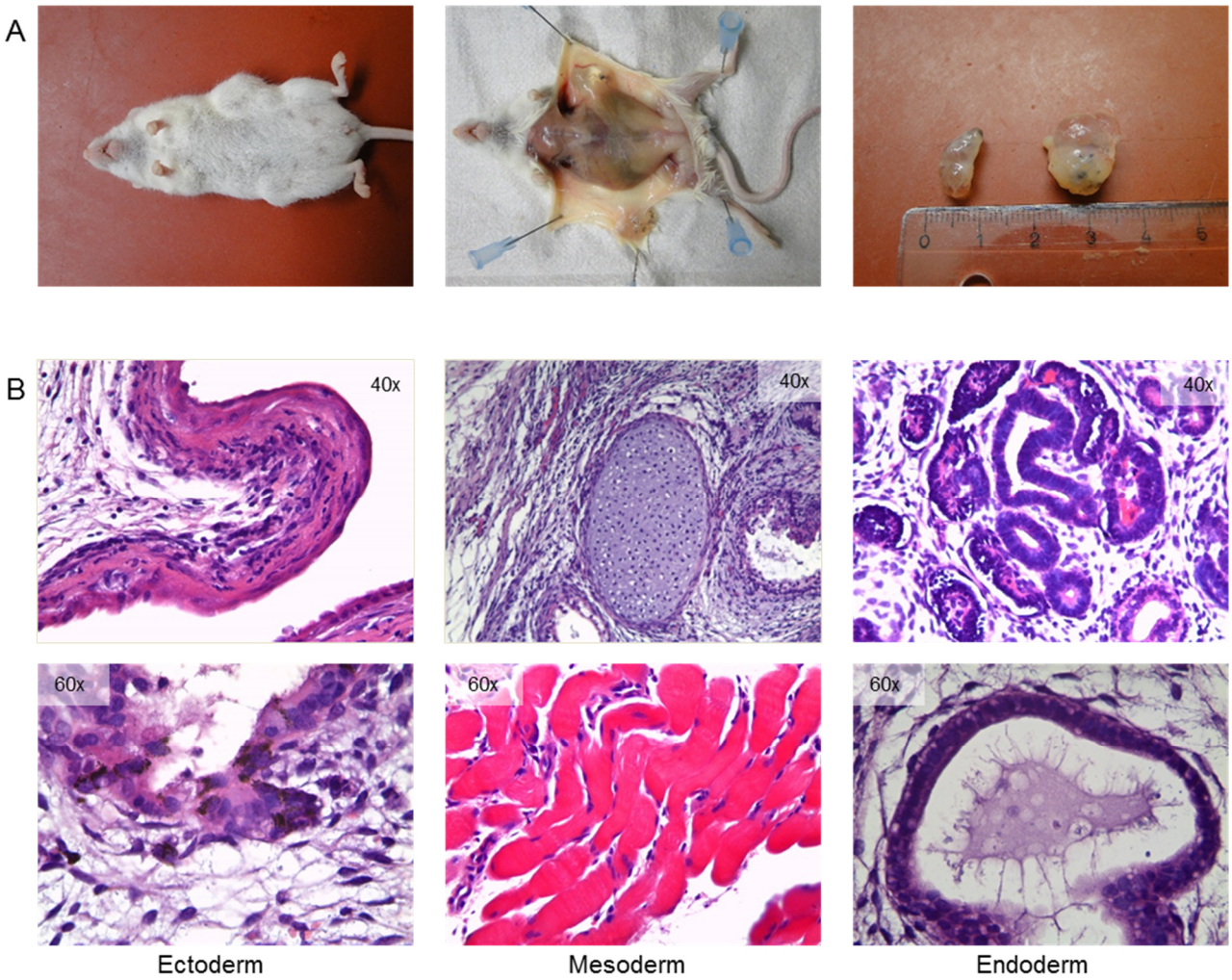

Figure 7: Teratoma assay indicating the pluripotent state of injected human induced pluripotent stem cells (hiPSCs). (A) HiPSCs were injected subcutaneously into an immunodeficient mouse. The mouse was sacrificed after teratomas developed. The teratomas were excised and the size was measured. (B) Hematoxylin and eosin staining of teratomas. The excised teratomas were fixed and paraffin embedded. Sections were prepared and Hematoxylin and eosin stained. Shown are selected parts of ectodermal, mesodermal, and endodermal tissue. Magnifications were 40x for the upper panel, 60x for the lower panel.

3.2 Differentiation of human induced pluripotent stem cells into keratinocytes

In the field of dermatology, the differentiation of hiPSCs into keratinocytes is of particular interest, in order to generate skin equivalents. Therefore, hiPSCs were differentiated into keratinocytes, according to the differentiation protocol of Itoh and colleagues (Itoh et al., 2011) with minor changes (changes are described in section “2.2.4 Epithelial differentiation protocol”). Figure 8 shows the differentiation procedure. Cells were differentiated for 30 days, and harvested every 5 days for RNA isolation or fixed for further stainings. In addition, cells were imaged every 5 days, to record the differentiation progress (Figure 9).

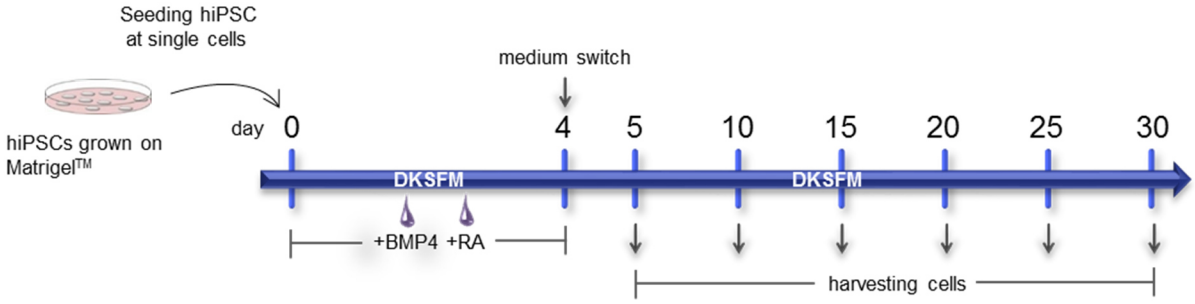

Figure 8: Schematic illustration of differentiation experiment. HiPSCs were seeded at single cells and differentiated for 30 days. Cells were harvested every 5 days.

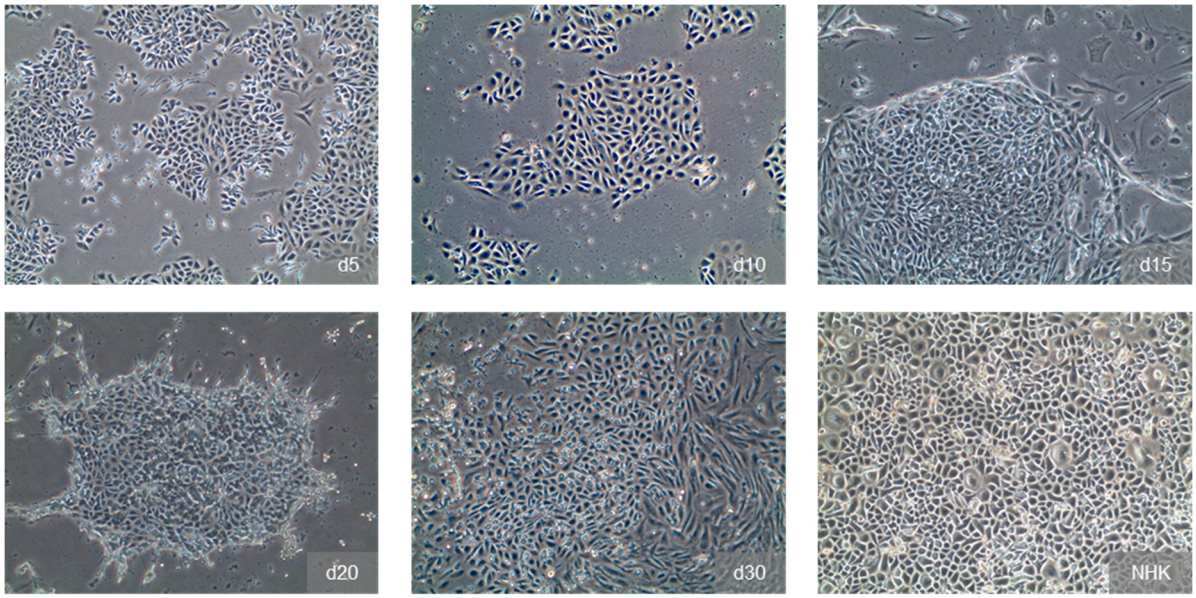

Figure 9: Bright field images of differentiated cells derived from human induced pluripotent stem cells. Shown are cells imaged at different time points, and normal human keratinocytes (NHK) for comparison. Magnification 10x.

Bright field images of the differentiating cells showed changes in morphology. Already at day 5 the morphology resembled that of epithelial cells rather than hiPSCs. To prove that the cells also undergo molecular changes, the expression of pluripotency-associated as well as keratinocyte markers was determined by QPCR. Figure 10A shows the QPCR results of one differentiation experiment, representative of three performed experiments. The data showed a clear decrease in expression of pluripotency-associated markers SOX2 and LIN28. While the expression of SOX2 on day 0 (represents undifferentiated hiPSCs) was 18,000 fold higher compared to NHK, it decreased strongly to a 3600 fold change on day 5, 236 fold change on day 10, and to a not detectable expression on day 30. The expression of the pluripotency-associated marker LIN28 displayed a similar tendency, showed a strongly decreasing expression, but remained ~25fold increased compared to NHK.

While the expression of pluripotency-associated markers diminished during the differentiation, the cells started to express epidermal markers (Figure 10B). Keratin 8 (K8) and keratin 18 (K18) are usually expressed by simple, single layered epithelia and during the embryonic development of the epidermis before stratification begins. During the *in vitro* differentiation of hiPSCs, the cells began to express K8 and K18, and the levels of both genes rose until day 15. From day 15, expression of K8 and K18 was replaced by the expression of another pair of keratins, keratin 5 (K5) and keratin 14 (K14). During embryonic development, the epidermis displays a single-layered epithelium, with cells expressing K8 and K18. As soon as the stratification begins, these keratins are replaced by K5 and K14, which are expressed in the basal layer of the stratified epithelium. Furthermore, differentiated hiPSCs at d5 started to express p63, which is an important regulator of keratinocyte differentiation, and responsible for the switch from K8 and K18 to K5 and K14 (Koster et al., 2004a).

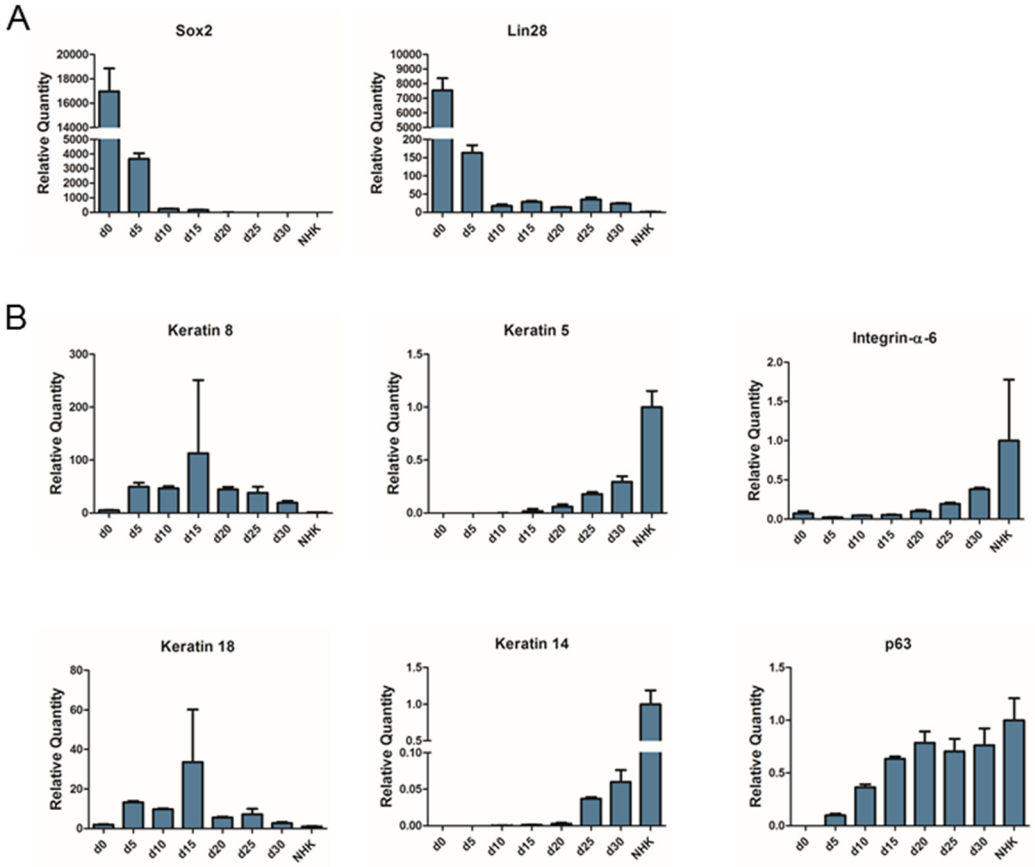

Figure 10: QPCR analysis of cells at several differentiation steps. (A) Relative expression quantities of SOX2 and LIN28 during differentiation. (B) Expression levels of keratin 8, keratin 18, keratin 5, keratin 14, integrin-α-6 and p63. Normalization with GAPDH, all values are relative to normal human keratinocytes (NHKs).

To demonstrate the expression of keratinocyte markers on protein level, immunofluorescence stainings of differentiated cells at several time points were performed (Figure 11). As already proved by QPCR, the cells showed a clear nuclear staining for p63 beginning on day 5, and K14 staining on day 20. In addition, markers for suprabasal layers, including involucrin (Inv) and keratin 1 (K1), could be detected on day 25.

To further prove that the differentiation protocol drives the cells towards a keratinocyte fate, a genome wide gene expression analysis (Microarray) was performed, to compare hiPSCs, cells differentiated for 10 days and NHK. All statistically significant genes (p.value ≤ 0.05) are displayed in a heatmap, hierarchically clustered in a dendrogram, as shown in figure 12. The analysis demonstrated that, as expected, the biological replicates grouped together. Furthermore, differentiated cells still clustered closer to hiPSCs than to NHK. This result was not surprising, since cells differentiated for 10 days still represent a progenitor stage.

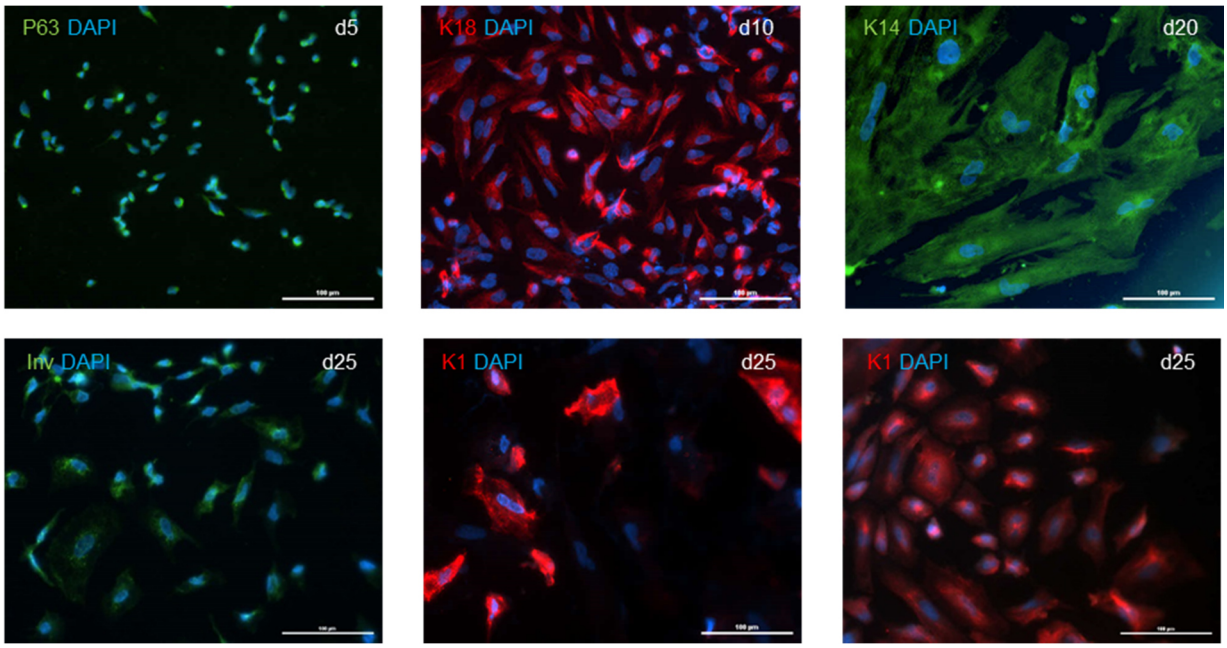

Figure 11: Immunofluorescence images of hiPSC-derived keratinocytes at several differentiation steps. Antibodies against keratinocyte markers p63, keratin 18 (K18), keratin 14 (K14), involucrin (Inv) and keratin 1 (K1) were used. Nuclei were stained with DAPI. Scale bars: 100 µm.

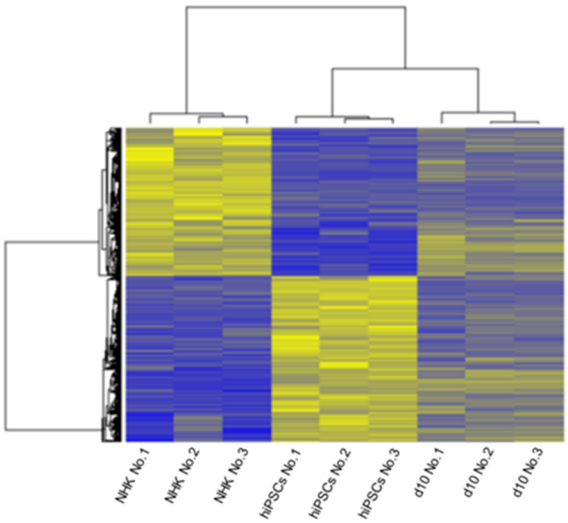

Figure 12: Dendrogram based on gene expression array results. Gene expression analysis of normal human keratinocytes (NHK), human induced pluripotent stem cells (hiPSCs) and cells differentiated for 10 days (d10), in biological triplicates. Heatmap of statistically significant genes, hierarchically clustered in a dendrogram.

In order to investigate the genes that are correlated to pluripotency and keratinocyte development, genes of interest were selected from the list of all statistically significantly regulated genes, and the fold changes were calculated (Figure 13). Pluripotency-associated genes, including SOX2, ZIC3 LIN28a or LIN28b, were significantly downregulated in differentiated cells compared to hiPSCs, and in NHK compared to hiPSCs. In addition, keratinocyte markers, including integrin-ß1 (ITGB1), TP63 or collagenVII were upregulated in differentiated cells and NHK compared to hiPSCs.

Taken together, a differentiation protocol was established and hiPSCs could be differentiated into early keratinocytes. Regarding the gene expression, the generated cells showed an upregulation of epithelial/keratinocyte markers, whereas the pluripotency-associated markers diminished.

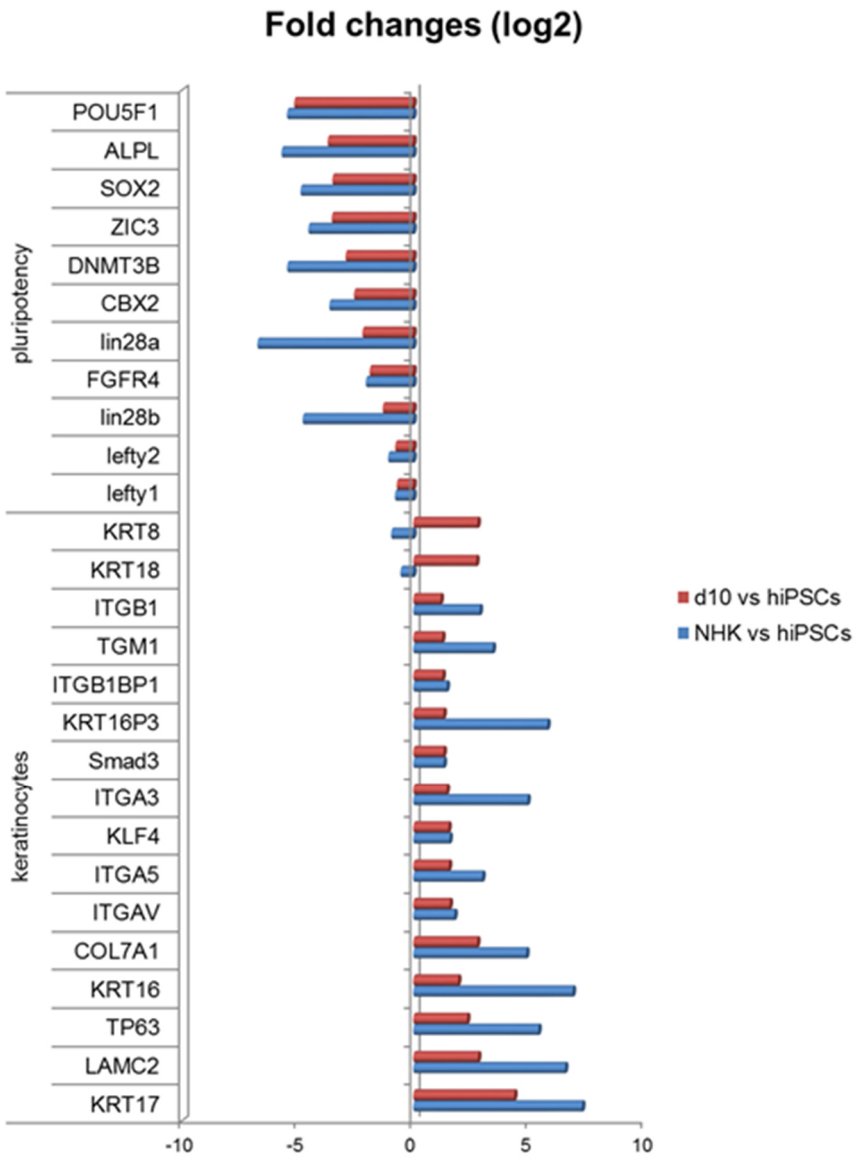

Figure 13: Significant fold changes of pluripotency associated genes and keratinocyte markers. Compared are fold changes in cells differentiated for 10 days (d10) and human induced pluripotent stem cells (hiPSCs) (red) and normal human keratinocytes (NHK) were compared to hiPSCs (blue).

3.3 High-throughput siRNA screen of differentiating human induced pluripotent stem cells

The expression of a specific protein can be knocked-down by transfecting cells with siRNAs. The siRNAs bind specifically to the mRNA with the complementary sequence (RNA interference) and thereby induce its degradation. The knock-down of genes is a common method to analyze their function. This method can help to find relevant factors or new pathways that are important for differentiation process. Furthermore, siRNA knock-down can be scaled up to high-throughput which enables the analysis of a lot of genes in one experiment.

The aim was to adapt the differentiation of hiPSCs into early epithelial cells to a high-throughput siRNA screen.

For the high-throughput siRNA screen, cells were seeded as single cells on 384well plates and transfected with the kinome siRNA library of ~800 siRNAs (siGenome, Dharmacon) (Figure 14). The cells were differentiated for 10 days under these conditions.

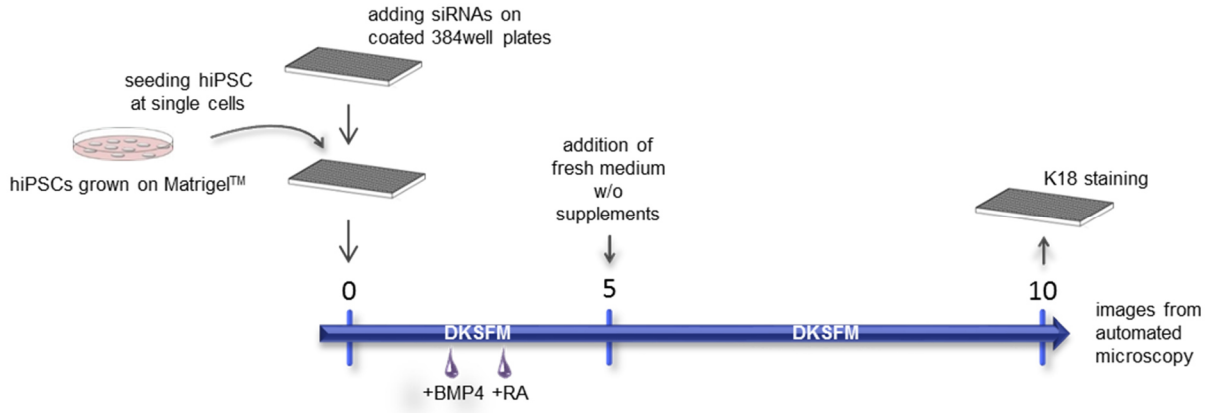

Figure 14: Schematic diagram of screen work flow. HiPSCs were seeded at single cells on siRNA containing 384well plates. Fresh medium was added on day 5. The cells were differentiated for 10 days followed by immunofluorescence staining against keratin 18 (K18). Cells were imaged by automated microscopy.

For the read-out the cells were stained against K18. K18 is usually expressed in simple, single layered epithelia and during embryonic development of the epidermis, before the epidermis begins to stratify. *In vitro* differentiation experiments presented before revealed that K18 was expressed at day 10, and it therefore represents a suitable marker to follow epithelial progenitor development. After imaging the stained cells, the number of K18 positive cells was determined, the values were normalized per assay plate and the z-scores were calculated (cellHTS2 software). The z-score represents the relationship of a certain sample to the mean of a group and thus generates a hit list of all used conditions .Figure 15A displays the distribution of the positive and the negative controls in the screens. The positive control yielded a mean value of 8.6% K18 positive cells and the negative control 0.5%. Furthermore, figure 15B shows the distribution of the controls by their z-scores, which indicates a clear distinction between positive and negative control.

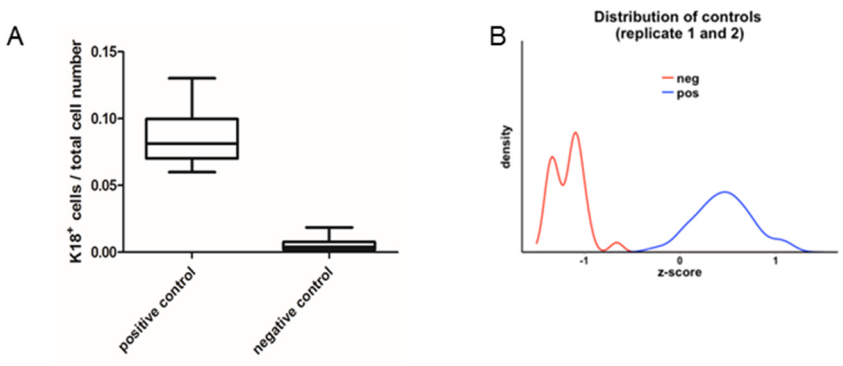

Figure 15: High-throughput siRNA screen analysis. (A) The boxplot depicts the ratio of the keratin 18 positive cells ($K18^+$) and the total cell number in the positive and the negative control. (B) Distribution of the positive and negative controls.

Up next, the z-score distribution of all siRNAs was investigated. As shown in figure 16, the negative (red) and positive (blue) samples grouped together, the positive controls at a value of -1 and the negative controls at a value of 1.3. Samples with a z-score lower than the positive control displayed higher amounts of K18 cells, and were of major interest. The top 50 candidates, with the lowest z-scores were investigated for their morphological differences compared to the positive controls. Figure 17 shows the immunofluorescence staining of the candidates HIPK4 and ADCK2, and the positive control for comparison.

Cells treated with siRNA against HIPK4 displayed a bigger cytoplasmic portion, more K18 fibers and fewer colonies of unstained cells, compared to the positive control. In contrast, nearly no K18 signals were detected in cells transfected with siRNA against ADCK2. HIPK4 was chosen for further analysis, due to the obtained screen results and because of the described morphological changes. It was of interest, to further analyze the role of HIPK4 during the epithelial determination.

In summary, the high-throughput screen is an effective method to screen numerous factors in a short time period. The high-throughput screen performed during the differentiation of hiPSCs into an epithelial lineage resulted in a list of potential candidates, for example HIPK4 and ADCK2, which are suggested to influence the differentiation process.

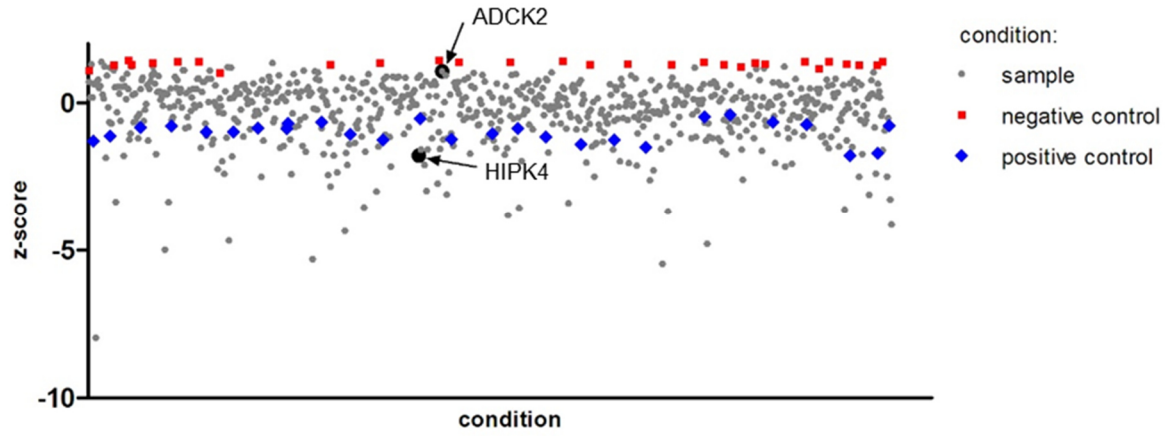

Figure 16: Distribution of the z-score values of all siRNAs. Blot includes negative (red) and positive (blue) controls. Arrows mark HIPK4 as a sample with increased numbers of keratin 18 positive cells, indicated by a lower z-score, and ADCK2 with decreased numbers of keratin 18 positive cells, indicated by a higher z-score.

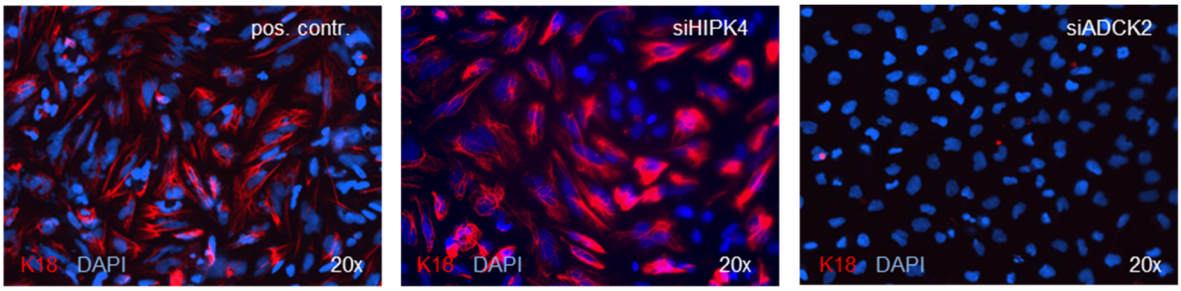

Figure 17: High-throughput siRNA screen read-out. Not transfected cells (positive control), cells transfected with siRNA against HIPK4 and against ADCK2 were differentiated for 10 days. These cells were then stained for keratin 18 (K18, red) and DAPI (nuclei stain, blue). Magnification: 20x.

3.4 Investigating the role of HIPK4 during early epithelial differentiation

3.4.1 The effect of HIPK4 knock-down on keratin 18 expression during early epithelial differentiation

After choosing HIPK4 as a candidate of interest, detailed investigations were performed. First the expression of HIPK4 during 30 days of differentiation was analyzed. Figure 18 shows the expression levels of HIPK4 during the differentiation process. Compared to NHK, hiPSCs (d0) showed an increased expression of HIPK4. The expression level decreased slightly until day5, but increased again until reaching a peak on day 15. After day 15 the expression levels declined again.

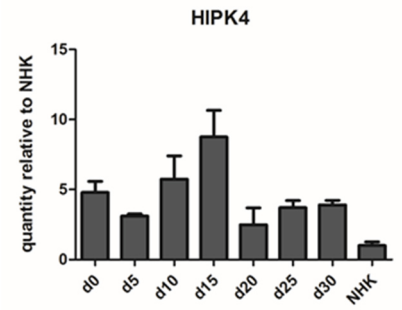

Figure 18: HIPK4 expression values during in vitro differentiation of hiPSCs into keratinocytes. Normalized to GAPDH and 18S. Reference sample NHK.

In order to validate the knock-down efficacy of the siRNA against HIPK4 on protein level, the differentiation with HIPK4 siRNA transfected hiPSCs was repeated in larger scale and protein was isolated at different time points. Figure 19 depicts the performed experiment. HiPSCs were dissociated into single cells and seeded on Matrigel™ coated cell culture plates. The next day, the cells were transfected with a pool of four siRNAs against HIPK4 and a pool of non-targeting siRNAs and differentiated for 10 days. The Cells were harvested on day 5 and day 10 and protein was isolated at both time points. Figure 20 shows a clear knock-down of HIPK4 compared to the control on day 5 of differentiation, detected by western blot. The transfection with siRNAs is transient, thus the knock-down effect lasts for a limited time. Because of that, a slight increase in protein expression was detected on day 10. ß-Actin served as a loading control.

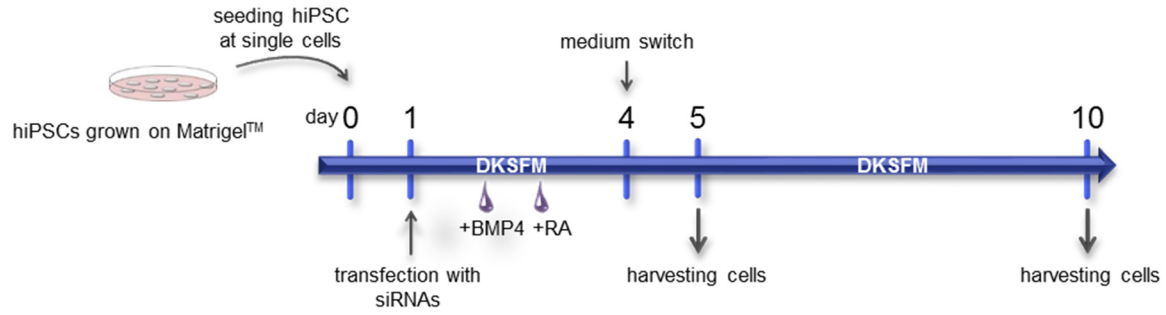

Figure 19: Illustration of the experimental set-up. HiPSCs were seeded at single cells on Matrigel™ coated plates. The next day cells were transfected with siRNAs. On day 4 medium was switched to defined keratinocyte serum free medium (DKSFM) without BMP and retinoic acid (RA). Cells were harvested on day 5 and day 10.

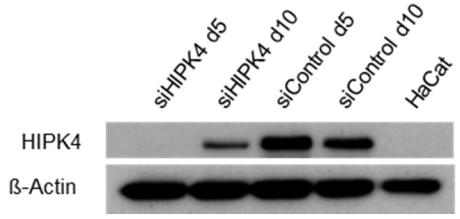

Figure 20: Western blot analysis of cells transfected with HIPK4 and non-targeting (control) siRNA. Cells were differentiated and harvested on day 5 and 10. Loading control: ß-Actin. Negative control: HaCat cells.

Figure 21 shows the QPCR analysis of differentiated cells which were either transfected with the pool of four HIPK4 siRNAs (blue bars), a pool of non-targeting siRNAs (siControl, yellow bars) or non-treated cells (gray bars). As already mentioned, the knock-down of HIPK4 was transient. Cells transfected with HIPK4 siRNAs expressed half as much HIPK4 compared to cells transfected with the non-targeting control. This effect was not persistent until day 10, where the expression level of HIPK4 was similar under both treatment conditions. The analysis revealed further that the knock-down of HIPK4 during early epidermal differentiation led to a significant increase of K8 and K18 expression, compared to the control- or non-treated cells. In addition, also the expression levels of K5 and K14 were significantly increased when cells were treated with siRNA against HIPK4. The depicted graphs demonstrate one experiment representative for three biological replicates.

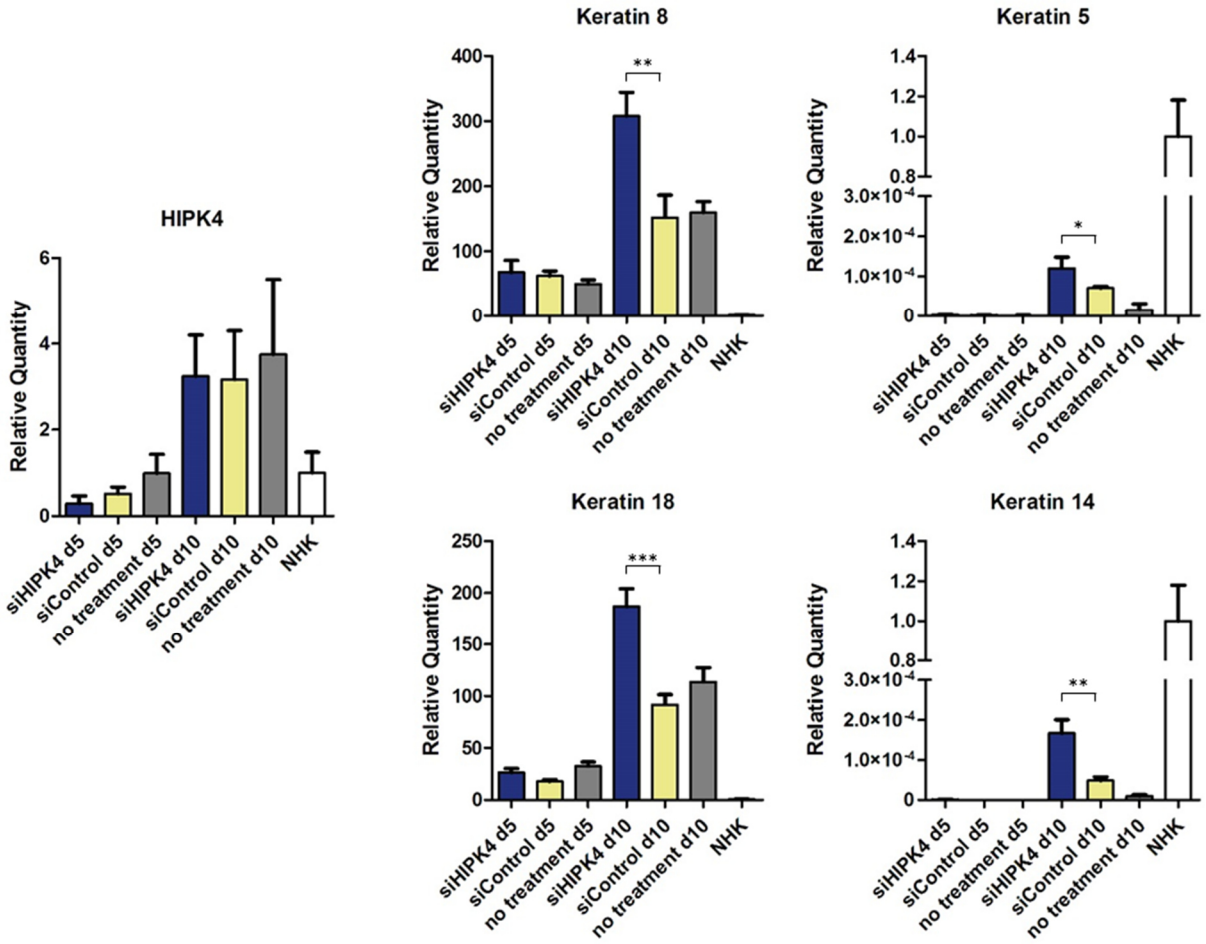

Figure 21: Expression values of keratinocyte markers in differentiated hiPSCs upon HIPK4 knock-down. Relative quantities of HIPK4, keratin 8, keratin 18, keratin 5, and keratin 14 RNA in cells differentiated for 5 and 10 days and transfected with HIPK4 siRNA (siHIPK4 d5, siHIPK4 d10), non-targeting siControl (siControl d5, siControl d10), and not treated cells (no treatment d5, no treatment d10). Normalized to GAPDH and 18S. Normal human keratinocytes (NHK) served as reference sample. Shown are results of one experiment, representative for 3 biological replicates. **: p.value < 0.01; ***: p.value <0.001.

Furthermore, differentiated cells were investigated for their expression of K18 antigens by flow cytometry. Figure 22 depicts flow cytometry analysis of untreated cells, cells transduced with a non-targeting siRNA (siControl) and transduced with siRNAs against HIPK4 (siHIPK4) after 10 days of differentiation. Unstained cells and secondary antibody stained cells were measured to set the gates.

The analysis confirmed the previous findings by showing an increased number of K18 positive cells (17.1%) compared to the siControl treated cells (11%) and the untransfected (untreated) cells (8.92%).

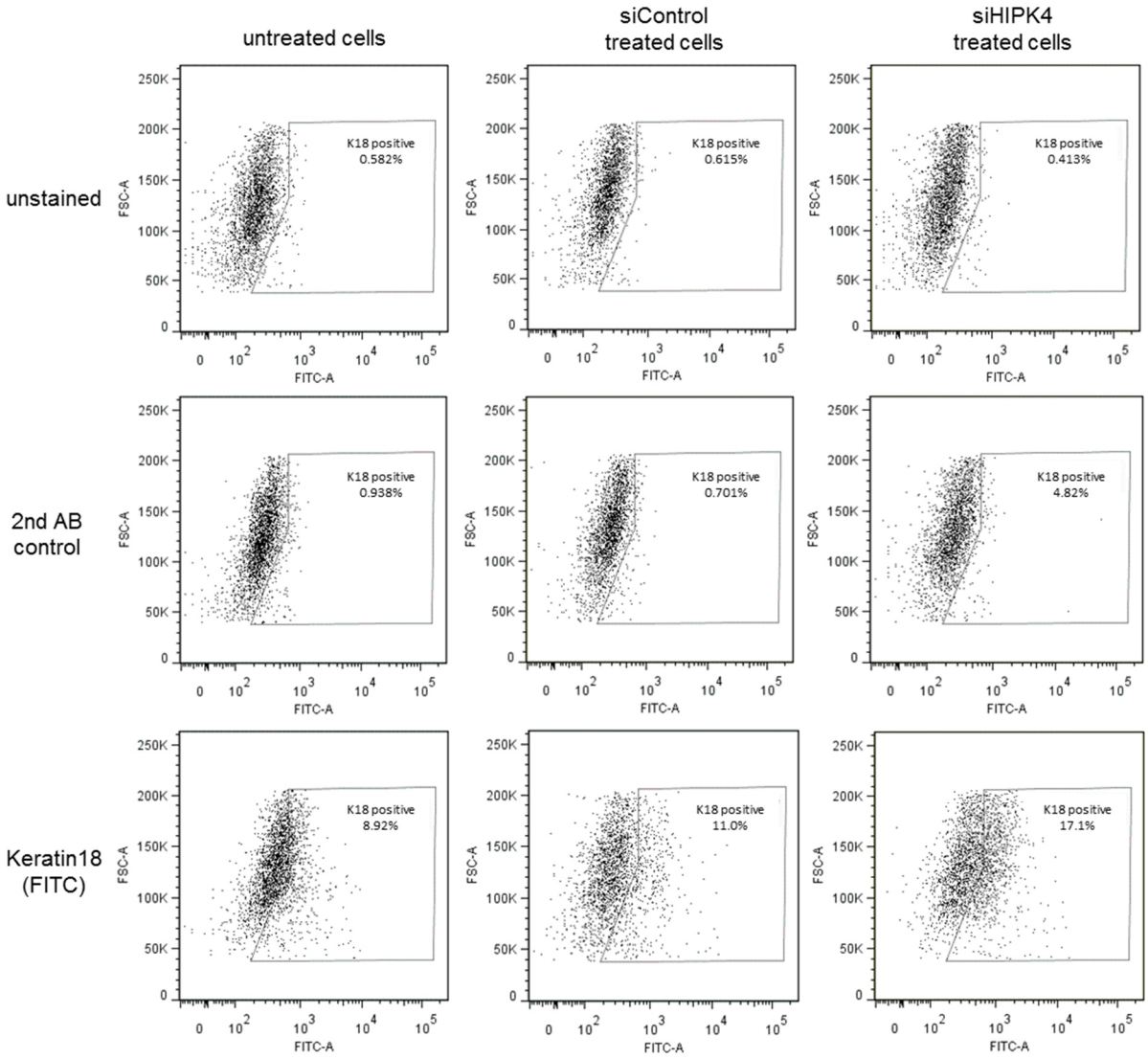

Figure 22: Flow cytometry analysis of differentiated hiPSCs upon HIPK4 knock-down. HiPSCs were transfected with siRNAs against HIPK4 (siHIPK4) or with non-targeting siRNAs (siControl) and differentiated for 10 days. Cells were then stained with an antibody against keratin 18 (K18) and the number of K18 positive cells quantified by flow cytometry. Unstained cells and cells only stained with the secondary antibody (2nd AB control) served ass control conditions. Gates were set on siControl treated cells only stained with the 2nd AB.

To further investigate morphological differences of differentiated cells after HIPK4 knock-down, immunofluorescence staining was performed. Figure 23 shows K18 stainings of cells which were differentiated for 10 days with and without HIPK4 knock-down. The cytoskeleton of cells which were transfected with HIPK4 siRNA was composed of larger and more interconnected fibers and a bigger cytoplasmic portion. This indicates a more advanced differentiation stage of cells which turn from a pluripotent into an early epithelial state.

In order to prove that this effect was not restricted to one specific hiPSC line, the experiment was repeated with the hiPSC line VG2, which was derived from another donor.

As depicted in figure 24, the transfection with HIPK4 siRNAs led to the reduction in HIPK4 expression in treated cells (blue bar) on day 5, compared to the cells transfected with non-targeting siRNA (yellow bar) on day 5. The knock-down of HIPK4 in turn, resulted in increased expression of K18 on day 10.

In summary, the knock-down of HIPK4 in hiPSCs increased the expression of keratins after 10 days of subsequent differentiation.

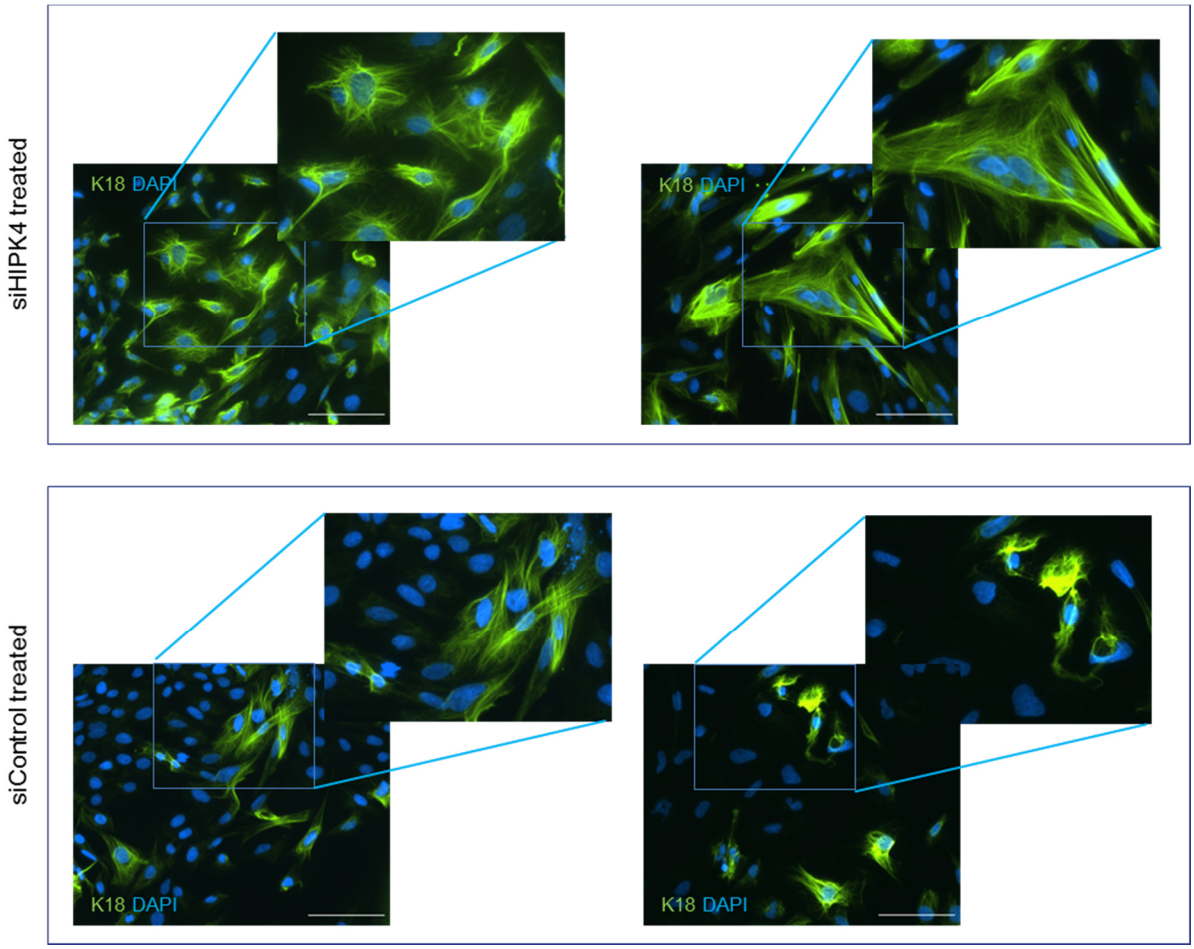

Figure 23: Immunofluorescence staining of Keratin18 (K18) on differentiated hiPSCs upon HIPK4 knock-down. HiPSCs were transfected with siRNAs against HIPK4 (siHIPK4 treated) or a non-targeting control (siControl treated) and subsequently differentiated into early epithelial cells. After 10 days of differentiation, cells were stained against keratin18 (K18, green). Nuclei were stained with 4′,6-Diamidin-2-phenylindol (DAPI). Scale bars: 100 µm.

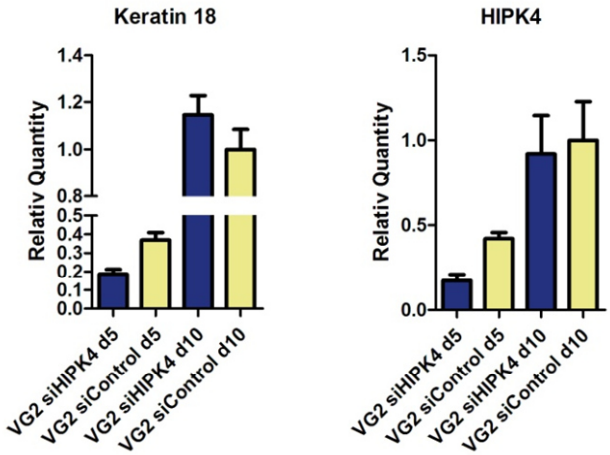

Figure 24: QPCR analysis of differentiated hiPSC line VG2 upon HIPK4 knock-down. Cells were transfected with siRNA against HIPK4 (siHIPK4) and a non-targeting siRNA (siControl) and differentiated for 10 days. Quantitative expression of HIPK4 and keratin 18 was analyzed after 5 (d5) and 10 days (d10) of differentiation. Normalized to GAPDH and 18S. Reference sample: VG2 siControl d10.

3.4.2 Transfection of hiPSCs with single siRNAs against HIPK4

In order to achieve a strong knock-down of a certain gene by using siRNAs, it is common to use a pool of siRNAs against different sequence locations. The drawback of this method is that some siRNAs can cause an off-target effect on the expression of other genes, instead of knocking-down the gene of interest. To prove that the used pool of four HIPK4 siRNAs results in the knock-down of HIPK4 and thus in an increase of K18 expression levels, the differentiation experiment was repeated by using the four single siRNAs against HIPK4 separately (Figure 25).

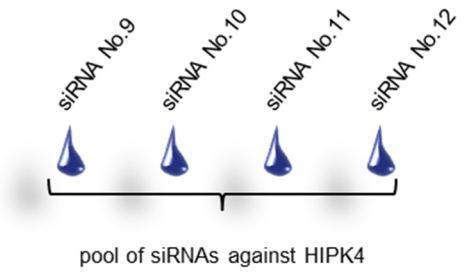

Figure 25: Pool of four single siRNAs against HIPK4. HIPK4 siRNA pool, composed of 4 single siRNAs (siRNA No.9, siRNA No.10, siRNA No.11, and siRNA No.12).

HiPSCs were seeded on Matrigel™ coated dishes and the next day they were transfected with single siRNAs (siNo.9, siNo.10, siNo.11, and siNo.12). After 5 and 10 days of differentiation, the cells were harvested and total RNA was isolated. The expression of HIPK4 and K18 was analyzed by QPCR. The analysis shown in figure 26 revealed that every single siRNA against HIPK4 leads to a knock-down of the gene although not to a similar level. The transfection with siNo.9 and siNo.12 resulted in the strongest knock-down, with 20% and 34% reduced expression on day 5, whereas siRNA No.11 and siNo.12 transfection yielded 2.5% and 10% knock-down efficiency on day 5 compared to the siControl treated cells.

As already mentioned, the transfection with siRNA is transient, thus the knock-down effect was detectable on day 5 before the expression levels increased again until day 10. The knock-down of HIPK4 resulted in increased expression levels of K18 after 5 and 10 days of differentiation. The levels of K18 expression increased at day 10 by 29% for siNo.9, 23% for siNo.10, 30% for siNo.11, and even 37% for siNo.12, compared to the control treatment.

Taken together, the transfection of hiPSCs with single siRNAs against HIPK4 and the subsequent differentiation into early epithelial cells led to the knock-down of HIPK4 and resulted in the upregulation of K18 after 5 and 10 days. This indicates that the upregulation of keratins and epithelial markers including p63, is not an off-target effect of the used siRNAs.

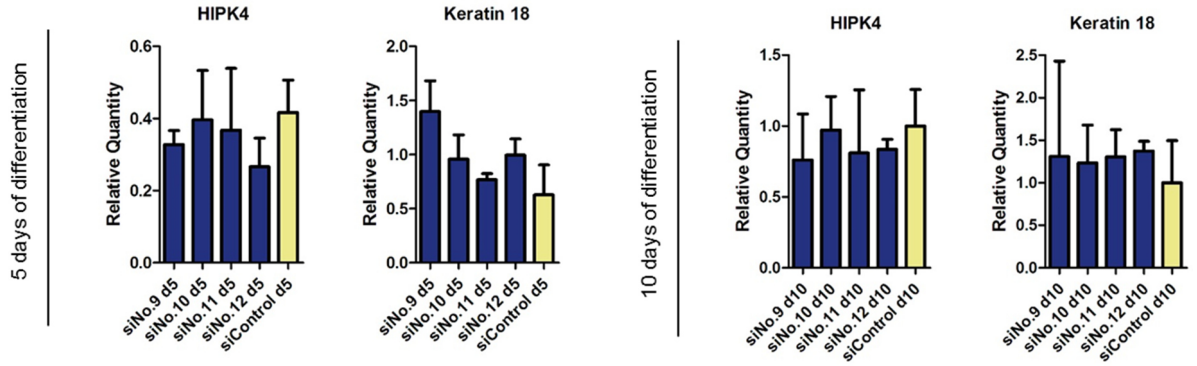

Figure 26: Expression analysis of differentiated hiPSCs transfection with single siRNAs against HIPK4. HiPSCs were transfected with four different siRNAs against HIPK4 (siNo.9, siNo.10, siNo.11 and siNo.12; blue bars) and non-targeting siRNA (siControl, yellow bar) and differentiated for 10 days. The expression level of HIPK4 and keratin 18 was determined by QPCR after 5 (left graphs) and 10 days (right graphs) of differentiation. Analysis was normalized to GAPDH. SiControl d10 served as reference sample.

3.4.3 Serial knock-down of HIPK4 during early epithelial differentiation of hiPSCs

As shown before, the transfection of hiPSCs with a pool of siRNAs against HIPK4 was transient. While the knock-down of HIPK4 was detectable on RNA and protein level on day 5 of differentiation, the effect was diminished on day 10. Nevertheless, the knock-down of HIPK4 led to the increase of keratin expression levels after 10 days of differentiation, which suggests the involvement of HIPK4 in very early events of differentiation. It was of interest to determine if a persistent knock-down during the differentiation of hiPSCs into early epithelial cells would result in even accelerated keratin expression levels. Therefore hiPSCs were again seeded for differentiation and transfected twice, on day 1 and on day 5 (2x) with a pool of siRNAs against HIPK4 and a non-targeting siControl, as shown in figure 27. In order to compare the results with the aforementioned experiments, one batch was only transfected once on day 1. The cells were differentiated under mentioned conditions for 10 days. Total RNA was isolated and the expression levels of epithelial markers on day 10 were analyzed.

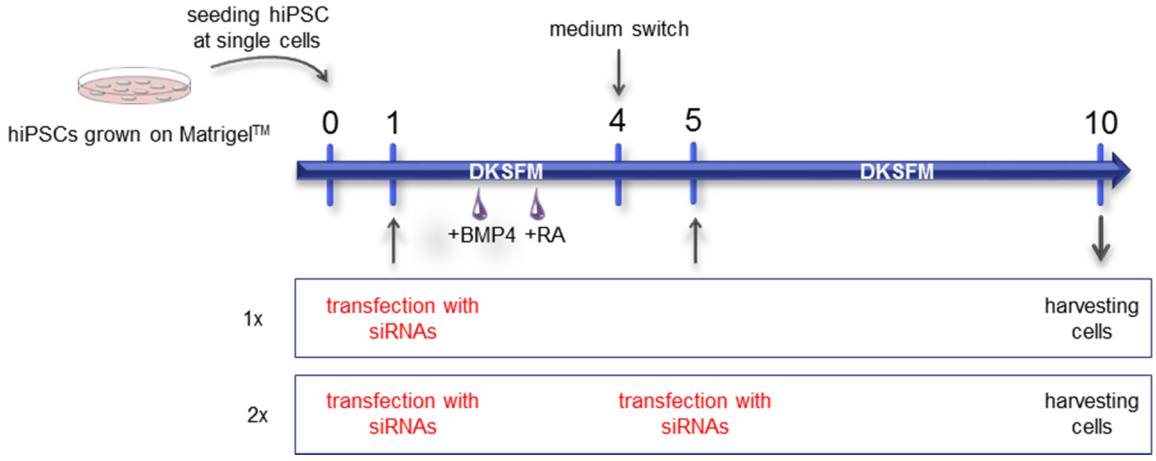

Figure 27: Schematic of serial transfection work flow. HiPSCs were seeded on Matrigel™ coated dishes for 10 days of differentiation into early epithelial cells. Defined keratinocyte serum free medium (DKSFM) was used for the directed differentiation, and supplemented the first 4 days with retinoic acid (RA) and bone morphogenetic factor 4 (BMP4). Cells were transfected either on day 1 and harvested on day 10 (1X), or transfected on day 1 and day 5 and harvested on day 10 (2X).

As shown in figure 28, a single knock-down of HIPK4 was not detectable anymore on day 10. In contrast, cells which were transfected twice (HIPK4 2x), still exhibited a persistent knock-down. Interestingly, the persistent knock-down of HIPK4 could not further increase the expression levels of keratins as well as the level of p63. The single knock-down of HIPK4 at the beginning of the differentiation process yielded the highest expression levels for all tested epithelial markers, as demonstrated in previous experiments. In contrast, cells with a persistent knock-down of HIPK4 did not show increased levels of keratins or of p63, but rather had expression levels comparable to the control cells.

From these results, one could suggest that HIPK4 might have an inhibitory role during the very early steps of development, but may be required for proper development after this initial phase.

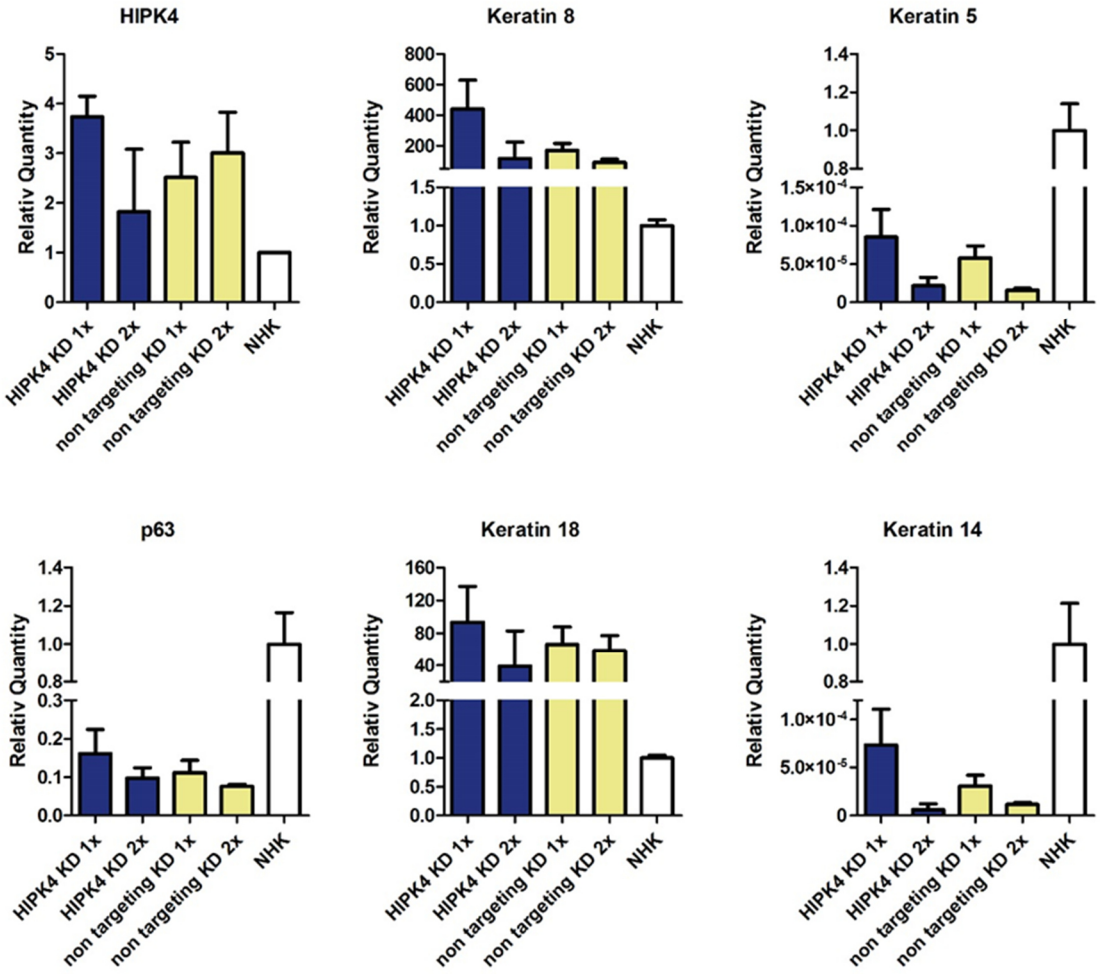

Figure 28: QPCR analysis of differentiated cells after serial knock-down. HiPSCs differentiated for 10 days were transfected on day 1 (1x) or on day 1 and 5 (2x) with siRNAs against HIPK4 (siHIPK4) or with a non-targeting control siRNA (siControl). The expression levels of HIPK4, p63, keratin 8, keratin 18, keratin 5 and keratin 14 were analyzed. Analyses were normalized to GAPDH and 18S. Normal human keratinocytes (NHK) served as reference sample.

3.4.4 The effect of HIPK4 knock-down under different culture conditions

The knock-down of HIPK4 during the very early differentiation steps led to an increase of epithelial markers, but a persistent knock-down did not increase their expression. Nevertheless, it is still unclear how HIPK4 affects the expression of epithelial markers.

For this reason, it was investigated whether the supplements in the differentiation medium have an influence on the upregulation of keratins induced by the HIPK4 knock-down. HiPSCs were seeded for differentiation under four different culture conditions for the first four days of differentiation. As depicted in figure 29, the cells were cultivated either in defined keratinocyte serum free medium (DKSFM) supplemented with retinoic acid (RA) and BMP4 (usual condition), DKSFM with RA, DKSFM with BMP4, or DKSFM without supplements. On day 4 the medium was replaced by DKSFM without supplements. RNA was isolated on day 5 and day 10. Furthermore bright field images were made to monitor morphological changes.

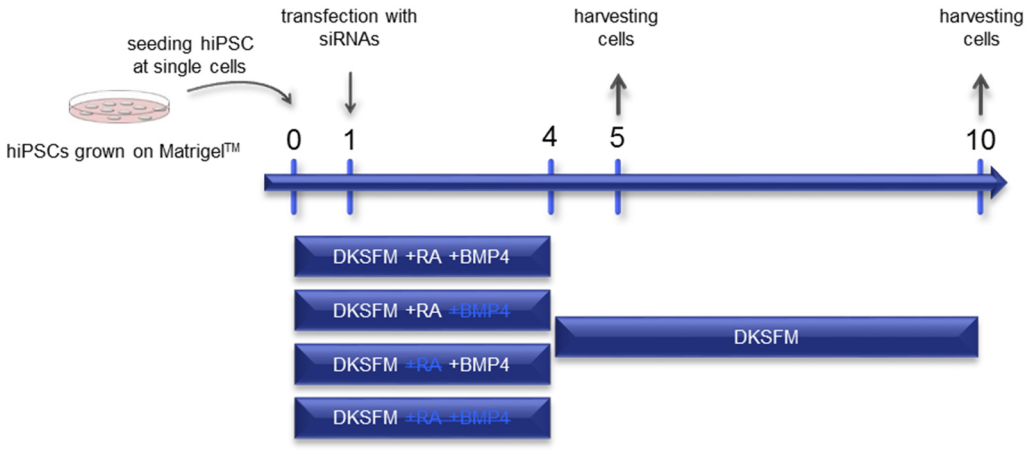

Figure 29: Schematic of varying culture conditions during differentiation. Human induced pluripotent stem cells (hiPSCs) were seeded for differentiation in four different culture conditions for the first four days, defined keratinocyte serum free medium (DKSFM) supplemented with retinoic acid (RA) and BMP4, with just RA, or just BMP4, or without both. On day 4 medium was change to DKSFM without supplements. Cells were harvested on day 5 and 10.

Figure 30 shows bright field images of cells after 10 days of differentiation under described culture conditions, with and without HIPK4 knock-down. Furthermore, it depicts QPCR analysis from the different conditions after 5 and 10 days. The first culture condition, DKSFM supplemented with RA and BMP4 was routinely used for differentiation. As shown in previous experiments, the knock-down of HIPK4 was detectable on day 5, but not on day 10. Compared to the non-targeting siControl, the transfection with siRNA against HIPK4 yielded a knock-down of 90%. As already shown in previous experiments, a detectable knock-down of HIPK4 on day 5 resulted in an upregulation of K18 on day 10 (one and a half higher more) compared to the non-targeting control. As seen on the bright field images, both treatments (siHIPK4 and siControl) resulted in a heterologous population of differentiating cells. Large colonies of epithelial-like cells could be found in between other cell types, but no stem cells like colonies were present.

The second condition, DKSFM with RA, showed similar results. QPCR analysis revealed a 46% knock-down of HIPK4 on day 5 after treatment with siRNAs against HIPK4, accompanied with an increase of K18 at day 10. Interestingly, the non-targeting siRNA treated cells showed no increase in K18 on day 10 compared to day 5. Bright field images illustrate the presence of epithelial-like colonies, surrounded by a heterologous cell population in both conditions. Furthermore, no stem cell colonies were found.

In contrast, cells grown for 4 days in DKSFM supplemented with BMP4 yielded colonies of hiPSCs in between differentiating cells. Furthermore, QPCR analysis of siHIPK4 treated cells after 10 days of differentiation detected no increase in K18, even though the HIPK4 knock-down efficiency reached 30%. Compared to the fully supplemented medium, this condition led to much lower levels of K18, in both, siHIPK4 treated and non-targeting siControl treated cells.

Similar results were obtained during the differentiation with DKSFM without any supplements. Bright field images showed remaining hiPSC colonies in between differentiating cells. Regarding the QPCR analysis, there was no increase in K18 levels after 10 days in siHIPK4 treated cells compared to the non-targeting control, even though the knock-down efficiency reached 59%. Furthermore, the K18 levels remained low (relative quantity value of 0.23) in both treatments, compared to cells grown in fully supplemented medium.

Taken together, the effect of HIPK4 knock-down on the expression level of K18 was only detectable in the presence of RA, whereas the withdrawal of RA from the initial differentiation medium (Differentiation Medium I) diminished the effect.

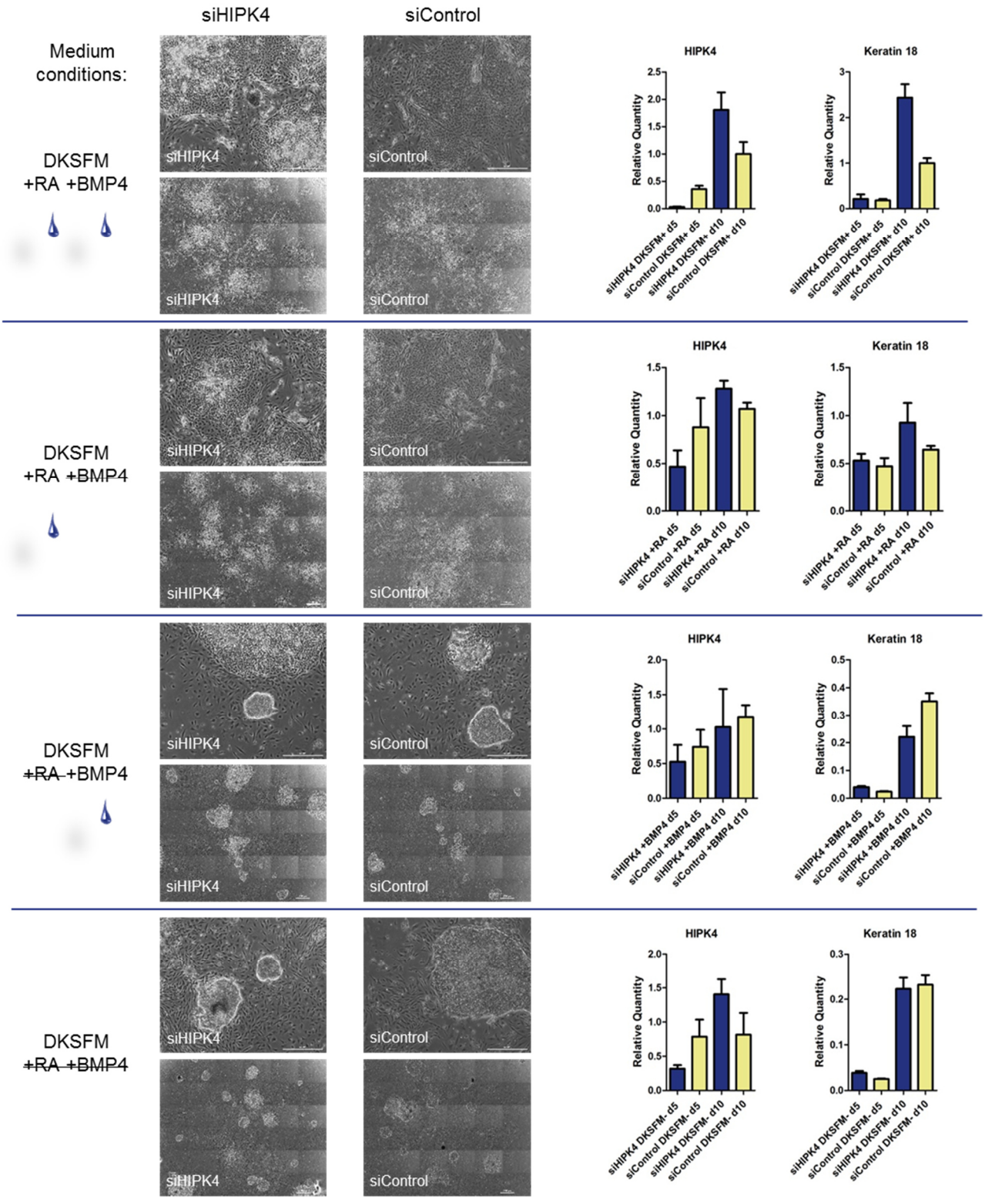

Figure 30: Influence of medium composition on the HIPK4 knock-down effect during differentiation. HIPK4 was knocked-down in hiPSCs using siRNAs (siHIPK4), and differentiated for 10 days. Control cells were transfected with a non-targeting control. Differentiation was induced in four different culture conditions, defined keratinocyte serum free medium (DKSFM) with retinoic acid (RA) and bone morphogenetic protein 4 (BMP4) (DKSFM+), with RA (DKSFM+RA) or BMP4 ((DKSFM+BMP4) or without both (DKSFM-). Large bright field images were combined from 36 images. On day 5 (d5) and 10 (d10) cells were harvested and expression levels of HIPK4 and keratin 18 were analyzed using QPCR. Normalization to GAPDH. Quantities are relative to siControl in DKSFM+ d10.

3.4.5 Influence of HIPK4 overexpression on differentiating cells

As shown before, the knock-down of HIPK4 in hiPSCs and their subsequent differentiation into epithelial cells, led to an increase in K18 expression. This finding raised the question, if the overexpression of HIPK4 also affects the expression of K18. In order to answer this question, hiPSCs were transduced with a lentiviral HIPK4 expression vector and an empty lentiviral vector as a control. Differentiation was induced by exposing the cells to Differentiation Medium I for 4 days. At day 4 medium was switched to Differentiation Medium II until day 10. Cells were harvested on day 5 and on day 10, as in previous experiments, and total RNA was isolated. Figure 31 displays the QPCR analysis of this experiment. As expected, the HIPK4 level in HIPK4-transduced cells was increased, compared to the control or non-treated cells. However, the levels of epithelial markers, including K8, K18, and p63 on day5, were not significantly different under control conditions. The expression levels of K8 and K18 on day 10 were slightly increased for HIPK4 overexpressing cells, but the level of p63 was identical for all three conditions.

In summary, in contrast to the knock-down of HIPK4, the overexpression of HIPK4 showed no significant effect on the differentiation of hiPSCs into an epithelial lineage.

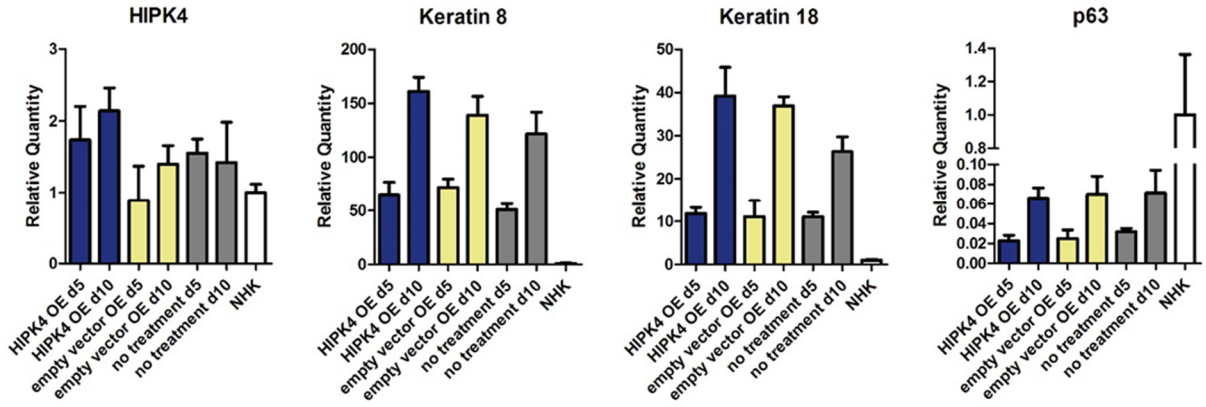

Figure 31: QPCR analysis of epithelial markers and HIPK4 in HIPK4 overexpressing cells. HiPSCs were transduced with a lentiviral HIPK4 expression vector (HIPK4 OE), or with an empty vector (empty vector OE) as a control, and differentiated for 10 days. Cells were harvested after 5 (d5) and 10 days (d10) and analyzed for their expression of HIPK4, keratin 8, keratin 18, and p63. Values were normalized to GAPDH and 18S. Normal human keratinocytes (NHK) served as a reference sample.

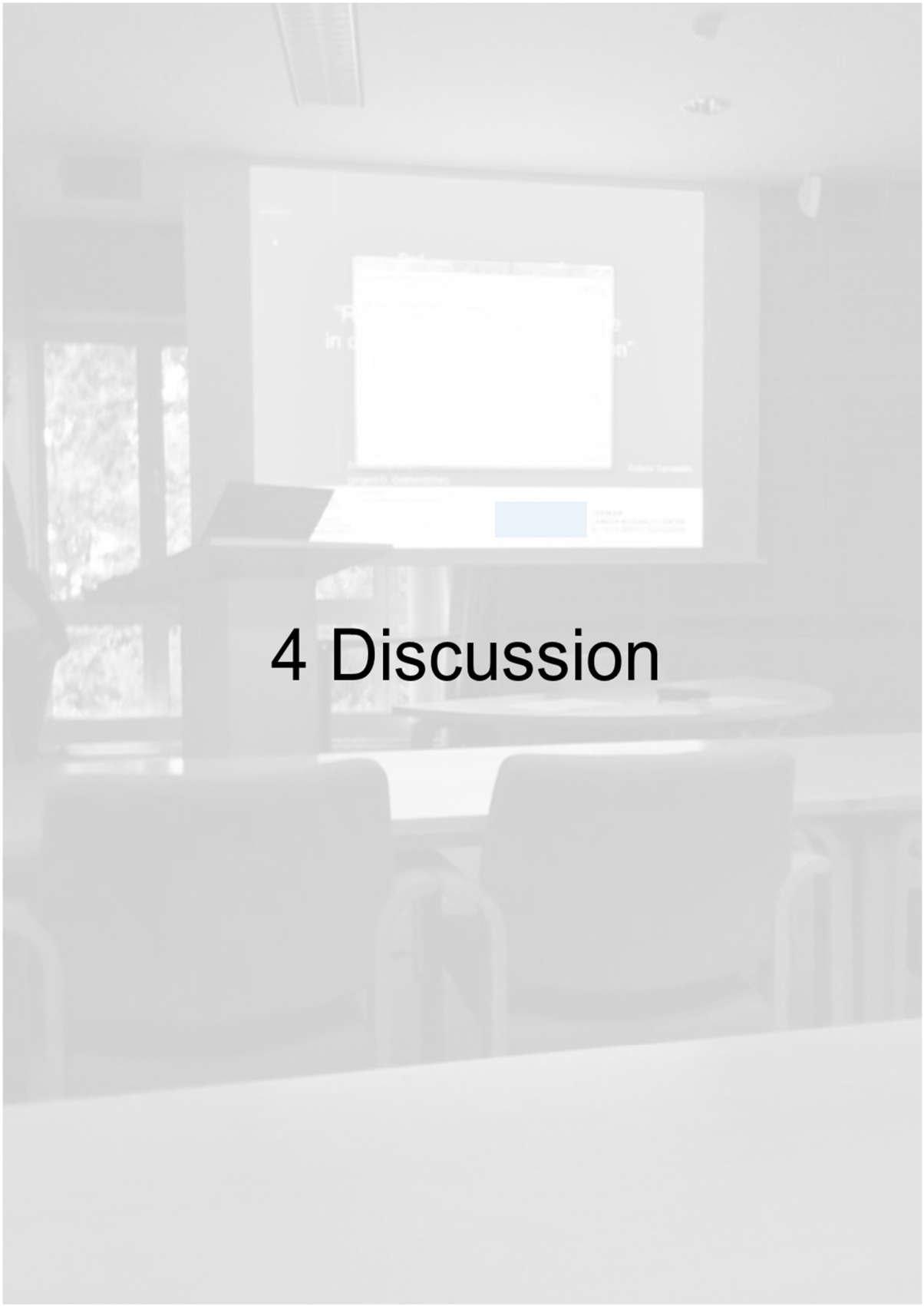

4 Discussion

4 Discussion

4.1 Advantages of using induced pluripotent stem cells

The technology of induced pluripotency offers great possibilities for various fields of research and application. It enables the investigation of developmental processes, especially in humans, since the generation of human induced pluripotent cells is not burdened with ethical concerns, in contrast to research with human embryonic stem cells. Besides studying embryonic development in healthy cells, the development of genetic diseases can be examined. HiPSCs can be derived from patients with a specific disease or they can be genetically modified in order to introduce disease-specific mutations. Subsequent differentiation into a cell type of interest would offer the possibility to monitor the pathogenesis and to investigate the involved pathways. Furthermore, disease specific hiPSCs can be differentiated into affected cell types and serve as an *in vitro* model for drug testing.

One major goal of iPSC research is to use these cells as a source of healthy cells for transplantation, as it is already in process for adult stem cells. To date, haematopoietic stem cells are used for the treatment of leukemia patients or patients after chemotherapies. Many clinical trials on adult stem cells transplanted into patients are already in process, for example for the treatment of spinal trauma (ClinicalTrials.gov identifier: NCT01772810), heart failures (ClinicalTrials.gov identifier: NCT01758406), or diabetes mellitus (ClinicalTrials.gov identifier: NCT01121029). However, adult stem cells are rare and the search for matching donors, in the case of allogeneic transplantations, is complicated. Furthermore, the extraction of bone marrow as a source of haematopoietic stem cells is a painful process for the patients.

HiPSCs represent a nearly inexhaustible source of pluripotent cells. They can be generated from adult somatic cells of nearly every differentiation lineage. For example, a small punch biopsy from the skin is sufficient to obtain fibroblasts, which can be expanded in culture, reprogrammed, and differentiated into the cell type of interest. Unfortunately, this process is not as trivial as it seems. Before using hiPSCs for transplantations, many open questions need to be answered and problems need to be solved.

A crucial issue concerning the use of hiPSCs for cell replacement therapy is the establishment of simple and effective protocols for the differentiation of these pluripotent cells towards cell lineages of interest. To date, no published differentiation protocol yielded 100% pure populations of differentiated cells (Robinton and Daley, 2012). Methods to enrich cells of interest, including fluorescence activated cell sorting, showed to be promising (Doi et al., 2014). Nevertheless, these methods require high amounts of cells and due to the exhausting procedure the cells need to recover afterwards.

Even though the differentiated cells can be investigated for their expression of cell type specific markers and tested for their functionality, they are still artificially generated and it is not clear how they behave in a living organism, especially in humans.

Since the discovery of induced pluripotent stem cells, (Takahashi and Yamanaka, 2006) much effort has been put into the investigation and study of these cells and their potential. Although many questions have been solved there still remain a lot of unresolved issues which need to be addressed.

In this work hiPSCs were generated by infecting somatic cells with lentiviral vectors harboring the four Yamanaka factors. This is a very efficient method for the generation of pluripotent cells. Since the focus of this work laid on the differentiation of hiPSCs towards an

epidermal fate, the aspect of generating iPSCs without genomic integrations was therefore neglected. Nevertheless, genomic instabilities due to the transduction with lentiviral particles are possible. Furthermore, the genomic integration of reprogramming factors into the genome and the subsequent reprogramming can cause genomic rearrangements and epigenetic changes. The cultured hiPSCs used for the experiments described in this thesis show no phenotypic changes and remain stably pluripotent in culture. The pluripotent state was proved by expression analysis via QPCR, by immunofluorescence stainings, to demonstrate the expression of pluripotency associated markers on protein level, and by the most stringent test, the teratoma assay.

4.2 Differentiation of hiPSCs into epithelial cells and the importance of generating efficient protocols

The differentiation of pluripotent cells into any kind of somatic cell is of major interest, especially in the field of regenerative medicine in dermatology. Skin replacements for patients with large burn injuries could be generated from patient-specific hiPSC-derived keratinocytes.

Establishing reliable and efficient protocols for the differentiation of hiPSCs into keratinocytes, the predominant cell type of the epidermis, enables the investigation of processes of homeostasis and development of healthy skin as well as the pathogenesis of skin diseases. In addition, it allows to investigate the dysregulation during skin development which leads to skin diseases.

Existing protocols (summarized in paragraph “1.3 Differentiation of pluripotent cells into keratinocytes in vitro”) have progressively improved the efficiency of generating pluripotent cell-derived keratinocytes. Nevertheless, in order to use the generated keratinocytes for skin-replacements, they need to yield 100% pure populations. Differentiation protocols are usually based on processes which take place during the *in vivo* development. The optimization of these protocols require a fundamental knowledge about these processes, which are not completely solved to date.

The focus of this work is on unknown factors, which play a role during the early steps of differentiation of pluripotent stem cells into keratinocytes.

The used differentiation protocol was modified from a published protocol (Itoh et al., 2011). The modifications comprise the seeding of hiPSCs as single cells, rather than culturing them in colonies. Seeding hiPSCs as single cells for the induction of differentiation has the effect, that every cell has the same exposure to the differentiation medium. When grown in colonies, the tightly packed formation makes it difficult to expose every cell in the same way to the differentiation medium, especially the cells in the center of the colony.

However, hiPSCs as well as hESCs show low clonal expansion potential and easily undergo apoptosis under single cell conditions. Therefore, the cells were treated with ROCK-Inhibitor prior to seeding, to avoid dissociation-induced apoptosis (Watanabe et al., 2007).

The medium used for the differentiation is a fully supplemented medium without the addition of fetal calf/bovine serum. The addition of serum supplements the medium with a black box of undefined factors with unknown concentrations (Evans et al., 1956; van der Valk et al., 2010). The used serum-free medium ensures comparable, stable culture conditions in every experiment.

According to published protocols, BMP4 and RA were added for the first four days of differentiation (described in paragraph “2.2.4 Epithelial differentiation protocol”).

At the beginning of differentiation, the cells represent a heterogeneous population, but as shown in figure 9, within the heterogeneous population, colonies of keratinocyte-like cells occur. During the 30-day differentiation process, keratinocytes are enriched due to the medium composition, which favors and promotes keratinocyte growth. The aim of the differentiation experiment was to confirm that the generated hiPSCs are able to be directed into an epidermal lineage. This was proven by real-time qPCR analysis, genome wide expression analysis and immunofluorescence stainings.

During the first 5-10 days of differentiation, the cells show a decrease in expression of pluripotency associated markers (Figure 10A). On the other hand, they show an upregulation of K8 and K18 (Figure 10B). The expression of K8 and K18 reaches a peak on day 15 and subsequently decreases. K8 and K18 are the first pair of keratins which are expressed during the epidermal development *in vivo*, when the epidermis consists of a single-layered epithelium (see paragraph “The embryonic development of the epidermis”). The cells of this single-layered primitive ectoderm proliferate and migrate upwards to build suprabasal layers and a stratified epithelium. K8 and K18 are then replaced by K5 and K14. These markers are characteristic for the cells of the basal layer of a stratified epidermis.

The downregulation of pluripotency associated markers and the subsequent upregulation of K8 and K18 demonstrates the transition of an undifferentiated state towards an epithelial fate. Furthermore, the switch in expression from K8 and K18 to K5 and K14 shows the maturation of these cells at later time points (~ day 25).

Genome wide expression analysis of cells differentiated for 10 days, compared to hiPSCs, allowed to establish a list of 5741 significantly regulated genes. Subsequent hierarchical clustering was performed and presented as a heat map (Figure 12).

As expected the biological replicates clustered together to build three groups, indicating good quality of samples. Interestingly, differentiated cells grouped closer to hiPSCs then to NHK, due to the fact that they are in a very early state of differentiation.

Furthermore, the fold changes of pluripotency-associated genes and keratinocyte markers, shown in figure 13, indicate that the differentiated cells show a comparable gene expression level to NHK. It is interesting to notice that K8 and K18 are upregulated in differentiated cells and not in NHK. This result was expected, since NHKs are differentiated and do not express K8 or K18 anymore.

The performed differentiation experiments could confirm the successful generation of keratinocytes from reprogrammed human fibroblasts. The hiPSC-derived keratinocytes express markers of basal keratinocytes on RNA and protein level.

4.3 High-throughput screens as the method of choice to find single candidates involved in the development of keratinocyte precursors

High-throughput and high-content screens are utilized in many research fields. Growing drug and gene libraries, as well as advanced automation and computerized analysis, enables the application of this method to nearly every questioning, including screening of active factors, effective drugs or small compounds. Furthermore, it enables cost-effective, time saving experiments in large scales (Boutros and Ahringer, 2008; Desbordes and Studer, 2013).

High-throughput can be applied to knock-down experiments, by transfecting cells with a library of siRNAs, to small compound screens, in order to investigate the effect of small compounds on the cell behavior, or to drug toxicity screens.

Drug toxicity screens are inalienable in clinical trials of new therapeutics and are of major interest for pharmaceutical industry. To date, these screens are performed with highly proliferative immortalized cell lines or cancer cells, since large amounts of cells are needed. However, the results obtained with these cells are not always applicable to normal human cells. The use of hiPSC-derived differentiated cells in high-throughput drug screens ensures an unlimited source of fully differentiated adult human cells (Ebert and Svendsen, 2010).

In this work, a protocol was established to knock-down specific genes (kinome library of about 800 siRNAs) during the differentiation of hiPSCs into early epithelial cells in a high-throughput procedure. The application of high-throughput screens during differentiation opens new possibilities to study developmental processes. Furthermore, it enables to generate gene expression patterns for precursor cells in different stages, and to find key factors which are characteristic for these stages.

The establishment of this experiment included preliminary experiments in order to determine the right settings.

As performed in above described differentiation experiments, the seeding of single cells instead of cell clumps ensures the same medium exposure for every cell. Therefore, a single cell seeding was also performed for the high-throughput experiments. Again, the cells were pre-treated with ROCK-inhibitor to prevent single cells induced apoptosis.

Further, the right cell number had to be determined. Therefore, the cells were seeded in different cell numbers. After a culture time of 10 days the cells were stained using an antibody against K18 together with a nuclear stain. The cell number and the number of positively stained cells were detected with a cell counter software. To ensure the proper detection of stained single cells, it has to be taken into account, that the wells should not be 100% confluent, after 10 days of culture, while reaching a minimum of 1000 cells/well. The most promising results were obtained by seeding 4000 cells per well (data not shown), whereas higher seeding numbers resulted in confluent wells, and lower seeding numbers show poor attachment of the cells.

Beside the right cell number, the control conditions and the seeding procedure, also the right marker for the read out was determined. Most convenient are markers with a nuclear expression, because they are easier to detect by the software. Since, however, the proper binding of the antibody is more important than the location of the antigen, an efficient and specific antibody should always be preferred, even if it detects a cytoplasmic antigen. For the differentiation into early epithelial cells, the search for quantitative markers was limited to K8 and 18, which are cytoplasmic, and p63, which is expressed in the nucleus. Unfortunately, stainings with commercially available p63 antibodies did not achieve the desired quality and intensity, compared to the results obtained by using K18 antibodies. For this reason, an antibody against K18 was used for the final screen readout.

Another aspect is the duration of culture. The drawback of an experiment in a high-throughput process is the rather small size of the cavities (0.109 cm^2) and the maximum volume is 100 µL. Furthermore, changing the medium by the automated workstation should be avoided in order to protect the cells from being aspirated. All these points taken into account, thus the cells were seeded in 50 µL medium and after 5 days additional 50 µL fresh medium were added and the cells cultured until day 10. A culture time longer than 10 days is not recommended, due to the aforementioned reasons.

Trial runs without siRNAs and transfection reagent are necessary, in order to standardize the performance, which results in saving costs.

The high-throughput screen was performed one time in duplicate and one time with a single set. The analysis of the screen data includes the plate normalization, where the relative signal of each well was compared to the median of the sample wells of the whole

plate. The purpose of normalization is to avoid technical discrepancies, including evaporation in the edge wells, pipetting errors or medium gradients. The normalized values were then transformed into z-scores, which include also the mean and the standard deviation of the normalized sample values.

In knock-down assays, a strong effect is indicated by a negative z-score. From the resulting hit list the first fifty candidates were analyzed for their effect on morphological changes, colony formation and intensity of the signals. Since screen data were analyzed using computerized tools it is needful to verify their “hit” status and compare the obtained images by eye. In some cases, the secondary antibody precipitates and leads to unspecific signals which result in false positive signals.

By examining the images of the first fifty hits, the size and amount of keratin fibers as a measure of the state of differentiation, was of major interest. Hits with clear positive stainings were chosen for further analysis, in order to validate the screen results.

In a pilot experiment, the chosen candidates were knocked-down in hiPSCs, which were subsequently differentiated for 10 days, and analyses were performed using real-time qPCR (data not shown).

However, the K18 expression results obtained upon HIKP4 knock-down were the most meaningful, and yielded high K18 expression levels (Figure 17). Regarding the morphology, the cells treated with HIPK4 siRNA showed the highest potential to develop into epithelial-like colonies. Due to these pilot results, HIPK4 was chosen as the candidate of interest for further analysis, even though the knock-down of HIPK4 did not result in the lowest z-score.

High-throughput experiments are great methods to screen large amounts of factors, compounds or genes, in a cost-effective and timesaving process. Even though the screen data need to be validated by additional experiments, it is a method-of-choice to obtain a general direction and first indications.

In addition to the performed high-throughput differentiation experiment, also precursor cells could be used for the screens. Therefore, cells could be pre-differentiated for 10 days and then be used for following 10 days of differentiation in a high-throughput process. This would enable to characterize precursors and identify markers for different stages.

4.4 The role of HIPK4 during the differentiation of human induced pluripotent stem cells into epithelial precursors

HIPK4 is the last described member of the homeodomain-protein kinase family of serine/threonine kinases. They all harbor a highly conserved serine/threonine catalytic domain at their N-terminus (He et al., 2010). While HIPK1, 2 and 3 are localized in nuclear speckles in the nucleus, HIPK4 demonstrates a rather cytoplasmic localization, which is supported by the fact that it does not have a nuclear localization signal (NLS) (Arai et al., 2007). HIPK2 was shown to phosphorylate p53 at Ser49 after UV irradiation (D’Orazi et al., 2002), and ΔNp63α upon treatment with genotoxic agents (Lazzari et al., 2011). Similar to HIPK2, HIPK4 was shown to phosphorylate p53 at serine 9 (Arai et al., 2007). Further functions of HIPK4 are not yet known and it is unclear if ΔNp63α is also phosphorylated by this kinase.

As described in the introduction (see paragraph “1.1.2.1 P63”), p63 is a very important regulator of epithelial development. Especially during the early phase of differentiation the ΔNp63α isoform plays a pivotal role (Guerrini et al., 2011). Interestingly, p63 is known to be phosphorylated, and thus degraded at later phases, when cells are postmitotic and in a

process of terminal differentiation. One could speculate that HIPK4 phosphorylates p63, which then results in the degradation of p63 and enhanced differentiation towards the epithelial lineage. Further experiments are necessary to test this hypothesis.

During 30 days of differentiation, the expression pattern of HIPK4 (Figure 18) mimics the one of K8/K18 (Figure 10B). This led to the assumption, that HIPK4 might play a role during the early stages of keratinocyte differentiation when K8 and K18 are expressed.

It could be clearly demonstrated, that the knock-down of HIPK4 significantly affects the expression levels of K8 and K18, as well as K5 and K14 (Figure 21). However, as shown in figure 28, this effect is due to the inhibition of HIPK4 during the first 5 days of differentiation. The results demonstrate, that a persistent knock-down for 10 days did not enhance the expression of epithelial markers. During these first days the pluripotent cells undergo a determination towards an epidermal lineage and the results obtained by the performed experiments indicate, that HIPK4 exerts its effect during this phase.

The supplementation of the differentiation medium with BMP4 and RA was shown to promote the differentiation process significantly. BMP4 was shown to enhance epidermal specification (Archer et al., 2011), and RA induces the expression of p63 (Metallo et al., 2008). In order to determine if the effect of HIPK4 correlates with the action of BMP4 and/or RA, they were withdrawn from the medium (Figure 30).The withdrawal of BMP4 could not diminish the effect of HIPK4 knock-down on K18 expression, even though the overall K18 expression levels were lower in both siHIPK4 treated cells and in the control. Interestingly, in control treated cells, K18 levels did not increase from day 5 to day 10, whereas siHIPK4 transfected cells show an increase. As already mentioned, BMP4 promotes the differentiation into an epidermal lineage. Without BMP4, the enhancing effect is diminished in control conditions, but upon HIPK4 knock-down, the levels of K18 increase from day 5 to day 10. This lead to the suggestion, that in the absence of BMP4 during epithelial differentiation, the knock-down of HIPK4 rescues the increasing expression levels of K18. Nevertheless, this only holds true in the presence of RA.

In contrast, upon withdrawal of RA, no HIPK4 knock-down induced increase of K18 is detectable. Also in this condition, the overall K18 expression is lower than under culture condition in the presence of both BMP4 and RA. Interestingly, upon withdrawal of RA, the effect of HIPK4 knock-down on the expression of K18 is abolished. Under these conditions, HIPK4 siRNA treated cells demonstrate even lower K18 levels compared to the control treatment. Also under withdrawal of both BMP4 and RA there is no detectable increase in K18 under HIPK4 knock-down.

These results show, that the HIPK4 knock-down effect on K18 is strongly RA dependent, and no increase of K18 under HIPK4 knock-down is detected upon withdrawal of RA. Furthermore, these results lead to the assumption, that in the presence of RA but under withdrawal of BMP4, the knock-down of HIPK4 can either enhance the RA pathway or rescue the function of BMP4.

It is known that during *in vitro* differentiation of pluripotent cells into an epidermal lineage, the addition of RA and BMP4 results in the enhanced expression of K18 and p63. While BMP4 actively blocks neural fate and induces apoptosis in neural precursors, RA leads to the induction of p63. It is not yet resolved how RA induces p63, since there is no RA responsive element in the p63-promoter (Metallo et al., 2008). Further, it is known that during differentiation, the phosphorylation of p63 and thus its degradation marks the transition of basal to suprabasal cells. To date, it is not clear, which kinase induces p63 degradation by phosphorylating it (Suzuki and Senoo, 2012).

The results obtained in this work clearly demonstrate a role of HIPK4 during the early steps of epithelial differentiation. It is not clear how HIPK4 acts, but it has a regulating role on the K8/K18 expression.

The investigations in this work show that the overexpression of HIPK4 did not result in decreased levels of epithelial markers. The absence of a detectable effect after HIPK4 overexpression lead to the suggestion, that the endogenous level of HIPK4 could be sufficient to phosphorylate p63, thus a higher HIPK4 level would not increase the level of phosphorylated p63. During development, the phosphorylation of p63 results in its degradation, and thus reduced p63 levels would be expected after HIPK4 overexpression. On the other hand, the investigation of the expression levels of epithelial markers was performed after 10 days; this period could be too short for a final prediction about the influence of HIPK4 overexpression on p63. It would be of great help to analyze the phosphorylation status of p63 after HIPK4 overexpression, as well as after the knock-down.

Further experiments need to answer the question, if HIPK4 phosphorylates p63 and thereby leads to the degradation of p63 and the subsequent differentiation of epithelial precursors into keratinocytes, as it is the case during the development. In this case, the early knock-down of HIPK4 would reduce the phosphorylation of p63, resulting in higher p63 levels (which was shown in figure28), and lead to an increase of epithelial precursors. The dependency of HIPK4 on RA might be due to the induction of p63 by RA.

Further investigations are needed to determine the role of HIPK4. For example, HIPK4 and a kinase-deficient mutant form could be overexpressed in cells, which do not express HIPK4 at all. The subsequent analysis of the phosphorylation status of p63 by specific phospho-p63 antibodies would help to investigate if p63 is phosphorylated. Co-immunoprecipitation could also determine the interaction of HIPK4 and p63, by pulling down HIPK4 and detecting the presence of p63 in the received fraction by western blot.

In addition, the differentiation time could be prolonged up to 30 days, in order to investigate, if the early knock-down of HIPK4 still has an influence at later differentiation stages.

It would also be of interest, to perform differentiation experiments without siRNA transfection, but instead using kinase inhibitors, to block HIPK4 kinase activity. If blocking of HIPK4 kinase activity results in increased expression of epithelial markers, this would indicate that it is in fact the kinase activity, which negatively regulates the epithelial development.

Unfortunately, HIPK4 is a relatively unknown kinase, and to date there is no specific inhibitor known, which only inhibits HIPK4 or HIPKs. Therefore, it would be more specific to perform gene targeting using zink-finger nucleases, which induce site-specific deletions in the kinase domain through homologous recombination. This would enable to investigate the kinase activity of HIPK4.

This work demonstrates for the first time that the kinase HIPK4 is involved in the process of epithelial differentiation. On this basis, it will be possible to investigate the function of HIPK4 in more detail and eventually exploit the gained knowledge in order to establish novel and more effective protocols for the differentiation of human pluripotent stem cells towards the epithelial lineage. Improving the efficiency of differentiation protocols is necessary in order to use iPS-derived cells for therapeutically purpose.

References

Aberdam, D. (2004). Derivation of keratinocyte progenitor cells and skin formation from embryonic stem cells. Int. J. Dev. Biol. *48*, 203–206.

Allen, M., Grachtchouk, M., Sheng, H., Grachtchouk, V., Wang, A., Wei, L., Liu, J., Ramirez, A., Metzger, D., Chambon, P., et al. (2003). Hedgehog signaling regulates sebaceous gland development. Am. J. Pathol. *163*, 2173–2178.

Ando, H., Niki, Y., Yoshida, M., Ito, M., Akiyama, K., Kim, J.-H., Yoon, T.-J., Matsui, M.S., Yarosh, D.B., and Ichihashi, M. (2011). Involvement of pigment globules containing multiple melanosomes in the transfer of melanosomes from melanocytes to keratinocytes. Cell. Logist. *1*, 12–20.

Anokye-Danso, F., Trivedi, C.M., Juhr, D., Gupta, M., Cui, Z., Tian, Y., Zhang, Y., Yang, W., Gruber, P.J., Epstein, J.A., et al. (2011). Highly efficient miRNA-mediated reprogramming of mouse and human somatic cells to pluripotency. Cell Stem Cell *8*, 376–388.

Arai, S., Matsushita, A., Du, K., Yagi, K., Okazaki, Y., and Kurokawa, R. (2007). Novel homeodomain-interacting protein kinase family member, HIPK4, phosphorylates human p53 at serine 9. FEBS Lett. *581*, 5649–5657.

Archer, T.C., Jin, J., and Casey, E.S. (2011). Interaction of Sox1, Sox2, Sox3 and Oct4 during primary neurogenesis. Dev. Biol. *350*, 429–440.

Aumailley, M., and Rousselle, P. (1999). Laminins of the dermo-epidermal junction. Matrix Biol. *18*, 19–28.

Aumailley, M., El Khal, A., Knöss, N., and Tunggal, L. (2003). Laminin 5 processing and its integration into the ECM. Matrix Biol. *22*, 49–54.

Banks-Schlegel, S.P. (1982). Keratin alterations during embryonic epidermal differentiation: a presage of adult epidermal maturation. J. Cell Biol. *93*, 551–559.

Barlow, P., Owen, D.A, and Graham, C. (1972). DNA synthesis in the preimplantation mouse embryo. J. Embryol. Exp. Morphol. *27*, 431–445.

Blanpain, C., and Fuchs, E. (2006). Epidermal stem cells of the skin. Annu. Rev. Cell Dev. Biol. *22*, 339–373.

Blanpain, C., Lowry, W., and Geoghegan, A. (2004). Self-renewal, multipotency, and the existence of two cell populations within an epithelial stem cell niche. Cell *118*, 635–648.

Blelloch, R., Venere, M., Yen, J., and Ramalho-Santos, M. (2007). Generation of induced pluripotent stem cells in the absence of drug selection. Cell Stem Cell *1*, 245–247.

Borradori, L., and Sonnenberg, A (1999). Structure and function of hemidesmosomes: more than simple adhesion complexes. J. Invest. Dermatol. *112*, 411–418.

Botchkarev, V.A. (2013). Bone Morphogenetic Proteins and Their Antagonists in Skin and Hair Follicle Biology. Prog. Dermatology *120*, 36–47.

Botchkarev, V.A, Botchkareva, N.V, Roth, W., Nakamura, M., Chen, L.H., Herzog, W., Lindner, G., McMahon, J.A, Peters, C., Lauster, R., et al. (1999). Noggin is a mesenchymally derived stimulator of hair-follicle induction. Nat. Cell Biol. *1*, 158–164.

Botchkarev, V.A, Botchkareva, N.V, Sharov, A.A, Funa, K., Huber, O., and Gilchrest, B.A (2002). Modulation of BMP signaling by noggin is required for induction of the secondary (nontylotrich) hair follicles. J. Invest. Dermatol. *118*, 3–10.

Boutros, M., and Ahringer, J. (2008). The art and design of genetic screens: RNA interference. Nat. Rev. Genet. *9*, 554–566.

Brakebusch, C., Grose, R., Quondamatteo, F., Ramirez, A, Jorcano, J.L., Pirro, A, Svensson, M., Herken, R., Sasaki, T., Timpl, R., et al. (2000). Skin and hair follicle integrity is crucially dependent on beta 1 integrin expression on keratinocytes. EMBO J. *19*, 3990–4003.

Braun, K.M., Niemann, C., Jensen, U.B., Sundberg, J.P., Silva-Vargas, V., and Watt, F.M. (2003). Manipulation of stem cell proliferation and lineage commitment: visualisation of label-retaining cells in wholemounts of mouse epidermis. Development *130*, 5241–5255.

Briggs, R., and King, T.J. (1952). Transplantation of Living Nuclei From Blastula Cells into Enucleated Frogs' Eggs. Proc. Natl. Acad. Sci. U. S. A. *38*, 455–463.

Brown, J.C., and Timpl, R. (1995). The collagen superfamily. Int. Arch. Allergy Immunol. *107*, 484–490.

Burdsal, C.A, Damsky, C.H., and Pedersen, R.A (1993). The role of E-cadherin and integrins in mesoderm differentiation and migration at the mammalian primitive streak. Development *118*, 829–844.

Byrne, C., Tainsky, M., and Fuchs, E. (1994). Programming gene expression in developing epidermis. Development *120*, 2369–2383.

Candi, E., Melino, G., Mei, G., Tarcsa, E., Chung, S.I., Marekov, L.N., and Steinert, P.M. (1995). Biochemical, structural, and transglutaminase substrate properties of human loricrin, the major epidermal cornified cell envelope protein. J. Biol. Chem. *270*, 26382–26390.

Candi, E., Tarcsa, E., Idler, W.W., Kartasova, T., Marekov, L.N., and Steinert, P.M. (1999). Transglutaminase cross-linking properties of the small proline-rich 1 family of cornified cell envelope proteins. Integration with loricrin. J. Biol. Chem. *274*, 7226–7237.

Candi, E., Schmidt, R., and Melino, G. (2005). The cornified envelope: a model of cell death in the skin. Nat. Rev. Mol. Cell Biol. *6*, 328–340.

Carvajal-Vergara, X., Sevilla, A., D'Souza, S.L., Ang, Y.-S., Schaniel, C., Lee, D.-F., Yang, L., Kaplan, A.D., Adler, E.D., Rozov, R., et al. (2010). Patient-specific induced pluripotent stem-cell-derived models of LEOPARD syndrome. Nature *465*, 808–812.

La Celle, P.T., and Polakowska, R.R. (2001). Human homeobox HOXA7 regulates keratinocyte transglutaminase type 1 and inhibits differentiation. J. Biol. Chem. *276*, 32844–32853.

Champliaud, M.F., Lunstrum, G.P., Rousselle, P., Nishiyama, T., Keene, D.R., and Burgeson, R.E. (1996). Human amnion contains a novel laminin variant, laminin 7, which like laminin 6, covalently associates with laminin 5 to promote stable epithelial-stromal attachment. J. Cell Biol. *132*, 1189–1198.

Chapman, S.J., and Walsh, A. (1990). Desmosomes, corneosomes and desquamation. An ultrastructural study of adult pig epidermis. Arch. Dermatol. Res. *282*, 304–310.

Chen, M., Marinkovich, M.P., Jones, J.C., O'Toole, E.A., Li, Y.Y., and Woodley, D.T. (1999). NC1 domain of type VII collagen binds to the beta3 chain of laminin 5 via a unique subdomain within the fibronectin-like repeats. J. Invest. Dermatol. *112*, 177–183.

Ciruna, B., and Rossant, J. (2001). FGF signaling regulates mesoderm cell fate specification and morphogenetic movement at the primitive streak. Dev. Cell *1*, 37–49.

Clayton, E., Doupé, D.P., Klein, A.M., Winton, D.J., Simons, B.D., and Jones, P.H. (2007). A single type of progenitor cell maintains normal epidermis. Nature *446*, 185–189.

Coraux, C., Hilmi, C., Rouleau, M., and Spadafora, A. (2003). Reconstituted skin from murine embryonic stem cells. Curr. Biol. *13*, 849–853.

Cotsarelis, G., Sun, T.T., and Lavker, R.M. (1990). Label-retaining cells reside in the bulge area of pilosebaceous unit: implications for follicular stem cells, hair cycle, and skin carcinogenesis. Cell *61*, 1329–1337.

Coulombe, P.A., and Wong, P. (2004). Cytoplasmic intermediate filaments revealed as dynamic and multipurpose scaffolds. Nat. Cell Biol. *6*, 699–706.

D'Orazi, G., Cecchinelli, B., Bruno, T., Manni, I., Higashimoto, Y., Saito, S., Gostissa, M., Coen, S., Marchetti, A., Del Sal, G., et al. (2002). Homeodomain-interacting protein kinase-2 phosphorylates p53 at Ser 46 and mediates apoptosis. Nat. Cell Biol. *4*, 11–19.

D'Souza, S.J., Pajak, A, Balazsi, K., and Dagnino, L. (2001). Ca2+ and BMP-6 signaling regulate E2F during epidermal keratinocyte differentiation. J. Biol. Chem. *276*, 23531–23538.

Dajee, M., Tarutani, M., Deng, H., Cai, T., and Khavari, P.A. (2002). Epidermal Ras blockade demonstrates spatially localized Ras promotion of proliferation and inhibition of differentiation. Oncogene *21*, 1527–1538.

Davidson, P., and Hardy, M.H. (1952). The development of mouse vibrissae in vivo and in vitro. J. Anat. *86*, 342–356.

Desbaillets, I., Ziegler, U., Groscurth, P., and Gassmann, M. (2000). Embryoid bodies: an in vitro model of mouse embryogenesis. Exp. Physiol. *85*, 645–651.

Desbordes, S.C., and Studer, L. (2013). Adapting human pluripotent stem cells to high-throughput and high-content screening. Nat. Protoc. *8*, 111–130.

Detmer, K., Lawrence, H.J., and Largman, C. (1993). Expression of class I homeobox genes in fetal and adult murine skin. J. Invest. Dermatol. *101*, 517–522.

Dick, A, Risau, W., and Drexler, H. (1998). Expression of Smad1 and Smad2 during embryogenesis suggests a role in organ development. Dev. Dyn. *211*, 293–305.

DiPersio, C.M., Hodivala-Dilke, K.M., Jaenisch, R., Kreidberg, J. a, and Hynes, R.O. (1997). alpha3beta1 Integrin is required for normal development of the epidermal basement membrane. J. Cell Biol. *137*, 729–742.

DiSepio, D., Jones, A., Longley, M.A., Bundman, D., Rothnagel, J.A., and Roop, D.R. (1995). The proximal promoter of the mouse loricrin gene contains a functional AP-1 element and directs keratinocyte-specific but not differentiation-specific expression. J. Biol. Chem. *270*, 10792–10799.

Doi, D., Samata, B., Katsukawa, M., Kikuchi, T., Morizane, A., Ono, Y., Sekiguchi, K., Nakagawa, M., Parmar, M., and Takahashi, J. (2014). Isolation of human induced pluripotent stem cell-derived dopaminergic progenitors by cell sorting for successful transplantation. Stem Cell Reports *2*, 337–350.

Le Douarin, N. (1980). Migration and differentiation of neural crest cells. Curr. Top. Dev. Biol. *16*, 31–85.

Doupé, D.P., Klein, A.M., Simons, B.D., and Jones, P.H. (2010). The ordered architecture of murine ear epidermis is maintained by progenitor cells with random fate. Dev. Cell *18*, 317–323.

Dowling, J., Yu, Q.C., and Fuchs, E. (1996). Beta4 integrin is required for hemidesmosome formation, cell adhesion and cell survival. J. Cell Biol. *134*, 559–572.

Ebert, A.D., and Svendsen, C.N. (2010). Human stem cells and drug screening: opportunities and challenges. Nat. Rev. Drug Discov. *9*, 367–372.

Ebert, A.D., Yu, J., Rose, F.F., Mattis, V.B., Lorson, C.L., Thomson, J.A., and Svendsen, C.N. (2009). Induced pluripotent stem cells from a spinal muscular atrophy patient. Nature *457*, 277–280.

Eckhart, L., Declercq, W., Ban, J., Rendl, M., Lengauer, B., Mayer, C., Lippens, S., Vandenabeele, P., and Tschachler, E. (2000). Terminal differentiation of human keratinocytes and stratum corneum formation is associated with caspase-14 activation. J. Invest. Dermatol. *115*, 1148–1151.

Economides, K.D., Zeltser, L., and Capecchi, M.R. (2003). Hoxb13 mutations cause overgrowth of caudal spinal cordand tail vertebrae. Dev. Biol. *256*, 317–330.

Evans, M.J., and Kaufman, M.H. (1981). Establishment in culture of pluripotential cells from mouse embryos. Nature *292*, 154–156.

Evans, V.J., Bryant, J.C., McQuilkin, W.T., Fioramonti, M.C., Sanford, K.K., Westfall, B.B., and Earle, W.R. (1956). Studies of nutrient media for tissue cells in vitro. II. An improved protein-free chemically defined medium for long-term cultivation of strain L-929 cells. Cancer Res. *16*, 87–94.

Fitzpatrick, T.B., and Breathnach, A.S. (1963). [The epidermal melanin unit system]. Dermatol. Wochenschr. *147*, 481–489.

Flanders, K.C., Kim, E.S., and Roberts, A.B. (2001). Immunohistochemical expression of Smads 1-6 in the 15-day gestation mouse embryo: signaling by BMPs and TGF-betas. Dev. Dyn. *220*, 141–154.

Freinkel, R.K., and Traczyk, T.N. (1985). Lipid composition and acid hydrolase content of lamellar granules of fetal rat epidermis. J. Invest. Dermatol. *85*, 295–298.

Friedmann-Morvinski, D., and Verma, I.M. (2014). Dedifferentiation and reprogramming: origins of cancer stem cells. EMBO Rep. *15*, 244–253.

Fuchs, E., and Horsley, V. (2008). More than one way to skin... Genes Dev. *22*, 976–985.

Fuchs, E., and Raghavan, S. (2002). Getting under the skin of epidermal morphogenesis. Nat. Rev. Genet. *3*, 199–209.

Fuchs, E., Merrill, B., Jamora, C., and DasGupta, R. (2001). At the roots of a never-ending cycle. Dev. Cell *1*, 13–25.

Fusaki, N., Ban, H., Nishiyama, A., Saeki, K., and Hasegawa, M. (2009). Efficient induction of transgene-free human pluripotent stem cells using a vector based on Sendai virus, an RNA virus that does not integrate into the host genome. Proc. Jpn. Acad. Ser. B. Phys. Biol. Sci. *85*, 348–362.

Galach, M., and Utikal, J. (2011). From skin to the treatment of diseases--the possibilities of iPS cell research in dermatology. Exp. Dermatol. *20*, 523–528.

Gallico, G.G., O'Connor, N.E., Compton, C.C., Kehinde, O., and Green, H. (1984). Permanent coverage of large burn wounds with autologous cultured human epithelium. N. Engl. J. Med. *311*, 448–451.

Gan, S.Q., McBride, O.W., Idler, W.W., Markova, N., and Steinert, P.M. (1990). Organization, structure, and polymorphisms of the human profilaggrin gene. Biochemistry *29*, 9432–9440.

Garrod, D.R. (1993). Desmosomes and hemidesmosomes. Curr. Opin. Cell Biol. *5*, 30–40.

Geissmann, F., Revy, P., Regnault, A, Lepelletier, Y., Dy, M., Brousse, N., Amigorena, S., Hermine, O., and Durandy, A (1999). TGF-beta 1 prevents the noncognate maturation of human dendritic Langerhans cells. J. Immunol. *162*, 4567–4575.

Ghazizadeh, S., and Taichman, L.B. (2001). Multiple classes of stem cells in cutaneous epithelium: a lineage analysis of adult mouse skin. EMBO J. *20*, 1215–1222.

Gipson, I.K., Spurr-Michaud, S.J., and Tisdale, A.S. (1987). Anchoring fibrils form a complex network in human and rabbit cornea. Invest. Ophthalmol. Vis. Sci. *28*, 212–220.

Green, H., Easley, K., and Iuchi, S. (2003). Marker succession during the development of keratinocytes from cultured human embryonic stem cells. Proc. Natl. Acad. Sci. U. S. A. *100*, 15625–15630.

Guan, E., Wang, J., Laborda, J., Norcross, M., Baeuerle, P.A., and Hoffman, T. (1996). T cell leukemia-associated human Notch/translocation-associated Notch homologue has I kappa B-like activity and physically interacts with nuclear factor-kappa B proteins in T cells. J. Exp. Med. *183*, 2025–2032.

Guenou, H., Nissan, X., Larcher, F., Feteira, J., Lemaitre, G., Saidani, M., Del Rio, M., Barrault, C.C., Bernard, F.-X., Peschanski, M., et al. (2009). Human embryonic stem-cell derivatives for full reconstruction of the pluristratified epidermis: a preclinical study. Lancet *374*, 1745–1753.

Guerrini, L., Costanzo, A., and Merlo, G.R. (2011). A symphony of regulations centered on p63 to control development of ectoderm-derived structures. J. Biomed. Biotechnol. *2011*, 864904.

Gurdon, J. (1962). The transplantation of nuclei between two species of Xenopus. Dev. Biol. *83*, 68–83.

Haase, I., Knaup, R., Wartenberg, M., Sauer, H., Hescheler, J., and Mahrle, G. (2007). In vitro differentiation of murine embryonic stem cells into keratinocyte-like cells. Eur. J. Cell Biol. *86*, 801–805.

Halata, Z., Grim, M., and Bauman, K.I. (2003). Friedrich Sigmund Merkel and his “Merkel cell”, morphology, development, and physiology: review and new results. Anat. Rec. A. Discov. Mol. Cell. Evol. Biol. *271*, 225–239.

Hamanaka, S., Nakazawa, S., Yamanaka, M., Uchida, Y., and Otsuka, F. (2005). Glucosylceramide accumulates preferentially in lamellar bodies in differentiated keratinocytes. Br. J. Dermatol. *152*, 426–434.

Han, G., Li, A.G., Liang, Y.-Y., Owens, P., He, W., Lu, S., Yoshimatsu, Y., Wang, D., Ten Dijke, P., Lin, X., et al. (2006). Smad7-induced beta-catenin degradation alters epidermal appendage development. Dev. Cell *11*, 301–312.

Hata, A., Lagna, G., Massagué, J., and Hemmati-Brivanlou, A. (1998). Smad6 inhibits BMP/Smad1 signaling by specifically competing with the Smad4 tumor suppressor. Genes Dev. *12*, 186–197.

He, Q., Shi, J., Sun, H., and An, J. (2010). Characterization of human homeodomain-interacting protein kinase 4 (HIPK4) as a unique member of the HIPK family. Mol. Cell. … *2*, 61–68.

Hennings, H., Michael, D., Cheng, C., Steinert, P., Holbrook, K., and Yuspa, S.H. (1980). Calcium regulation of growth and differentiation of mouse epidermal cells in culture. Cell *19*, 245–254.

Hess, J., Angel, P., and Schorpp-Kistner, M. (2004). AP-1 subunits: quarrel and harmony among siblings. J. Cell Sci. *117*, 5965–5973.

Hilger-Eversheim, K., Moser, M., Schorle, H., and Buettner, R. (2000). Regulatory roles of AP-2 transcription factors in vertebrate development, apoptosis and cell-cycle control. Gene *260*, 1–12.

Hopkinson, S.B., and Jones, J.C. (2000). The N terminus of the transmembrane protein BP180 interacts with the N-terminal domain of BP230, thereby mediating keratin cytoskeleton anchorage to the cell surface at the site of the hemidesmosome. Mol. Biol. Cell *11*, 277–286.

Hopkinson, S.B., Riddelle, K.S., and Jones, J.C. (1992). Cytoplasmic domain of the 180-kD bullous pemphigoid antigen, a hemidesmosomal component: molecular and cell biologic characterization. J. Invest. Dermatol. *99*, 264–270.

Horsley, V., O’Carroll, D., Tooze, R., Ohinata, Y., Saitou, M., Obukhanych, T., Nussenzweig, M., Tarakhovsky, A., and Fuchs, E. (2006). Blimp1 defines a progenitor population that governs cellular input to the sebaceous gland. Cell *126*, 597–609.

Houben, E., De Paepe, K., and Rogiers, V. (2007). A keratinocyte’s course of life. Skin Pharmacol. Physiol. *20*, 122–132.

Hu, Y., Baud, V., Oga, T., Kim, K.I., Yoshida, K., and Karin, M. (2001). IKKalpha controls formation of the epidermis independently of NF-kappaB. Nature *410*, 710–714.

Huangfu, D., Osafune, K., Maehr, R., Guo, W., Eijkelenboom, A., Chen, S., Muhlestein, W., and Melton, D.A. (2008). Induction of pluripotent stem cells from primary human fibroblasts with only Oct4 and Sox2. Nat. Biotechnol. *26*, 1269–1275.

Hwang, E.A, Lee, H.B., and Tark, K.C. (2001). Comparison of bone morphogenetic protein receptors expression in the fetal and adult skin. Yonsei Med. J. *42*, 581–586.

Ishitani, T., Ninomiya-tsuji, J., Nagai, S., Nishita, M., Meneghini, M., Barker, N., Waterman, M., Bowerman, B., Clevers, H., Shibuya, H., et al. (1999). The TAK1-NLK-MAPK-related pathway antagonizes signalling between beta-catenin and transcription factor TCF. Nature *399*, 798–802.

Itoh, M., Kiuru, M., Cairo, M.S., and Christiano, A.M. (2011). Generation of keratinocytes from normal and recessive dystrophic epidermolysis bullosa-induced pluripotent stem cells. Proc. Natl. Acad. Sci. U. S. A. *108*, 8797–8802.

Iuchi, S., Dabelsteen, S., Easley, K., Rheinwald, J.G., and Green, H. (2006). Immortalized keratinocyte lines derived from human embryonic stem cells. Proc. Natl. Acad. Sci. U. S. A. *103*, 1792–1797.

Jakob, T., Ring, J., and Udey, M.C. (2001). Multistep navigation of Langerhans/dendritic cells in and out of the skin. J. Allergy Clin. Immunol. *108*, 688–696.

Janes, S.M., and Watt, F.M. (2006). New roles for integrins in squamous-cell carcinoma. Nat. Rev. Cancer *6*, 175–183.

Ji, L., Allen-Hoffmann, B., and Pablo, J. (2006). Generation and differentiation of human embryonic stem cell-derived keratinocyte precursors. Tissue Eng. *12*, 665–679.

Jia, F., Wilson, K.D., Sun, N., Gupta, D.M., Huang, M., Li, Z., Panetta, N.J., Chen, Z.Y., Robbins, R.C., Kay, M.A., et al. (2010). A nonviral minicircle vector for deriving human iPS cells. Nat. Methods *7*, 197–199.

Johnson, K.O. (2001). The roles and functions of cutaneous mechanoreceptors. Curr. Opin. Neurobiol. *11*, 455–461.

Jones, P.H., and Watt, F.M. (1993). Separation of human epidermal stem cells from transit amplifying cells on the basis of differences in integrin function and expression. Cell *73*, 713–724.

Kachinskas, D.J., Phillips, M. a, Qin, Q., Stokes, J.D., and Rice, R.H. (1994). Arsenate perturbation of human keratinocyte differentiation. Cell Growth Differ. *5*, 1235–1241.

Kaghad, M., Bonnet, H., Yang, A, Creancier, L., Biscan, J.C., Valent, A, Minty, A, Chalon, P., Lelias, J.M., Dumont, X., et al. (1997). Monoallelically expressed gene related to p53 at 1p36, a region frequently deleted in neuroblastoma and other human cancers. Cell *90*, 809–819.

Kim, M.H., Cho, M., and Park, D. (1998). Sequence analysis of the 5'-flanking region of the gene encoding human HOXA-7. Somat. Cell Mol. Genet. *24*, 371–374.

Kimura, N., Matsuo, R., Shibuya, H., Nakashima, K., and Taga, T. (2000). BMP2-induced apoptosis is mediated by activation of the TAK1-p38 kinase pathway that is negatively regulated by Smad6. J. Biol. Chem. *275*, 17647–17652.

Kömüves, L.G., Ma, X.-K., Stelnicki, E., Rozenfeld, S., Oda, Y., and Largman, C. (2003). HOXB13 homeodomain protein is cytoplasmic throughout fetal skin development. Dev. Dyn. *227*, 192–202.

Koster, M., and Roop, D. (2004). Transgenic mouse models provide new insights into the role of p63 in epidermal development. CELL CYCLE-LANDES Biosci. *3*, 411–413.

Koster, M.I., and Roop, D.R. (2007). Mechanisms regulating epithelial stratification. Annu. Rev. Cell Dev. Biol. *23*, 93–113.

Koster, M., Kim, S., and Mills, A. (2004a). p63 is the molecular switch for initiation of an epithelial stratification program. Genes Dev. *18*, 126–131.

Koster, M.I., Kim, S., Mills, A.A, DeMayo, F.J., and Roop, D.R. (2004b). P63 Is the Molecular Switch for Initiation of an Epithelial Stratification Program. Genes Dev. *18*, 126–131.

Kusanagi, K., Inoue, H., Ishidou, Y., Mishima, H.K., Kawabata, M., and Miyazono, K. (2000). Characterization of a bone morphogenetic protein-responsive Smad-binding element. Mol. Biol. Cell *11*, 555–565.

Lazzari, C., Prodosmo, A., Siepi, F., Rinaldo, C., Galli, F., Gentileschi, M., Bartolazzi, A., Costanzo, A., Sacchi, A., Guerrini, L., et al. (2011). HIPK2 phosphorylates ΔNp63α and promotes its degradation in response to DNA damage. Oncogene *30*, 4802–4813.

Leask, A, Byrne, C., and Fuchs, E. (1991). Transcription factor AP2 and its role in epidermal-specific gene expression. Proc. Natl. Acad. Sci. U. S. A. *88*, 7948–7952.

Lechler, T., and Fuchs, E. (2005). Asymmetric cell divisions promote stratification and differentiation of mammalian skin. Nature *437*, 275–280.

Legué, E., and Nicolas, J.-F. (2005). Hair follicle renewal: organization of stem cells in the matrix and the role of stereotyped lineages and behaviors. Development *132*, 4143–4154.

Li, A.G., Koster, M.I., and Wang, X.J. (2003). Roles of TGFbeta signaling in epidermal/appendage development. Cytokine Growth Factor Rev. *14*, 99–111.

Li, W., Chen, F., Nagarajan, R.P., Liu, X., and Chen, Y. (2001). Characterization of the DNA-binding property of Smad5. Biochem. Biophys. Res. Commun. *286*, 1163–1169.

Li, X., Massa, P.E., Hanidu, A., Peet, G.W., Aro, P., Savitt, A., Mische, S., Li, J., and Marcu, K.B. (2002). IKKalpha, IKKbeta, and NEMO/IKKgamma are each required for the NF-kappa B-mediated inflammatory response program. J. Biol. Chem. *277*, 45129–45140.

Liew, F., and Yamanishi, K. (1992). of transglutaminase 1 gene expression by 12- O-tetradecanoylphorbol-13-acetate, dexamethasone, and retinoic acid in cultured human keratinocytes. Exp. Cell Res. *315*, 310–315.

Lippens, S., Denecker, G., Ovaere, P., Vandenabeele, P., and Declercq, W. (2005). Death penalty for keratinocytes: apoptosis versus cornification. Cell Death Differ. *12 Suppl 2*, 1497–1508.

List, K., Szabo, R., Wertz, P.W., Segre, J., Haudenschild, C.C., Kim, S.-Y., and Bugge, T.H. (2003). Loss of proteolytically processed filaggrin caused by epidermal deletion of Matriptase/MT-SP1. J. Cell Biol. *163*, 901–910.

Loomis, C.A. (2001). Development and morphogenesis of the skin. Adv. Dermatol. *17*, 183–210.

Lyons, K.M., Pelton, R.W., and Hogan, B.L. (1989). Patterns of expression of murine Vgr-1 and BMP-2a RNA suggest that transforming growth factor-beta-like genes coordinately regulate aspects of embryonic development. Genes Dev. *3*, 1657–1668.

Maas-Szabowski, N., Szabowski, A., Stark, H.J., Andrecht, S., Kolbus, A., Schorpp-Kistner, M., Angel, P., and Fusenig, N.E. (2001). Organotypic cocultures with genetically modified mouse fibroblasts as a tool to dissect molecular mechanisms regulating keratinocyte growth and differentiation. J. Invest. Dermatol. *116*, 816–820.

Mack, J.A, Anand, S., and Maytin, E.V (2005). Proliferation and cornification during development of the mammalian epidermis. Birth Defects Res. C. Embryo Today *75*, 314–329.

Mack, J.W., Steven, A.C., and Steinert, P.M. (1993). The mechanism of interaction of filaggrin with intermediate filaments. The ionic zipper hypothesis. J. Mol. Biol. *232*, 50–66.

Mangiulli, M., Valletti, A., Caratozzolo, M.F., Tullo, A., Sbisà, E., Pesole, G., and D'Erchia, A.M. (2009). Identification and functional characterization of two new transcriptional variants of the human p63 gene. Nucleic Acids Res. *37*, 6092–6104.

Mariniello, L., Qin, Q., Jessen, B.A., and Rice, R.H. (1995). Keratinocyte transglutaminase promoter analysis. Identification of a functional response element. J. Biol. Chem. *270*, 31358–31363.

Martí, M., Mulero, L., Pardo, C., Morera, C., Carrió, M., Laricchia-Robbio, L., Esteban, C.R., and Izpisua Belmonte, J.C. (2013). Characterization of pluripotent stem cells. Nat. Protoc. *8*, 223–253.

Martin, G.R. (1981). Isolation of a pluripotent cell line from early mouse embryos cultured in medium conditioned by teratocarcinoma stem cells. Proc. Natl. Acad. Sci. U. S. A. *78*, 7634–7638.

Massagué, J. (2012). TGFβ signalling in context. Nat. Rev. Mol. Cell Biol. *13*, 616–630.

Matoltsy, A.G. (1975). Desmosomes, filaments, and keratohyaline granules: their role in the stabilization and keratinization of the epidermis. J. Invest. Dermatol. *65*, 127–142.

Maytin, E., and Habener, J. (1998). Transcription factors C/EBPα, C/EBPβ, and CHOP (Gadd153) expressed during the differentiation program of keratinocytes in vitro and in vivo. J. Invest. Dermatol. 238–246.

Maytin, E.V, Lin, J.C., Krishnamurthy, R., Batchvarova, N., Ron, D., Mitchell, P.J., and Habener, J.F. (1999). Keratin 10 gene expression during differentiation of mouse epidermis requires transcription factors C/EBP and AP-2. Dev. Biol. *216*, 164–181.

McDonnell, M.A, Law, B.K., Serra, R., and Moses, H.L. (2001). Antagonistic effects of TGFbeta1 and BMP-6 on skin keratinocyte differentiation. Exp. Cell Res. *263*, 265–273.

McMillan, J.R., Akiyama, M., and Shimizu, H. (2003). Epidermal basement membrane zone components: ultrastructural distribution and molecular interactions. J. Dermatol. Sci. *31*, 169–177.

Menon, G.K., Feingold, K.R., and Elias, P.M. (1992). Lamellar body secretory response to barrier disruption. J. Invest. Dermatol. *98*, 279–289.

Metallo, C.M., Ji, L., de Pablo, J.J., and Palecek, S.P. (2008). Retinoic acid and bone morphogenetic protein signaling synergize to efficiently direct epithelial differentiation of human embryonic stem cells. Stem Cells *26*, 372–380.

Millar, S.E. (2002). Molecular mechanisms regulating hair follicle development. J. Invest. Dermatol. *118*, 216–225.

Mills, A.A, Zheng, B., Wang, X.J., Vogel, H., Roop, D.R., and Bradley, A (1999). P63 Is a P53 Homologue Required for Limb and Epidermal Morphogenesis. Nature *398*, 708–713.

Mischke, D., Korge, B.P., Marenholz, I., Volz, A., and Ziegler, A. (1996). Genes encoding structural proteins of epidermal cornification and S100 calcium-binding proteins form a gene complex ("epidermal differentiation complex") on human chromosome 1q21. J. Invest. Dermatol. *106*, 989–992.

Mishina, Y. (2003). Function of bone morphogenetic protein signaling during mouse development. Front. Biosci. *8*, d855–69.

Miyoshi, N., Ishii, H., Nagano, H., Haraguchi, N., Dewi, D.L., Kano, Y., Nishikawa, S., Tanemura, M., Mimori, K., Tanaka, F., et al. (2011). Reprogramming of mouse and human cells to pluripotency using mature microRNAs. Cell Stem Cell *8*, 633–638.

Moll, R., Moll, I., and Wiest, W. (1982). Changes in the pattern of cytokeratin polypeptides in epidermis and hair follicles during skin development in human fetuses. Differentiation. *23*, 170–178.

Montagna, W., and Carlisle, K. (1991). The architecture of black and white facial skin. J. Am. Acad. Dermatol. *24*, 929–937.

Morris, R.J., Liu, Y., Marles, L., Yang, Z., Trempus, C., Li, S., Lin, J.S., Sawicki, J.A, and Cotsarelis, G. (2004). Capturing and profiling adult hair follicle stem cells. Nat. Biotechnol. *22*, 411–417.

Nemes, Z., Marekov, L.N., Fésüs, L., and Steinert, P.M. (1999). A novel function for transglutaminase 1: attachment of long-chain omega-hydroxyceramides to involucrin by ester bond formation. Proc. Natl. Acad. Sci. U. S. A. *96*, 8402–8407.

Nickoloff, B.J., Qin, J.-Z., Chaturvedi, V., Denning, M.F., Bonish, B., and Miele, L. (2002). Jagged-1 mediated activation of notch signaling induces complete maturation of human keratinocytes through NF-kappaB and PPARgamma. Cell Death Differ. *9*, 842–855.

Niemann, C., Unden, A.B., Lyle, S., Zouboulis, C.C., Toftgård, R., and Watt, F.M. (2003). Indian hedgehog and beta-catenin signaling: role in the sebaceous lineage of normal and neoplastic mammalian epidermis. Proc. Natl. Acad. Sci. U. S. A. *100 Suppl* , 11873–11880.

Nishiyama, T., Amano, S., Tsunenaga, M., Kadoya, K., Takeda, A, Adachi, E., and Burgeson, R.E. (2000). The importance of laminin 5 in the dermal-epidermal basement membrane. J. Dermatol. Sci. *24 Suppl 1*, S51–9.

O'Sullivan, C.M., Rancourt, S.L., Liu, S.Y., and Rancourt, D.E. (2001). A novel murine tryptase involved in blastocyst hatching and outgrowth. Reproduction *122*, 61–71.

Oh, H.S., and Smart, R.C. (1998). Expression of CCAAT/enhancer binding proteins (C/EBP) is associated with squamous differentiation in epidermis and isolated primary keratinocytes and is altered in skin neoplasms. J. Invest. Dermatol. *110*, 939–945.

Okita, K., Ichisaka, T., and Yamanaka, S. (2007). Generation of germline-competent induced pluripotent stem cells. Nature *448*, 313–317.

Okita, K., Nakagawa, M., Hyenjong, H., Ichisaka, T., and Yamanaka, S. (2008). Generation of mouse induced pluripotent stem cells without viral vectors. Science *322*, 949–953.

Panchision, D., and Pickel, J. (2001). Sequential actions of BMP receptors control neural precursor cell production and fate. Genes … *6*, 2094–2110.

Park, G.T., and Morasso, M.I. (2002). Bone morphogenetic protein-2 (BMP-2) transactivates Dlx3 through Smad1 and Smad4: alternative mode for Dlx3 induction in mouse keratinocytes. Nucleic Acids Res. *30*, 515–522.

Perez-Moreno, M., and Fuchs, E. (2006). Catenins: keeping cells from getting their signals crossed. Dev. Cell *11*, 601–612.

Perona, R.M., and Wassarman, P.M. (1986). Mouse blastocysts hatch in vitro by using a trypsin-like proteinase associated with cells of mural trophectoderm. Dev. Biol. *114*, 42–52.

Potten, C.S. (1974). The epidermal proliferative unit: the possible role of the central basal cell. Cell Tissue Kinet. *7*, 77–88.

Potten, C.S. (1981). Cell replacement in epidermis (keratopoiesis) via discrete units of proliferation. Int. Rev. Cytol. *69*, 271–318.

Qin, J., Chaturvedi, V., and Denning, M. (1999). Role of NF-κB in the apoptotic-resistant phenotype of keratinocytes. J. Biol. ….

Ramathal, C., Wang, W., Hunt, E., Bagchi, I.C., and Bagchi, M.K. (2011). Transcription factor CCAAT enhancer-binding protein beta (C/EBPbeta) regulates the formation of a unique extracellular matrix that controls uterine stromal differentiation and embryo implantation. J. Biol. Chem. *286*, 19860–19871.

Ramji, D., and Foka, P. (2002). CCAAT/enhancer-binding proteins: structure, function and regulation. Biochem. J *575*, 561–575.

Rangarajan, A, Talora, C., Okuyama, R., Nicolas, M., Mammucari, C., Oh, H., Aster, J.C., Krishna, S., Metzger, D., Chambon, P., et al. (2001). Notch signaling is a direct determinant of keratinocyte growth arrest and entry into differentiation. EMBO J. *20*, 3427–3436.

Rice, R.H., and Green, H. (1977). The cornified envelope of terminally differentiated human epidermal keratinocytes consists of cross-linked protein. Cell *11*, 417–422.

Riedl, E., Stöckl, J., Majdic, O., Scheinecker, C., Rappersberger, K., Knapp, W., and Strobl, H. (2000). Functional involvement of E-cadherin in TGF-beta 1-induced cell cluster formation of in vitro developing human Langerhans-type dendritic cells. J. Immunol. *165*, 1381–1386.

Robinton, D.A, and Daley, G.Q. (2012). The promise of induced pluripotent stem cells in research and therapy. Nature *481*, 295–305.

Romani, N., Ratzinger, G., Pfaller, K., Salvenmoser, W., Stössel, H., Koch, F., and Stoitzner, P. (2001). Migration of dendritic cells into lymphatics-the Langerhans cell example: routes, regulation, and relevance. Int. Rev. Cytol. *207*, 237–270.

Rousselle, P., Keene, D.R., Ruggiero, F., Champliaud, M.F., Rest, M., and Burgeson, R.E. (1997). Laminin 5 binds the NC-1 domain of type VII collagen. J. Cell Biol. *138*, 719–728.

Rungarunlert, S., Techakumphu, M., Pirity, M.K., and Dinnyes, A. (2009). Embryoid body formation from embryonic and induced pluripotent stem cells: Benefits of bioreactors. World J. Stem Cells *1*, 11–21.

Scholl, F.A, Dumesic, P.A, Barragan, D.I., Harada, K., Bissonauth, V., Charron, J., and Khavari, P.A (2007). Mek1/2 MAPK kinases are essential for Mammalian development, homeostasis, and Raf-induced hyperplasia. Dev. Cell *12*, 615–629.

Seiji, M., and Fitzpatrick, T.B. (1961). The reciprocal relationship between melanization and tyrosinase activity in melanosomes (melanin granules). J. Biochem. *49*, 700–706.

Seitz, C.S., Lin, Q., Deng, H., and Khavari, P.A (1998). Alterations in NF-kappaB function in transgenic epithelial tissue demonstrate a growth inhibitory role for NF-kappaB. Proc. Natl. Acad. Sci. U. S. A. *95*, 2307–2312.

Seitz, C.S., Deng, H., Hinata, K., Lin, Q., and Khavari, P.A. (2000). Nuclear factor kappaB subunits induce epithelial cell growth arrest. Cancer Res. *60*, 4085–4092.

Sidhu, G.S., Chandra, P., and Cassai, N.D. (2005). Merkel cells, normal and neoplastic: an update. Ultrastruct. Pathol. *29*, 287–294.

Silva, J., and Smith, A. (2008). Capturing pluripotency. Cell *132*, 532–536.

Simon, M., and Green, H. (1988). The glutamine residues reactive in transglutaminase-catalyzed cross-linking of involucrin. J. Biol. Chem. *263*, 18093–18098.

Simpson, C.L., Patel, D.M., and Green, K.J. (2011). Deconstructing the skin: cytoarchitectural determinants of epidermal morphogenesis. Nat. Rev. Mol. Cell Biol. *12*, 565–580.

Somers, A., Jean, J.-C., Sommer, C.A, Omari, A., Ford, C.C., Mills, J.A, Ying, L., Sommer, A.G., Jean, J.M., Smith, B.W., et al. (2010). Generation of transgene-free lung disease-specific human induced pluripotent stem cells using a single excisable lentiviral stem cell cassette. Stem Cells *28*, 1728–1740.

Stadtfeld, M., and Hochedlinger, K. (2010). Induced pluripotency: history, mechanisms, and applications. Genes Dev. *24*, 2239–2263.

Stadtfeld, M., Maherali, N., Breault, D.T., and Hochedlinger, K. (2008a). Defining molecular cornerstones during fibroblast to iPS cell reprogramming in mouse. Cell Stem Cell *2*, 230–240.

Stadtfeld, M., Nagaya, M., Utikal, J., Weir, G., and Hochedlinger, K. (2008b). Induced pluripotent stem cells generated without viral integration. Science *322*, 945–949.

Steinert, P.M., and Marekov, L.N. (1995). The proteins elafin, filaggrin, keratin intermediate filaments, loricrin, and small proline-rich proteins 1 and 2 are isodipeptide cross-linked components of the human epidermal cornified cell envelope. J. Biol. Chem. *270*, 17702–17711.

Stern, C.D., and Downs, K.M. (2012). The hypoblast (visceral endoderm): an evo-devo perspective. Development *139*, 1059–1069.

Stoitzner, P., Pfaller, K., Stössel, H., and Romani, N. (2002). A close-up view of migrating Langerhans cells in the skin. J. Invest. Dermatol. *118*, 117–125.

Sun, X., Meyers, E.N., Lewandoski, M., and Martin, G.R. (1999). Targeted disruption of Fgf8 causes failure of cell migration in the gastrulating mouse embryo. Genes Dev. *13*, 1834–1846.

Suzuki, D., and Senoo, M. (2012). Increased p63 phosphorylation marks early transition of epidermal stem cells to progenitors. J. Invest. Dermatol. *132*, 2461–2464.

Szabowski, A., Maas-Szabowski, N., Andrecht, S., Kolbus, A., Schorpp-Kistner, M., Fusenig, N.E., and Angel, P. (2000). c-Jun and JunB antagonistically control cytokine-regulated mesenchymal-epidermal interaction in skin. Cell *103*, 745–755.

Takahashi, H., and Iizuka, H. (1993). Analysis of the 5'-upstream promoter region of human involucrin gene: activation by 12-O-tetradecanoylphorbol-13-acetate. J. Invest. Dermatol. *100*, 10–15.

Takahashi, H., and Ikeda, T. (1996). Transcripts for two members of the transforming growth factor-beta superfamily BMP-3 and BMP-7 are expressed in developing rat embryos. Dev. Dyn. *207*, 439–449.

Takahashi, K., and Yamanaka, S. (2006). Induction of pluripotent stem cells from mouse embryonic and adult fibroblast cultures by defined factors. Cell *126*, 663–676.

Takahashi, M., Tezuka, T., and Katunuma, N. (1992). Phosphorylated cystatin alpha is a natural substrate of epidermal transglutaminase for formation of skin cornified envelope. FEBS Lett. *308*, 79–82.

Takeda, H., Lyle, S., Lazar, A.J.F., Zouboulis, C.C., Smyth, I., and Watt, F.M. (2006). Human sebaceous tumors harbor inactivating mutations in LEF1. Nat. Med. *12*, 395–397.

Taylor, G., Lehrer, M.S., Jensen, P.J., Sun, T.T., and Lavker, R.M. (2000). Involvement of follicular stem cells in forming not only the follicle but also the epidermis. Cell *102*, 451–461.

Thomson, J.A. (1998). Embryonic Stem Cell Lines Derived from Human Blastocysts. Science (80-.). *282*, 1145–1147.

Thomson, J.A., Kalishman, J., Golos, T.G., Durning, M., Harris, C.P., Becker, R.A., and Hearn, J.P. (1995). Isolation of a primate embryonic stem cell line. Proc. Natl. Acad. Sci. U. S. A. *92*, 7844–7848.

Tolar, J., Xia, L., Riddle, M.J., Lees, C.J., Eide, C.R., McElmurry, R.T., Titeux, M., Osborn, M.J., Lund, T.C., Hovnanian, A., et al. (2011). Induced pluripotent stem cells from individuals with recessive dystrophic epidermolysis bullosa. J. Invest. Dermatol. *131*, 848–856.

Truong, A.B., and Khavari, P.A. (2007). Control of keratinocyte proliferation and differentiation by p63. Cell Cycle *6*, 295–299.

Tsuruta, D., Hashimoto, T., Hamill, K.J., and Jones, J.C.R. (2011). Hemidesmosomes and focal contact proteins: functions and cross-talk in keratinocytes, bullous diseases and wound healing. J. Dermatol. Sci. *62*, 1–7.

Tumbar, T., Guasch, G., Greco, V., Blanpain, C., Lowry, W.E., Rendl, M., and Fuchs, E. (2004). Defining the epithelial stem cell niche in skin. Science *303*, 359–363.

Van der Valk, J., Brunner, D., De Smet, K., Fex Svenningsen, A., Honegger, P., Knudsen, L.E., Lindl, T., Noraberg, J., Price, A., Scarino, M.L., et al. (2010). Optimization of chemically defined cell culture media--replacing fetal bovine serum in mammalian in vitro methods. Toxicol. In Vitro *24*, 1053–1063.

Verma, I.M., Stevenson, J.K., Schwarz, E.M., Van Antwerp, D., and Miyamoto, S. (1995). Rel/NF-kappa B/I kappa B family: intimate tales of association and dissociation. Genes Dev. *9*, 2723–2735.

Wall, N.A., Blessing, M., Wright, C. V, and Hogan, B.L. (1993). Biosynthesis and in vivo localization of the decapentaplegic-Vg-related protein, DVR-6 (bone morphogenetic protein-6). J. Cell Biol. *120*, 493–502.

Wang, H., and Dey, S.K. (2006). Roadmap to embryo implantation: clues from mouse models. Nat. Rev. Genet. *7*, 185–199.

Warren, L., Manos, P.D., Ahfeldt, T., Loh, Y.-H., Li, H., Lau, F., Ebina, W., Mandal, P.K., Smith, Z.D., Meissner, A., et al. (2010). Highly efficient reprogramming to pluripotency and directed differentiation of human cells with synthetic modified mRNA. Cell Stem Cell *7*, 618–630.

Watanabe, K., Ueno, M., Kamiya, D., Nishiyama, A., Matsumura, M., Wataya, T., Takahashi, J.B., Nishikawa, S., Nishikawa, S., Muguruma, K., et al. (2007). A ROCK inhibitor permits survival of dissociated human embryonic stem cells. Nat. Biotechnol. *25*, 681–686.

Watt, F.M., Estrach, S., and Ambler, C.A (2008). Epidermal Notch signalling: differentiation, cancer and adhesion. Curr. Opin. Cell Biol. *20*, 171–179.

Wernig, M., Meissner, A., Foreman, R., Brambrink, T., Ku, M., Hochedlinger, K., Bernstein, B.E., and Jaenisch, R. (2007). In vitro reprogramming of fibroblasts into a pluripotent ES-cell-like state. Nature *448*, 318–324.

Wernig, M., Lengner, C.J., Hanna, J., Lodato, M.A., Steine, E., Foreman, R., Staerk, J., Markoulaki, S., and Jaenisch, R. (2008). A drug-inducible transgenic system for direct reprogramming of multiple somatic cell types. Nat. Biotechnol. *26*, 916–924.

Williams, T.M., Williams, M.E., Heaton, J.H., Gelehrter, T.D., and Innis, J.W. (2005). Group 13 HOX proteins interact with the MH2 domain of R-Smads and modulate Smad transcriptional activation functions independent of HOX DNA-binding capability. Nucleic Acids Res. *33*, 4475–4484.

Woltjen, K., Michael, I.P., Mohseni, P., Desai, R., Mileikovsky, M., Hämäläinen, R., Cowling, R., Wang, W., Liu, P., Gertsenstein, M., et al. (2009). piggyBac transposition reprograms fibroblasts to induced pluripotent stem cells. Nature *458*, 766–770.

Yamaguchi, K., Nagai, S., Ninomiya-Tsuji, J., Nishita, M., Tamai, K., Irie, K., Ueno, N., Nishida, E., Shibuya, H., and Matsumoto, K. (1999). XIAP, a cellular member of the inhibitor of apoptosis protein family, links the receptors to TAB1-TAK1 in the BMP signaling pathway. EMBO J. *18*, 179–187.

Yamanaka, Y., Lanner, F., and Rossant, J. (2010). FGF signal-dependent segregation of primitive endoderm and epiblast in the mouse blastocyst. Development *137*, 715–724.

Yamazaki, M., Ishidoh, K., Suga, Y., Saido, T.C., Kawashima, S., Suzuki, K., Kominami, E., and Ogawa, H. (1997). Cytoplasmic processing of human profilaggrin by active mu-calpain. Biochem. Biophys. Res. Commun. *235*, 652–656.

Yang, A., Kaghad, M., Wang, Y., Gillett, E., and Fleming, M. (1998). p63, a p53 homolog at 3q27-29, encodes multiple products with transactivating, death-inducing, and dominant-negative activities. Mol. Cell *2*, 305–316.

Yang, A., Schweitzer, R., Sun, D., and Kaghad, M. (1999). p63 is essential for regenerative proliferation in limb, craniofacial and epithelial development. Nature *398*, 3–7.

Yoneda, K., and Steinert, P.M. (1993). Overexpression of human loricrin in transgenic mice produces a normal phenotype. Proc. Natl. Acad. Sci. U. S. A. *90*, 10754–10758.

Yu, J., Vodyanik, M.A, Smuga-Otto, K., Antosiewicz-Bourget, J., Frane, J.L., Tian, S., Nie, J., Jonsdottir, G.A, Ruotti, V., Stewart, R., et al. (2007). Induced pluripotent stem cell lines derived from human somatic cells. Science *318*, 1917–1920.

Yu, J., Hu, K., Smuga-Otto, K., Tian, S., Stewart, R., Slukvin, I.I., and Thomson, J.A. (2009). Human induced pluripotent stem cells free of vector and transgene sequences. Science *324*, 797–801.

Yuspa, S.H., Kilkenny, A E., Steinert, P.M., and Roop, D.R. (1989). Expression of murine epidermal differentiation markers is tightly regulated by restricted extracellular calcium concentrations in vitro. J. Cell Biol. *109*, 1207–1217.

Zeng, Y.X., Somasundaram, K., and el-Deiry, W.S. (1997). AP2 inhibits cancer cell growth and activates p21WAF1/CIP1 expression. Nat. Genet. *15*, 78–82.

Zenz, R., Scheuch, H., Martin, P., Frank, C., Eferl, R., Kenner, L., Sibilia, M., and Wagner, E.F. (2003). c-Jun regulates eyelid closure and skin tumor development through EGFR signaling. Dev. Cell *4*, 879–889.

Zhou, W., and Freed, C.R. (2009). Adenoviral gene delivery can reprogram human fibroblasts to induced pluripotent stem cells. Stem Cells *27*, 2667–2674.

Zhou, H., Wu, S., Joo, J.Y., Zhu, S., Han, D.W., Lin, T., Trauger, S., Bien, G., Yao, S., Zhu, Y., et al. (2009). Generation of induced pluripotent stem cells using recombinant proteins. Cell Stem Cell *4*, 381–384.

Danksagung

Mein besonderer Dank gilt:

Herrn Prof. Dr. Jochen Utikal, für die Möglichkeit meine Doktorarbeit in seiner Arbeitsgruppe anzufertigen, für sein Interesse und Engagement und das Vertrauen, welches er mir besonders in der Anfangszeit entgegen gebracht hat.

Herrn Prof. Dr. Viktor Umansky, für die Übernahme des Erstgutachtens, für sein Interesse und viele Anregungen für mein Projekt und, dass er immer ein offenes Ohr für mich hatte.

Herrn Prof. Dr. Michael Boutros, für die Möglichkeit der Durchführung der High-Throughput Screens in seinem Labor, für sein Interesse am Projekt, viele wertvolle Ideen und Anregungen und die Übernahme des Vorsitzes.

Frau Prof. Dr. Petra Boukamp für ihr Interesse, ihren Enthusiasmus und wertvolle Ideen. Unsere Meetings haben mich immer sehr motiviert und angespornt und ich bin mir sicher, dass das Hautäquivalent bald Früchte trägt. Vielen Dank für diese Möglichkeit.

Dr. Christian Volz für seine Screen Kenntnisse, sein Knowhow und dass er jede noch so nervige Mail von mir beantwortet hat.

Tatjana Wüst für die Mitarbeit am Screen, die am Schluss schon Hand-in-Hand ging.

Dr. Hans-Jürgen Stark für seine Hilfe, sein Interesse und Engagement und die schönsten Färbungen, die ich je gesehen habe.

Iris Martin für eine tolle und unproblematische Kooperation und ihre Kompetenz.

Melanie Bewerunge-Hudler, Oliver Heil und Tatjana Schmidt von der Genomics Core Facility am DKFZ für ihre großartige Arbeit und Hilfe bei der Durchführung und Analyse des Microarrays.

Roberta Scognamiglio for a great time and her help with the teratoma assay and many, many other things.

Nathalie „Nathaklaus“ Knappe geb. Schöler, Kasia „Kash“ Weina, Mathias „Matze“ Bernhardt, Sabrina „Sab“ Fehrenbach, Huizi Wu, Kathrin „Kadn“ Tarnanidis, Maike „Maiki“ Reith, Johannes „José“ Ridinger, Elias Orouji, Felix Wezel, Sachindra, Nicolaus Wagner, Sayran Arif-Said, Yvonne Nowak, Willi Eickelbaum und Dr. Christoffer Gebhardt, für einen tollen Zusammenhalt, schöne und lustige Zeiten. Ich vermisse euch schon und werde unsere Zeit nie vergessen. Thank you guys for a great time, I´ll never forget you.

Der gesamten G300 Abteilung für eine tolle Zeit.

Jenny „Jen/Jennoslav/JenJen“ Dworacek für ihre iPSC-Unterstützung, lustige Autofahrten und Zigarettenpausen, für schöne Stunden im Lavandou und die ein oder andere Mannheimer Party.

Janosh „Josh“ Geiger für so viel Spaß, ein tolles Jahr, Call-me-Maybe und dafür, dass ich jetzt Hipster bin.

Dr. Lionel “Lio” Larribere for his help and support, for correcting my thesis and his interest for my project. Thank you for coffee brakes, funny retreats and for being a great desk neighbor, I had so much fun.

Dr. Daniel “Schnobi/Schnob/Schnobsen/Dr.No/Carlos“ Novak für eine tolle Zeit, für seine Hilfe und Unterstützung, lustige Videoabende und immer eine helfende Hand. Du warst der beste Nachbar, lang lebe die Karl-Mathy-Strasse. Ich denke immer gerne an unsere „Zeit-zu-Dritt“ in Mannheim zurück und bin froh, dass du auch so einen Dachschaden hast wie ich…Eckbus-Mitgaaat…

Daniel „Penny/Pan/Pan-the-man/Pan-of-steel“ Roth für einfach alles…dafür dass ich dich kennenlernen durfte, dass du immer das gleiche denkst wie ich, du immer für mich da warst. Danke für Steffen, sau dumm, „…das ist Martagalach“, Kino-Geschichten, die Einführung in den Pälzer-Dialekt, Valerie Denser, Mülltüten-Brautkleider und unsagbar viele Videos, die mich an diese Zeit erinnern werden.

Henry Haigler for correcting my thesis and his interest in the topic.

Meinen Mädels Dr. Daniela „Dani-Schatz“ Straube, Carolin Knell, Teresa „Resi“ Dierlam und Tanja Bachmeyer, dafür dass sie mich immer unterstützt haben und mir nie böse waren, wenn ich mal wieder keine Zeit hatte.

Sara, René und Tom Rückert dafür, dass sie immer da waren und mich auch in stressigen Zeiten immer aufgebaut haben.

Agata „Agi“ and Charles „Charlie“ Schwab for being proud of me, and supporting me, even though they were so far away.

Kevin Chileong Lee, für seine Liebe, Geduld, Unterstützung und Hilfe. Du hast mich immer aufgebaut und warst mein Fels in der Brandung. Danke für deine Ruhe und, dass du meine stressige Art ertragen hast.

Meinen Eltern, ohne die ich das nie geschafft hätte. Mein größtes Ziel ist es euch stolz zu machen. Ihr habt alles richtig gemacht. Ich liebe euch.

Eidesstattliche Erklärung

Hiermit erkläre ich Eides statt, dass ich die vorliegende Dissertation selbstständig und nur mit den angegebenen Hilfsmitteln ausgeführt habe.

Heidelberg, den 30 Juli 2014

_____

(Marta Galach)